High sulfur content polymeric materials for energy storage

2018

Autor: Iñaki Gomez

Supervisors: Prof. David Mecerreyes

Dr. J. Alberto Blazquez

Universidad
del País Vasco

Euskal Herriko
Unibertsitatea

EUSKAL HERRIKO UNIBERTSITATEA / UNIVERSIDAD DEL PAÍS VASCO

Facultad de Ciencias Químicas Departamento de Química Aplicada

"High Sulfur content Polymeric Materials for Energy Storage"

A thesis presented for the degree of PhD to the University of the Basque Country in fulfilments of the requirements.

By

Iñaki Gomez

2018

Thesis Advisors:

Prof. David Mecerreyes   Dr. Alberto Blazquez

Dedicado a Jesusa Antón, Angel Agundez, Jose Antonio Gomez y Maria Agote

""It´s no so toxic"

D.*P*.M.

"All we have to decide is what to do with the time is given to us"

G.

Index

3

4

ATR-FTIR	Attenuated total reflection - fourier transformed infrared spectroscopy
CMC	Carboxy Methyl Cellulose
CV	Cyclic voltammetry
DAS	Diallyl sulfide
DCAQ	1,5-dichloroanthraquinone
DCPD	Dicyclopentadiene
DIB	1,3-diisopropenyl benzene
DMSO-d6	Dimethylsulfoxide hexadeuterated
DSC	Differential scanning calorimetry
DVB	Divinylbenzene
EES	Electrical Energy Storage
EIS	Electrochemical Impedance Spectroscopy
FT-IR	Fourier transformed infrared spectroscopy
GPC	Gel Permeation Chromatography
GPE	Gel Polymer Electrolyte
HEV	Hibrid Electric Vehicle
L-b-L	Layer-by-Layer
LIB	Lithium-ion battery
Li-O2	Lithium-air (oxygen) batteries
LiPAA	Poly(acrylic acid) lithium salt
Li-S	Lithium-Sulfur batteries
LiTFSI	Lithium bis(trifluoromethane sulfonyl) imide
MeOH	Methanol
Myr	Myrcene
Na-S	Sodium-Sulfur batteries
NMP	N-methyl pyrrolidone
NMR	Nuclear Magnetic Resonance
P(DADMAC)	Poly(diallyl dimethyl ammonium chloride)
P(S-DAS)	Poly(Sulfur-Diallylsulfide)
P(S-DCPD)	Poly(Sulfur-Dicyclopentadiene)
P(S-DIB)	Poly(Sulfur-1,3-diisopropenylbenzene)
P(S-DVB)	Poly(Sulfur-Divinylbenzene)
P(SeS-DIB)	Poly(Selenium-Sulfur-1,3-Diisopropenylbenzene)
P(S-Myr)	Poly(Sulfur-Myrcene)
P(S-VBC)	Poly(Sulfur-1,4-Vinylbenzyl chloride)
P(S-VBMImC)	Poly(Sulfur-1,4-Vinylbenzyl methylimidazolium chloride)

P(S-VBMImTFSI)	Poly(Sulfur-1,4-Vinylbenzyl methylimidazolium bis(trifluoromethane sulfonyl) imide)
PAN	Poly(acrylonitrile)
PANI	Poly(aniline)
PAQdS	Poly(anthraquinone disulfide)
PAQnS	Poly(anthraquinone nonasulfide)
PAQpS	Poly(anthraquinone pentasulfide)
PAQS	Poly(anthraquinone sulfide)
PAQxS	Poly(anthraquinone polysulfide)
PEDOT	Poly(3,4-ethylenedioxotiophene)
PEG	Poly(ethylene glycol)
PEGDA	Poly(ethylene glycol) diacrylate
PEI	Poly(ethylene imine)
PEO	Poly(ethylene oxide)
PMMA	Poly(methyl methacrylate)
PS	Polysulfides
PSS	Poly(Styrene sulfonate)
PTFE	Poly(tetrafluoro ethylene)
PVDF	Poly(vinylidene fluoride)
PVDF-co-HFP	Poly(vinylidene fluoride-co-hexafluoro propylene)
PVP	Poly(vinylene pyrrolidone)
Pyr14	N-methyl-N-butyl pyrrolidinium
SEI	Solid Electrolyte Interface
SPE	Solid Polymer Electrolyte
TEM	Transmission Electron Microscopy
Tg	Glass Transition Temperature
TGA	Thermogravimetric analysis
TTCA	Tritiocyanuric acid
UV	Ultra-violet
VBC	1,4-Vinylbenzyl chloride
VBMImC	Vinylbenzyl methylimidazolium chloride
VBMImTFSI	Vinylbenzyl methylimidazolium bis(trifluoromethane sulfonyl) imide

Acknowledgments

I will not fall into the cliché of saying that acknowledgments "are the hardest part of the thesis." Not much less. It is true that throughout these 4-5 years I have been lucky to witness and to be part of the coming and going of many people, and I have to do a bit of memory. This exercise has helped me to remember so many people and good moments lived throughout this stage that in brief I will close, and open another equally exciting. I am of the firm belief that the human being is forged and molded constantly by the people around with an exchange of experiences, problems, successes and failures, victories and defeats. Therefore, I will try to mention and thank all the people who have accompanied me throughout these last years and with whom I have shared so many things.

My first thought is for my supervisor Professor David Mecerreyes. Without him this would not be possible as he (luckily for me) convinced me to do the master thesis and gave me the opportunity of doing this PhD within his group. I consider him as a model leader of a very multidisciplinary and multicultural group of people and I really admire his impressive ability of see beyond of what people shows to him. I really wish that at least something of this have stuck on me.

The following people that comes into my mind is the Innovative Polymers Group. I would like to write many many things that I have shared with every single friend I have made within this group, but it would take me days and pages, so I will try to summarize. Starting from Guiomar (who taught me how to use a Schlenk line for the first time), Nerea (from Bachelor´s degree, through PhD and we will see what the future brings), Mehmet (widest and deepest knowledge of synthetic chemistry I´ve ever known), Ana Margarida (always with a bright smile in her face, good luck!!), Ana Pascual (a model of tenacity and perseverance spiced with good humor and a pinch of madness) and Giulia (you have been always part of the group for me!!) who made my landing into research smooth. Also, the people who started the PhD with me, Alex (you are becoming European!!) and Isabel (a sweet shell with a spicy core!!). Without

forgeting Sufi (always willing to share a beer talking either about chemistry or life, or both together) and Leire (from synthesis to euskal dantza!). In the office of the faculty… Andere (Japanese surfing lady!!), Amaury (good wine lover!), Naroa (arriba Navarra!), Elena (you will be always the youngest of the lab), Coralie (wish you all the best!) and Irma (estás muy cerquita!). Can´t forget the couple of Asier (from south) and Antonio (from even more south). And the last message for the last batch of young students with Sara, Fermín, Ester Udabe, Alvaro, Marine, Jorge and the new Master students; keep the good mood, the friendship, the brotherhood of this amazing research group.

However, this group could not work without researchers, post-docs, visitors and collaborators that I have to mention. Firstly I have to mention Dr (or prof?) Haritz Sardon, who recently have started his most important project and I wish him the best. Prof. Maria Forsyth, from whom I learned a lot of electrochemistry just only by listening in the group meetings. Dr. Ester Verde, master of organic chemistry and organization of the lab. Dr. Luca Porcarelli, that I have been witness of his rise and promises a bright future. Prof. Sonia Zulfiqar, always a pleasure to talk with her in the office of the faculty. Prof. Vijayakrisna Kari with whom I had the privilege to work with during the master. Dr. Alexander Shaplov, from whom always something could be learned. Dr. Ana Sanchez Sanchez, I wish you the best in Cambridge!! And many others like Prof. Laurent Rubatat, Dr. Maitane Salsamendi, Dr. Klemen Pirnat, Dr. Jeremy Demarteau and Dr. Nicolas Zivic that deserve to be remembered. Also PhD students that spent some time in San Sebastian and we had the luck to meet at least a short period of time. Like Dr. Manoj Kumar (always with a smile in his face and a column in his hands), Antonella Gallastegi (Awesome farewell party!!), Miguel Angel (Iodine… Iodine everywhere), Marta Ribeiro, David Patinha and many others that scape from my memory.

Special mention to a person with whom I have share so many good and bad moments, laughter, beers, problems, discussions, brainstormings and so on. Daniele Mantione sei diventato un fratello. La mia porta sarà sempre aperta e la mia casa avrà sempre un letto così potrai tornare al nostro amato Euskadi.

8

Broadening the scope, our group is part of an ever-growing polymer institute, POLYMAT. I feel privileged for have spent so many years in this institute and really thank the possibility of have assisted and have been part of several Polymat seminars and share discussions with the principal researchers like Prof. Jose M. Asua, Prof. Joserra Leiza, Prof. Mariaje Barandiaran, Prof. Maria Paulis, and other Polymat Researchers. Also the section of the faculty with Prof. Lourdes Irusta and Dr Alba Gonzalez, always willing to help with any difficult characterization. The students from the 3rd floor!! Stefano, Jessica, Sevilay, Verónica, Adrián, Sil, Alex (Simula! Et Oui!!), Ali, Aitor, Iñaki, Nerea and many many others that I can´t remember and to whom I wish the best. The students from the faculty like Oihane and June. Also special mention to my friend since many years Bea (por todos los cafés y los desayunos que nos hemos pegado contando penas y arreglando el mundo!!). Students from the other sections of Polymat, I remember you! Valentina, Cristian, Silvia and Silvia and Juanpe and many others, a huge hug to all of you! Special mention to Inés Plaza, without her unpayable work Polymat would crumble.

Moving towards South East of Donosti, we place in Cidetec, where I belong since last April, mainly thanks to my co-supervisor (and now my JP) Dr. Alberto Blazquez. It has been a privilege to have been your PhD student, and going to Cidetec to leave my materials and bringing new ideas, always with a smile in the face and always finding time in your tight schedule. Special mention to Olatz Leonet, who is the real person in charge of making the LiS group work. Also Amane Lago, who taught me for the first time how to prepare a slurry and coin cells (although it was a Li-ion cell, ☺). And the current group of LiS were I belong, Eneko, Jasmina, Julen and former Manu. Por aguantar mi mal humor durante los difíciles meses de escritura de la tesis.

I really thing that a PhD student should do an internship far from home, as is an experience that change people, usually for good. By crossing the Atlantic Ocean, I would like to thank Professon Jeffrey Pyun for hosting me 6 months in his lab in Tucson, Arizona. It has been a real pleasure and an honor to have met you, and I will never forget what I learned under your guidance. The Pyun

9

group, with special mention to Metin Karayilan who took care of me during these months sharing lunches, beers, money and a lot of time with me. I keep all the moments lived as a treasure (fossil creek!!). Also the rest of the group, that made me feel like home in the middle of the Sonoran desert. Dr. Nick Pavlopoulos (for opening to me the doors of yout home in my first American night!), Frida Zhang, Tristan Kleine, Kyle Carothers, Michael Manchester, Katrina Konopka, Laura Anderson and Junhyuk Lee. Thank you from the deep of my heart for the time we spent together!! Miriam Rodriguez, con infinito buen humor canario, esos cafés me salvaron la vida!! Carmen a quien envío un abrazo muy fuerte, mucho ánimo con tu tesis y suerte en tu futuro (cuando vayas a Gijón pásate por Donosti!). Miriam Diaz, una Zarauztarra en Tucson con quien era un placer y una alegría pasar el rato tomando café o un brunch en su casa de los años 70. And the Tucson Magpies, who show me that there is a universal common language called rugby.

Solo me queda agradecer a mi cuadrilla, que aun llevando meses sin aparecer, cuando vuelves es como si no pasase el tiempo. A mi equipo de rugby del Atlético San Sebastián, que aun sin saberlo me han ayudado mucho (todo se ve diferente después de un entrenamiento). Y sobre todo a mi familia, mis hermanos (Iosu, Esther y Mikel), que sé que están orgullosos de mí, aunque no me lo digan muy a menudo. A Rafa, Kristina y Jon que nos han ayudado de muchas y diferentes maneras en los últimos años. Y a mis aitas, en quienes tengo mi modelo de vida y persona, y que estaré muy orgulloso si algún día soy la mitad de íntegros que ellos.

Eta ez pentsa zutaz ahaztu naizela. Baina ez det uste ez dakizun zeoze idatzi dezakeela. Maite zaitut Potxoli.

Resumen de la tesis

Este trabajo de investigación se ha realizado en una colaboración entre el BERC Polymat (Universidad del País Vasco, Centro Joxe Mari Korta - Avda. Tolosa, 72, 20018, Donostia-San Sebastian) y Cidetec Energy Storage (Parque Científico y Tecnológico de Gipuzkoa Pº Miramón, 196, 20014 Donostia - San Sebastián). Durante la tesis se ha hecho una estancia de 6 meses en el laboratorio del Profesor Jeffrey Pyun en la Universidad de Arizona (Chemistry and Biochemistry, 1306 E. University Blvd., Room 221, 85721, Tucson, Arizona).

Introducción:

La producción de energía a partir de fuentes renovables está en la agenda de instituciones, gobiernos y organizaciones a nivel mundial para mitigar los problemas asociados al uso combustibles fósiles manteniendo el estilo de vida actual. Unas de las limitaciones de estas tecnologías es el hecho de que son intermitentes y en algunos casos poco accesibles, por lo que para su competitividad económica contra la producción de energía actualmente implantada los sistemas de almacenamiento de energía (SAE) son cruciales. Las baterías de litio ion están entre los SAE predominantes en el mercado y abarcan una amplia variedad de aplicaciones. Sin embargo, este tipo de baterías está alcanzando su techo debido a la creciente demanda de SAE con mayor densidad de energía y menor coste. De entre las baterías de nueva generación las baterías de litio-azufre son una de las más prometedoras y las más avanzadas en su desarrollo hacia su comercialización gracias en gran medida a las propiedades intrínsecas del azufre como material activo, esto es, altas capacidad específica (1672 mAh g_S^{-1}) y alta densidad de energía (aprox. 2500 Wh Kg^{-1} vs Li/Li$^+$), bajo coste y respetuoso con el medio ambiente.

Sin embargo, esta tecnología sufre de varios problemas críticos que limitan sus prestaciones finales y están directamente asociados al uso del azufre elemental como material activo. Por un lado, el azufre es un aislante eléctrico e iónico,

11

con lo que se necesita una gran cantidad de aditivo conductor (como carbones, polímeros y cargas inorgánicas) que dificultan el procesado de los electrodos y disminuyen la densidad de energía final. Por otro lado, debido al mecanismo redox de la batería, se forman polisulfuros de litio (Li_2S_x, 8≤x≤4) que son muy solubles en los disolventes orgánicos del electrolito. Esta solubilidad causa lo que se denomina "polysulfide shuttle", que se trata de la migración de estos intermedios hacia el ánodo causando reacciones secundarias que disminuyen la eficiencia de la batería, así como la corrosión del cátodo por pérdida de material activo y pasivación de la superficie del ánodo por la formación de una capa electroquímica sólida (SEI) insoluble, irreversible y aislante formada por Li_2S y Li_2S_2. Por último, los cambios de volumen que ocurren en el cátodo durante el ciclado de la batería causan un estrés mecánico en el cátodo que terminan por destruir la estructura, dando lugar a un fallo drástico de la batería. Adicionalmente, están los problemas asociados al uso de litio metal como material activo. Por un lado, la no homogénea disolución/deposición durante los procesos de ciclado causa formaciones dendríticas que crecen a lo largo del electrolito y atravesando el separador pueden llegar a un contacto físico con el cátodo causando un cortocircuito.

A lo largo de los últimos años, gracias a numerosos esfuerzos que se han destinado a la mejora de los diferentes componentes de la batería, como el encapsulado del azufre con materiales avanzados, diseño de electrolitos para disminuir el efecto "shuttle", así como separadores específicos para bloquear los polisulfuros solubles, o configuraciones avanzadas de celda, se han conseguido importantes avances en esta tecnología. En este aspecto los materiales poliméricos han tenido un papel muy significativo. Como por ejemplo, recubrimientos poliméricos como protección de la superficie del ánodo, con el fin de progeterlo del contacto con el electrolito y minimizar las reacciones parasíticas debidas a su alta reactividad. La capacidad de tunear fácilmente las propiedades químicas de estos materiales ha dado lugar a separadores funcionales que consiguen evitar la migración de los polisulfuros por medio de diferentes mecanismos. Otro aspecto en los que han cobrado

gran importancia ha sido aplicación de polímeros conductores iónicos como electrolito sólido con el fin de bloquear los polisulfuros y mejorar la seguridad de las baterías. Gracias a la capacidad de tunear su microestructura, los polímeros han sido aplicados en el cátodo como recubrimientos avanzados de las partículas de azufre, como de las partículas de composite como del cátodo completo con el fin de mejorar la utilización del azufre así como restringir las reacciones electroquímicas del azufre al cátodo, evitando la migración de los polisulfuros. Para mejorar la estabilidad mecánica del cátodo a lo largo de los procesos de ciclado de las baterías de litio azufre, se han diseñado materiales funcionales específicos como binders de cátodos de azufre. Por último, con el fin de evitar la solubilidad de los polisulfuros en el electrolito por medio de enlazar covalentemente el azufre a materiales poliméricos.

En este contexto, en 2013 Pyun y colaboradores presentaron una nueva ruta de síntesis bautizada como vulcanización inversa para sintetizar polímeros de alto contenido en azufre. Inversamente a la vulcanización normal, donde pequeñas cantidades de azufre hacen de puentes covalentes entre polidienos, en la vulcanización inversa el azufre polimérico es estabilizado por una pequeña cantidad de un dieno, en este caso el 1,3-diisopropil benceno (DIB). De esta manera se pueden conseguir materiales poliméricos con cantidades de azufre de hasta 90% en peso. Esta nueva familia de polímeros presenta propiedades muy interesantes (como alto índice de refracción y capacidad de atrapar metales pesados como mercurio), pero el área donde más se han desarrollado ha sido como material catódico en baterías de litio azufre. Estos materiales resultaron tener una capacidad específica similar a la del azufre elemental, pero con mejor retención de la capacidad durante el ciclado así como una eficiencia coulómbica superior. El éxito de estos materiales atrajo el interés de investigadores de todo el mundo, y desde entonces han aparecido muchas publicaciones con materiales poliméricos sintetizados mediante la vulcanización inversa del azufre para su uso como materiales catódicos en baterías de litio azufre.

Este trabajo supuso un punto de partida de la presente tesis doctoral y enmarcado en el proyecto europeo IPES (Innovative Polymers for Energy Storage), este trabajo ha tenido como objetivo desarrollar nuevas generaciones de polímeros de alto contenido en azufre como materiales catódicos para baterías de litio con el objetivo de mejorar resultados anteriores. A continuación, se resumirán los capítulos presentados en esta tesis.

Capítulo 1: "Inverse vulcanization of sulfur with divinyl benzene: Stable and easy processable cathode materials for lithium sulfur batteries".

El divinil benceno (DVB) es una molécula orgánica muy utilizada en química macromolecular como entrecruzante de polímeros lineales (como poliestireno). Presenta una estructura molecular similar a la del monómero original de la vulcanización inversa, con el añadido de tener un peso molecular menor, lo que puede traducirse en una mayor cantidad de azufre con una composición similar. La síntesis de los copolímeros poli(azufre-DVB) resultó ser más rápida que con el DIB, debido a la mayor reactividad del DVB. Tanto era así que con fracciones en peso superiores al 20% iniciales de monómero orgánico, la reacción se descontrolaba y los tiempos y temperatura tenían que ser ajustados. Después de la optimización de la reacción de síntesis, se obtuvieron una serie de copolímeros poli(azufre-DVB) variando las cantidades iniciales. Estos polímeros fueron caracterizados por técnicas espectroscópicas como el RMN y FTIR así como técnicas calorimétricas como el DSC y la TGA. Los resultados de las caracterizaciones mostraron materiales totalmente amorfos y estructura similar a copolímeros de azufre previamente reportados. Estos polímeros fueron molidos en polvos muy finos y procesados hasta obtener electrodos para su caracterización y testeo en pila botón frente a litio. Los resultados mostraron unas propiedades electroquímicas muy similares a la del azufre elemental. Sin embargo, estos materiales mostraron una alta capacidad específica incluso a su ciclado a altas densidades de corriente y una ciclabilidad muy estable manteniendo un 78% de la capacidad inicial en el ciclo 500. Estos copolímeros resultan muy atractivos gracias a su bajo coste, su

14

síntesis rápida y fácil, su estabilidad química y sus propiedades electroquímicas.

Capítulo 2: "Inverse Vulcanization of Sulfur using Natural Dienes as Sustainable Materials for Lithium–Sulfur Batteries".

Los materiales sintetizados vía vulcanización inversa reportados hasta el momento se basaban en la utilización de monómeros aromáticos tanto sintéticos como provenientes de refinamientos del petróleo. En este capítulo se explora la vulcanización inversa del azufre con monómeros de origen natural o de desechos industriales. Uno de los requisitos para la copolimerización del azufre es la miscibilidad de los monómeros con el azufre fundido. Para ello los monómeros deben ser relativamente planos y apolares. En este capítulo se presenta la vulcanización inversa del azufre con el dialil sulfuro (DAS, responsable del olor característico del ajo), del mirceno (Myr, 7-Metil-3-metilen-1,6-octadieno, parte de los aceites aromáticos de plantas como el tomillo) y del diciclopentadieno (DCPD, proveniente de desechos industriales del cracking del naphta para la obtención de etileno). La síntesis de estos materiales se llevó a cabo después de la fusión del azufre a 170 ºC y la subsecuente adición del monómero correspondiente. En todos los casos la reacción tuvo un tiempo de homogeneización y después una rápida auto aceleración, en la que se observaba una rápida degradación y evolución de gas. Por tanto, las reacciones de síntesis se paraban mediante la inmersión del medio de reacción en nitrógeno líquido, y seguidamente, con el fin de promover la reacción de todos los grupos funcionales, se les sometía a un curado a 120 ºC durante varias horas. Los materiales finales se caracterizaron por RMN y FTIR mostrando que las señales relacionadas con los grupos reactivos desaparecían. Las propiedades térmicas fueron estudiadas por DSC y TGA. Los copolímeros poli(azufre-DAS) y poli(azufre-Myr) mostraban comportamientos similares con un aumento gradual de la Tg y el residuo de la TGA con el aumento de monómero orgánico añadido. Sin embargo, el poli(azufre-DCPD) mostraba un comportamiento diferente, en que se veía un aumento de la Tg hasta un máximo en la composición de 30:70 (DCPD:azufre),

15

donde la temperatura de transición vítrea volvía a bajar gradualmente. Un comportamiento similar se podía observar en la TGA, con una estabilidad térmica máxima en la coposición 30:70. Después de caracterizar estos materiales, se procedió a su testeo en baterías de litio azufre como materiales catódicos. De nuevo, se pudo observar que la electroquímica era muy similar a la del azufre, con unas prestaciones superiores en términos de retención de la capacidad, con unos valores superiores al 80% de la capacidad inicial en el ciclo 200. Por lo tanto, se puede concluir que la vulcanización inversa del azufre se puede realizar con monómeros baratos y sostenibles manteniendo las prestaciones finales en su aplicación como materiales catódicos en baterías de litio azufre.

Capítulo 3: Hybrid Sulfur Selenium Co-polymers as Cathodic Materials for Lithium Batteries

Hasta ahora, este trabajo de tesis se había dedicado a la modificación del azufre con diferentes moléculas orgánicas. En este apartado, se modificó la parte calcógena de copolímero de azufre. Recientemente se reportó el uso del selenio como alternativa de material activo en baterías de litio metal. Se observó que el selenio presenta un mecanismo redox similar al del azufre con el añadido de una conductividad eléctrica de cerca de 30 órdenes de magnitud superior y una estabilidad durante el ciclado excelente. Sin embargo, el selenio es un material escaso y de una densidad mayor, lo que aumenta su precio y reduce su capacidad específica teórica. Recientemente, se estudió el sistema azufre-selenio como opción para buscar una sinergia de propiedades con resultados muy prometedores. Sin embargo, la preparación de las mezclas de azufre-selenio requiere de altas temperaturas y tiempos largos de síntesis. En este trabajo se presenta la hibridación del polímero de azufre sintetizado via vulcanización inversa mediante la adición de selenio elemental al medio de reacción. Para ello se someten mezclas físicas de azufre y selenio a la vulcanización inversa. Se prepararon una serie de copolímeros híbridos variando los ratios molares de azufre:selenio (basados en publicaciones anteriores). Por RMN se confirmó el éxito de la copolimerización del azufre con

16

el DIB y por DSC se estudió la variación de Tg del polímero de azufre con la adición del selenio. Para estudiar el sistema azufre:selenio se utilizó el RMN de [77]Se y la espectroscopía Raman. En ninguna de las dos técnicas su pudo detectar selenio elemental residual, y los resultados de ambas coincidieron en mezclas moleculares de azufre selenio. Después de la exitosa síntesis y detallada caracterización de los polímeros poli(selenio-azufre-DIB), se procedió a su caracterización electroquímica. La voltametría cíclica mostró las señales relativas a la reducción de la mezcla azufre-selenio, confirmando de nuevo la exitosa hibridación del polímero. Las prestaciones electroquímicas mostraron una mejoría de la capacidad con la densidad de corriente de los polímeros hibridados con selenio así como la característica propia de los polímeros de azufre de la alta retención de la capacidad con el ciclado. De esta manera, se confirma la sinergia de propiedades entre el sistema de azufre-selenio y la copolimerizción del azufre por vulcanización inversa con un método de síntesis fácil, rápido y escalable.

Capítulo 4: Poly(anthraquinonyl sulfides): High Capacity Redox Polymers for Energy Storage

Una de las limitaciones de la vulcanización inversa es la limitada opción de monómeros disponibles para la copolimerización del azufre, ya que se necesitan moléculas planas y relativamente apolares. Sin embargo, la mayoría de moléculas con algún tipo de funcionalidad interesante no cumple estos requisitos, ya que no suelen ser planas y mucho menos apolares. Por lo tanto, en este capítulo se busca una alternativa a la vulcanización inversa para la síntesis de polímeros de alto contenido en azufre. El poli(sulfuro de antraquinona) es un polímero redox que ha demostrado tener unas propiedades y prestaciones electroquímicas muy interesantes, con una estabilidad en el ciclado excelente. De hecho, este polímero se ha usado como material catódico en pruebas de concepto en sistemas de baterías emergentes como baterías de magnesio. Sin embargo, este material presenta una baja densidad, lo que se traduce en una capacidad específica teórica menor. Teniendo en cuenta que la síntesis involucra la policondensación de la 1,8-

dicloroantraquinona con sulfuro de sodio a altas temperaturas y aprovechando la capacidad del azufre en formar polisulfuros de sodio en solución, se han sintetizado una serie de poli(polisulfuros de antraquinona) variando la cantidad de azufre en la unidad repetitiva. La síntesis de estos materiales pasa primeramente por la obtención de los polisulfuros de sodio disolviendo azufre y sulfuro de sodio en NMP a altas temperaturas y segundo la adición de la 1,8-dicloroantraquinona al medio de reacción. Después de varias horas de reacción, se recoge un precipitado que cambia de color con la cantidad de azufre en la unidad repetitiva. Estos materiales se han estudiado por RMN en estado sólido, FTIR y espectroscopía raman. Entre las tres técnicas se confirma la reacción de la molécula orgánica inicial, así como la existencia de cadenas largas de azufre. Por TGA y análisis elemental, se confirma que los valores de azufre y parte orgánica se acercan a los valores calculados. Por tanto, después de la caracterización fisicoquímica, se realizó la caracterización electroquímica. En la voltametría cíclica se pueden observar las señales características de los procesos de reducción y oxidación tanto de la antraquinona como de los segmentos de azufre. En términos de prestaciones, el nuevo copolímero de azufre-antraquinona mostró una sinergia de propiedades, en las que se observó una alta capacidad inicial debido a la presencia de alto contenido en azufre y una alta estabilidad con el ciclado relativo a la antraquinona. De esta manera, se demuestra que la síntesis de polímeros de azufre se pueden extender más allá de la vulcanización inversa y dar mayores funcionalidades y diferentes características a esta familia de polímeros.

Capítulo 5: Sulfur polymers meet poly(ionic liquid)s: bringing new properties to both polymer families

Este capítulo se realizó en colaboración con el laboratorio del profesor Jeffrey Pyun, en la Universidad de Arizona. Uno de los mayores inconvenientes de los polímeros de azufre es relativo a la solubilidad de materiales con alto contenido en azufre. Recientemente, la copolimerización del azufre con estireno a bajas temperaturas fue reportada, dando materiales solubles en disolventes

orgánicos. Este ejemplo abre una puerta a monómeros con puntos de ebullición por debajo de la autopolimerización del azufre, así como el uso de monómeros estirénicos funcionales. En este caso se ha estudiado la copolimerización del azufre con 4-cloruro de vinilbenzeno (VBC) y su modificación post-polimerización con N-metilimidazol para obtener el primer líquido iónico polimérico en base a azufre reportado hasta ahora. La cinética de la copolimerización del azufre con VBC se estudió por RMN, dando tiempos de reacción que varían desde 3 a 8 horas dependiendo de ratio azufre:VBC. Después de la purificación del polímero resultante se procedió a la modificación post-polimerización en cloroformo. El material final resultó ser soluble en disolventes orgánicos polares e, interesantemente, en agua. La reacción se estudió por RMN confirmando la exitosa modificación y síntesis del poli(azufre-cloruro de 4-vinilbenzil imidazolio). Una de las características más distintivas de los líquidos iónicos poliméricos es su capacidad de ajustar la solubilidad mediante el intercambio del contraión. En este caso, se añadió LiTFSI a una disolución en agua del poli(líquido iónico) dando como resultado un precipitado amarillo-naranja, que resultó ser soluble en disolventes orgánicos poco polares, como en cloroformo o THF. La modificación se estudió por FTIR, revelando las señales distintivas al ion TFSI. Estos últimos materiales mostraron características típicas de los líquidos iónicos poliméricos como la conductividad iónica así como propiedades de los polímeros de azufre, como la activdad redox. Después se caracterizaron las propiedades térmicas de los materiales por DSC y TGA, dando tendencias similares independientemente del ratio azufre:VBC inicial. Finalmente se probaron posibles aplicaciones. Por un lado los polímeros solubles en agua como estabilizantes de nanopartículas de azufre en suspensión, dando como resultado suspensiones de azufre estables, con partículas con tamaños por debajo de los 200 nm. Por otro lado, los polímeros iónicos con contraionoes de TFSI se probaron en baterías de litio azufre tanto como aditivos en el electrolito como cobinders en el cátodo, con resultados insatisfactorios. De esta manera se reportan los primeros líquidos iónicos poliméricos en base a azufre con propiedades sinérgicas de

conductividad y solubilidad ajustable de los líquidos iónicos poliméricos con la actividad redox de los polímeros de azufre.

Summary of the PhD thesis

This research Project has been developed framed in a collaboration between BERC Polymat (Universidad del País Vasco, Centro Joxe Mari Korta - Avda. Tolosa, 72, 20018, Donostia-San Sebastian) and Cidetec Energy Storage (Parque Científico y Tecnológico de Gipuzkoa Pº Miramón, 196, 20014 Donostia - San Sebastián). During this PhD thesis, an internship was carried out in the University of Arizona (Chemistry and Biochemistry, 1306 E. University Blvd., Room 221, 85721, Tucson, Arizona)under the supervision of Professor Jeffrey Pyun.

Introduction:

The production of energy from renewable sources is on the agenda of institutions, governments and organizations worldwide to mitigate the problems associated with the use of fossil fuels while maintaining the current lifestyle. One of the limitations of these technologies is the fact that they are intermittent and in some cases not very accessible, therefore for their economic competitiveness against currently implemented energy production systems, energy storage systems (ESS) are crucial. Lithium ion batteries are among the predominant ESSs on the market and cover a wide variety of applications. However, this type of batteries is reaching its ceiling due to the growing demand for ESS with higher energy density and lower cost. Among the new generation batteries lithium-sulfur batteries are one of the most promising and the most advanced in their development towards commercialization thanks in large part to the intrinsic properties of sulfur as an active material, that is, high specific capacity (1672 mAh gS-1) and high energy density (approx 2500 Wh Kg-1 vs Li/Li+), low cost and environmentally friendliness.

Nevertheless, this technology suffers from several critical problems that limit its final performance and are directly associated with the use of elemental sulfur as active material. On the one hand, sulfur is an electrical and ionic insulator, which requires a large amount of conductive additive (such as carbons, polymers and inorganic fillers) that hinder the processing of the electrodes and

21

reduce the final energy density. On the other hand, due to the redox mechanism of the battery, lithium polysulfides (Li_2S_x, $8 \leq x \leq 4$) are formed which are very soluble in the organic solvents of the electrolyte. This solubility causes the so-called "polysulfide shuttle", which involves the migration of these intermediates towards the anode causing parasitic secondary reactions that decrease the efficiency of the battery, as well as corrosion of the cathode due to loss of active material and passivation of the surface of the anode by the formation of an insoluble, irreversible and insoluble solid electrochemical layer (SEI) formed by Li_2S and Li_2S_2. Finally, volume changes that occur at the cathode during battery cycling cause mechanical stress on the cathode that ultimately destroy the structure, leading to drastic battery failure. Additionally, there are the problems associated with the use of lithium metal as an active material. On the one hand, the inhomogeneous plating/stripping during cycling processes causes dendritic formations that grow along the electrolyte and through the separator can reach a physical contact with the cathode causing a short circuit.

Over the last few years, thanks to numerous efforts that have been devoted to the improvement of the different components of the battery, such as the encapsulation of sulfur with advanced materials, design of electrolytes to reduce the "shuttle" effect, as well as specific separators in order to block the migration of polysulfides, or advanced cell configurations, have promoted important advances in this technology. In this aspect the polymeric materials have played a very significant role. For instance, as polymer coatings for the anode surface, in order to protect it from contact with the electrolyte and minimize parasitic reactions due to its high reactivity. The ability to easily tune the chemical properties of these materials has given rise to functional separators that manage to avoid the migration of polysulfides by means of different mechanisms. Another aspect in which they have gained great importance has been the application of ionic conductor polymers as a solid electrolyte in order to block the polysulfides and improve the safety of the batteries. Thanks to the ability to tune its microstructure, the polymers have been applied at the cathode as advanced coatings of the sulfur particles, as well as the composite particles

and the complete cathode in order to improve the use of sulfur as well as to restrict the reactions electrochemical from sulfur to cathode, avoiding the migration of polysulfides. To improve the mechanical stability of the cathode during the lithium sulfur battery cycling processes, specific functional materials have been designed as binders of sulfur cathodes. Finally, in order to avoid the solubility of the polysulfides in the electrolyte by means of covalently binding the sulfur to polymeric materials.

In this context, in 2013 Pyun and coworkers presented a new synthetic route named inverse vulcanization to synthesize high sulfur content polymers. In contrast to normal vulcanization, where small amounts of sulfur act as covalent bridges between polydienes, in reverse vulcanization the polymeric sulfur is stabilized by a small amount of a diene, in this case 1,3-diisopropylbenzene (DIB). In this way polymeric materials with amounts of sulfur of up to 90% by weight can be obtained. This new family of polymers has very interesting properties (such as high refractive index and ability to trap heavy metals such as mercury), but the field where they have attracted more attention has been as cathode material in lithium sulfur batteries. These materials were found to have a specific capacity similar to that of elemental sulfur, but with superior capacity retention during cycling as well as enhanced coulombic efficiency. The success of these materials attracted the interest of researchers from all over the world, and many publications have appeared with polymeric materials synthesized by the reverse vulcanization of sulfur for use as cathode materials in lithium sulfur batteries.

This work was a starting point of the present doctoral thesis and framed in the European project IPES (Innovative Polymers for Energy Storage), this work has aimed to develop new generations of high sulfur polymers as cathode materials for lithium batteries with the aim of improving previous results. Next, the chapters presented in this thesis will be summarized.

23

Chapter 1: "Inverse vulcanization of sulfur with divinyl benzene: Stable and easy processable cathode materials for lithium sulfur batteries".

The divinyl benzene (DVB) is an organic molecule widely used in macromolecular chemistry as a crosslinker of linear polymers (such as polystyrene). It has a molecular structure similar to that of the original monomer of reverse vulcanization, with the addition of having a lower molecular weight, which can result in a greater amount of sulfur with a similar composition. The synthesis of the poly (sulfur-DVB) copolymers was found to be faster than with the DIB, due to the higher reactivity of the DVB; in fact with fractions by weight greater than the initial 20% organic monomer, the reaction became uncontrolled and the times and temperature had to be adjusted. After optimization of the synthesis reaction, a series of poly (sulfur-DVB) copolymers were obtained by varying the initial amounts. These polymers were characterized by spectroscopic techniques such as NMR and FTIR as well as calorimetric techniques such as DSC and TGA. The results of the characterizations showed totally amorphous materials and structure similar to previously reported sulfur copolymers. These polymers were ground into very fine powders and processed until the obtention of electrodes for their characterization and testing in a button cell versus lithium. The results showed some electrochemical properties very similar to that of elemental sulfur. However, these materials showed a high specific capacity even when cycled at high current densities and a very stable cyclability maintaining 78% of the initial capacity in cycle 500. These copolymers are very attractive thanks to their low cost, their synthesis quick and easy, its chemical stability and its electrochemical properties.

Chapter 2: "Inverse Vulcanization of Sulfur using Natural Dienes as Sustainable Materials for Lithium–Sulfur Batteries".

The materials synthesized via inverse vulcanization reported so far were based on the use of aromatic monomers both synthetic and from refinements of petroleum. This chapter explores the inverse vulcanization of sulfur with natural sourced monomers of or industrial waste. One of the requirements for the copolymerization of sulfur is the miscibility of the monomers with the molten

24

sulfur. For this the monomers must be relatively flat and apolar. This chapter presents the inverse vulcanization of sulfur with diallyl sulfide (DAS, responsible for the characteristic smell of garlic), myrcene (Myr, 7-Methyl-3-methylene-1,6-octadiene, part of the aromatic oils of plants such as thyme) and dicyclopentadiene (DCPD, from industrial waste from the cracking of naphta to obtain ethylene). The synthesis of these materials was carried out after the melting of the sulfur at 170 ° C and the subsequent addition of the corresponding monomer. In all cases, the reaction had a homogenization time and then a rapid self-acceleration, in which a rapid degradation and evolution of gas was observed. Therefore, the synthesis reactions were quenched by immersing the reaction medium in liquid nitrogen, and then, in order to promote the reaction of all the functional groups, they were subjected to a cure at 120 ° C for several hours. The final materials were characterized by NMR and FTIR showing that the signals related to the reactive groups disappeared. The thermal properties were studied by DSC and TGA. Poly (sulfur-DAS) and poly (sulfur-Myr) copolymers exhibited similar behaviors with a gradual increase in Tg and the residue of TGA with the increase in added organic monomer. However, the poly (sulfur-DCPD) showed a different behavior, in which an increase in Tg was seen to a maximum in the composition of 30:70 (DCPD: sulfur), where the glass transition temperature gradually decreased again . A similar behavior could be observed in the TGA, with a maximum thermal stability in the 30:70 coposition. After characterizing these materials, they were tested in lithium sulfur batteries as cathode materials. Again, it was observed that electrochemistry was very similar to sulfur, with superior performance in terms of capacity retention, with values higher than 80% of the initial capacity in cycle 200. Therefore, it can be concluded that the inverse vulcanization of sulfur can be carried out with cheap and sustainable monomers maintaining the final benefits in its application as cathode materials in lithium sulfur batteries.

Chapter 3: Hybrid Sulfur Selenium Co-polymers as Cathodic Materials for Lithium Batteries

25

Recently the use of selenium was reported as an alternative of active material in lithium metal batteries. It was observed that selenium has a redox mechanism similar to that of sulfur with the addition of an electrical conductivity of about 30 orders of magnitude and higher stability during cycling. However, selenium is a scarce material with a higher molecular weight, which increases its price and reduces its theoretical specific capacity. Recently, the sulfur-selenium system was studied as an option to look for a synergy of properties with very promising results. However, the preparation of the sulfur-selenium mixtures requires high temperatures and long synthesis times. In this work, the hybridization of the sulfur polymer synthesized by inverse vulcanization is presented by the addition of elemental selenium to the reaction medium. For this purpose, physical mixtures of sulfur and selenium are subjected to inverse vulcanization. A series of hybrid copolymers were prepared by varying the molar ratios of sulfur: selenium (based on previous publications). The success of the copolymerization of the sulfur with the DIB was confirmed by NMR and by DSC the variation of Tg of the sulfur polymer with the addition of selenium was studied. To study the sulfur: selenium system, 77Se NMR and Raman spectroscopy were used. In none of the two techniques residual elemental selenium was detected, and the results of both coincided in molecular mixtures of sulfur selenium. After the successful synthesis and detailed characterization of the poly(selenium-sulfur-DIB) polymers, they were electrochemically characterized. The cyclic voltammetry showed the signals relative to the reduction of the sulfur-selenium mixture, further confirming the successful hybridization of the polymer. The electrochemical performance showed an improvement in capacity with the current density of the selenium-annealed polymers as well as the characteristic of the sulfur polymers of the high capacity retention with cycling. In this way, the synergy of properties between the sulfur-selenium system and the copolymerization of sulfur by inverse vulcanization with an easy, fast and scalable synthesis method is confirmed.

Capítulo 4: Poly(anthraquinonyl sulfides): High Capacity Redox Polymers for Energy Storage

26

One of the limitations of the inverse vulcanization technique is the limited choice of monomers available for the copolymerization of sulfur, since flat and relatively apolar molecules are needed. However, most molecules with some interesting functionality do not meet these requirements, since they are not usually flat and much less apolar. Therefore, in this chapter an alternative to reverse vulcanization is sought for the synthesis of high sulfur polymers. Poly(anthraquinone sulfide) is a redox polymer that has been shown to have very interesting electrochemical properties and performance, with excellent cycling stability. In fact, this polymer has been used as cathode material in emerging battery systems such as magnesium batteries. However, this material has a low density, which translates into a lower theoretical specific capacity. Taking into account that the synthesis involves the polycondensation of 1,8-dichloroanthraquinone with sodium sulfide at high temperatures and taking advantage of the capacity of sulfur to form sodium polysulfides in solution, a series of poly(anthraquinone polysulfides) has been synthesized varying the amount of sulfur in the repetitive unit. The synthesis of these materials goes through first by obtaining the sodium polysulfides dissolving sulfur and sodium sulfide in NMP at high temperatures and secondly the addition of 1,8-dichloroanthraquinone to the reaction medium. After several hours of reaction, a precipitate is collected which a color change with the amount of sulfur in the repetitive unit. These materials have been studied by solid state NMR, FTIR and raman spectroscopy. Among the three techniques, the reaction of the initial organic molecule is confirmed, as well as the existence of sulfur long chains. By TGA and elemental analysis, it is confirmed that the values of sulfur and organic part are close to the calculated values. Therefore, after the physico-chemical characterization, the electrochemical characterization was carried out. In cyclic voltammetry, the characteristic signals of the reduction and oxidation processes of anthraquinone and sulfur segments can be observed. In terms of performance, the new sulfur-anthraquinone copolymer showed a synergy of properties, in which a high initial capacity was observed due to the presence of high sulfur content and a high stability with cycling relative to anthraquinone. In this way, it is demonstrated that the synthesis of sulfur polymers can extend

27

beyond the inverse vulcanization and give greater functionalities and different characteristics to this family of polymers.

Capítulo 5: Sulfur polymers meet poly(ionic liquid)s: bringing new properties to both polymer families

This chapter was conducted in collaboration with the laboratory of Professor Jeffrey Pyun, at the University of Arizona. One of the major disadvantages of sulfur polymers is relative to the solubility of materials with high sulfur content. Recently, the copolymerization of sulfur with styrene at low temperatures was reported, giving materials soluble in organic solvents. This example opens a door to monomers with boiling points below self polymerization of sulfur, as well as the use of functional styrenic monomers. In this case, the copolymerization of sulfur with 4-vinylbenzene chloride (VBC) and its post-polymerization modification with N-methylimidazole was studied to obtain the first polymeric ionic liquid based on sulfur reported hitherto. The kinetics of the copolymerization of sulfur with VBC was studied by NMR, giving reaction times ranging from 3 to 8 hours depending on the sulfur: VBC ratio. After the purification of the resulting polymer, the post-polymerization modification in chloroform was carried out. The final material turned out to be soluble in polar organic solvents and, interestingly, in water. The reaction was studied by NMR confirming the successful modification and synthesis of the poly (sulfur-4-vinylbenzyl imidazolium chloride). One of the most distinctive characteristics of polymeric ionic liquids is their ability to adjust solubility through the exchange of counter ion. In this case, LiTFSI was added to a solution in water of the poly (ionic liquid) resulting in a yellow-orange precipitate, which was found to be soluble in low polar organic solvents, as in chloroform or THF. The modification was studied by FTIR, revealing the distinctive signals to the TFSI ion. These latter materials showed typical characteristics of polymeric ionic liquids such as ionic conductivity as well as properties of sulfur polymers, such as redox activity. The thermal properties of the materials were then characterized by DSC and TGA, giving similar trends independently of the sulfur: initial VBC ratio. Finally, possible applications were tested. On the one hand, water-soluble

polymers as stabilizers of suspended sulfur nanoparticles, resulting in stable sulfur suspensions, with particles with sizes below 200 nm. On the other hand, ionic polymers with TFSI counterions were tested in lithium sulfur batteries as both electrolyte additives and cobinders at the cathode, with unsatisfactory results. In this way, the first polymeric ionic liquids based on sulfur are reported with synergistic properties of conductivity and adjustable solubility of polymeric ionic liquids with the active.

Introduction

1. Introduction

In the XXIst century, we are being witnesses of the twilight of the fossil fuels and the dawn of renewable resources (figure 0.1 a)). Since the industrial revolution, the combustion of fossil fuels has been the major process from which humanity has obtained energy, a process that releases Gigatones of greenhouse gasses (such as CO_2, CO or CH_4) as a byproduct every year to the atmosphere. This effect leads to an abnormal overheating of the planet, driving to the climate change. Furthermore the increasing demand of energy from the ever-growing human population has made the climate issue to become a humanitarian and political concern[1] (Figure 0.1, b)). Moreover, fossil fuel largest reserves are located in politically unstable countries, what leads to political
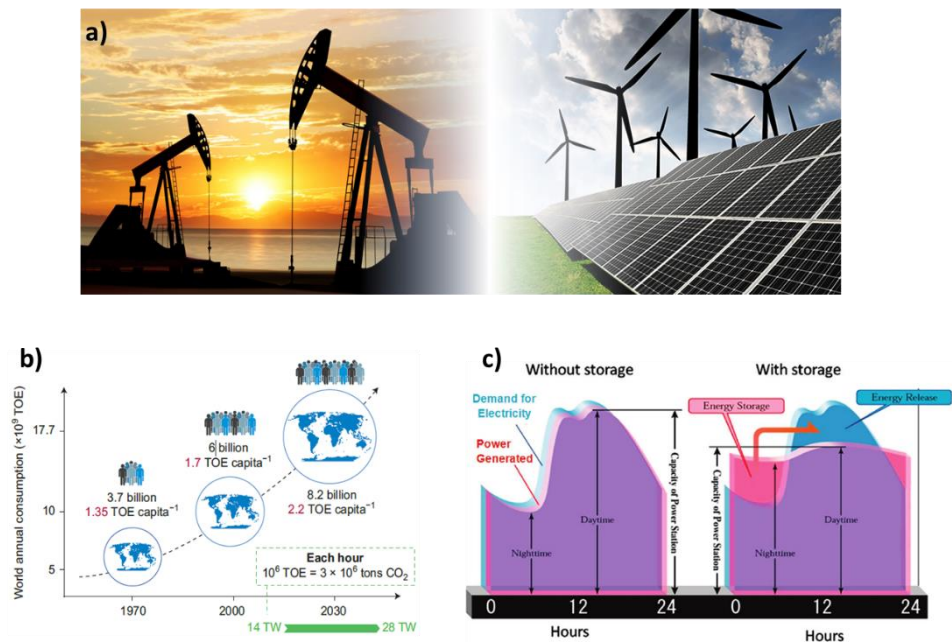

Figure 0.1: a) Digital image representing the twilight of the fossil fuels and the dawn of energy production by renewable sources. b) Exponential energy demand with the population growth expectation from 1970 to 2030. c) Schematic representation of balancing generation and demand via load leveling of energy.

tensions, and in some cases armed conflicts[2,3]. Therefore, energetic transition towards more sustainable energy production systems is already in the world governments work agenda. Solar, wind, hydropower and geothermal energy generation technologies can effectively answer the energy demand without the emission of further greenhouse gasses[4,5].

Electrical energy storage (EES) systems constitute an essential element in the development of sustainable energy technologies. Electrical energy generated from renewable resources such as solar radiation or wind provides great potential to meet our energy needs in a sustainable manner. However, these renewable energy technologies generate electricity intermittently and thus require efficient and reliable electrical energy storage methods (Figure 1, c)). For commercial and residential end-use, electricity must be reliably available at any time of the day. In fact, second-to-second fluctuations can cause major disruptions with costs estimated to be in the tens of billions of dollars annually. Thus, the development of new EES systems will be critical in the use of large-scale solar or wind-based electricity generation. Moreover, greatly improved EES systems are required to enable the widespread use of hybrid electrical vehicles (HEV), plug-in hybrids, and all-electric vehicles. Improvements in ESS performance, reliability, and efficiency are needed in the development of modern portable electronic devices such as laptops and smart phones[2,6,7].

There are a variety of energy storage system that can be classified in mechanical, thermal, chemical, electrochemical and electrical energy storage[8]. All these systems embrace the wide range of applications, from large scale energy storage for the support of electrical grid to small scale energy storage of portable electronics (Figure 0.2 a))[9]. Electrochemical energy storage is the most versatile energy storage system, with applications from stationary plants in order to support the grid to small electronic devices (laptops and smartphones) passing through automotive applications (electric cars). Four types of

electrochemical energy storage systems can be found, namely batteries, fuel cells, redox flow cells and supercapacitors, and each one has its own store mechanism that governs over the store capacity (or energy density) and the energy release rate (Power density) (Figure 0.2 b))[9]. Batteries offer an excellent energy storage technology for the integration of renewable energy production thanks to a compact size, that makes them suited for distributed locations, as well as providing frequency control to mitigate output fluctuations (figure 0.1 c))[9].

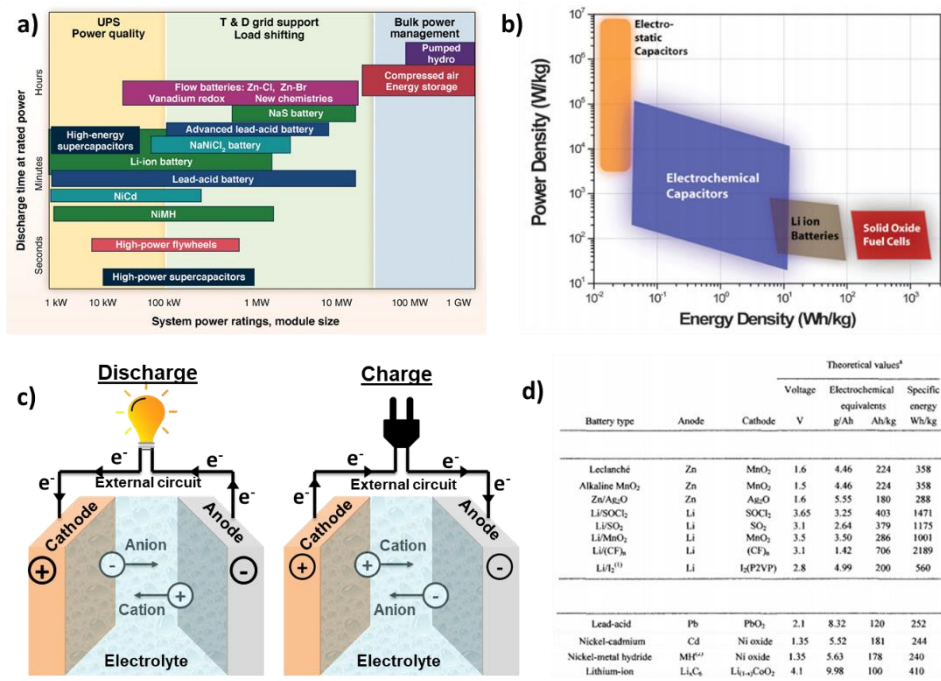A battery consists in two electrodes separated by an electrolyte and connected

Figure 0.2: a) Classification of energy storage systems by the power that can store v the power release rate. b) Classification of electrochemical storage systems by energy density vs power density. c) Basic elements of a battery and the mechanism of charge discharge processes. d) List of the principal primary and secondary battery systems.

through an external electrical circuit. During the discharge the negative electrode (or the anode) is oxidized releasing ions to the electrolyte, whereas the positive electrode (or the cathode) is reduced by accepting ions from the electrolyte (figure 0.2 c)). Along this process the electrons travel from the anode to the cathode through the external circuit generating the electrical current. Batteries can be divided into two categories based on the reversibility of the redox processes. First, primary batteries, such as Zinc-carbon (Leclanché), Magnesium alkaline, silver-zinc and lithium primary among others, where the electrochemical reaction is not reversible and therefore are the batteries are not rechargeable. This kind of batteries provide high energy density and long shelf life with low cost. Next, secondary or rechargeable batteries, that after the first discharge process the system can be recovered by passing an equivalent current in the opposite direction. Secondary batteries offer high power density and high cycle life of more than 2000 cycles. Battery systems such as Lead-acid and Nickel-Cadmium are well known as they have a long history (developed in 1860´s and 1910´s respectively), although they are being widely used nowadays. New battery systems such as Nickel-Metal hydride and specially Li-ion have allowed the revolution of portable electronics (smartphones, laptops, electric cars) in the last 20 years, as they allowed more compact, high energy density and long cycle life batteries.

Lithium ion batteries (LIB) own their name to the electrochemical intercalation mechanism in which are based on, where lithium ions are exchanged between the anode (based in graphite) and the cathode (an inorganic lithium transition metal oxide, such as $LiCoO_2$, or a phosphate, $LiFePO_4$) (Figure 0.3 a))[10–12]. The intercalation reaction occurs at an average voltage of 3.8V what leads to an energy density of 180-250 Wh kg^{-1}. Besides, this kind of batteries provide excellent cycling stability, long cycle life and high C-rate capability. These features have made lithium-ion batteries to revolutionize and dominate the market of portable electronics and look like they will be the principal choice for both, automotive and grid applications in near future. Nevertheless, LIBs suffer

from several drawbacks that are hindering the definitive market penetration of either electric mobility and renewable energy production[12]. The electrode materials have limited specific capacity, what limits the energy density of the battery, for the long-term future application that will demand batteries with increased energy density for longer autonomy. Furthermore, the cathodic materials are composed of rare metals, what makes these batteries not sustainable[13]. Nevertheless, although the limited specific capacity of the lithium-ion batteries has been suggested to be most important challenge for the short-term electrification of transportation, is no the energy density but the cost of LIBs, that nowadays is still quite above the goal of 150 US\$ kWh^{-1} for commercialization[16].
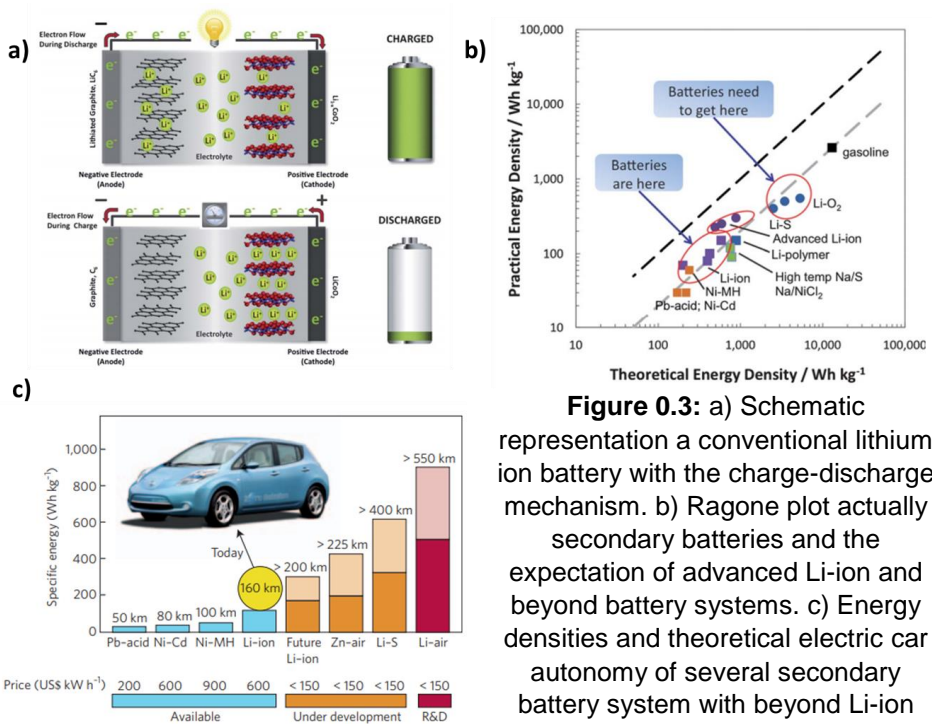

Figure 0.3: a) Schematic representation a conventional lithium ion battery with the charge-discharge mechanism. b) Ragone plot actually secondary batteries and the expectation of advanced Li-ion and beyond battery systems. c) Energy densities and theoretical electric car autonomy of several secondary battery system with beyond Li-ion battery systems, Li-S and Li-O$_2$ among them.

These limitations have moved governments, companies, institutions and researchers to find other kind of technologies that can complement or replace the actually implanted Lithium-ion technology (Figure 0.3 b))[11]. Lithium metal possess excellent properties such as low density (0.59 g cm^{-3}), high theoretical specific capacity (3860 mAh g^{-1}) and enough negative redox potential (-3.04 V vs SHE), what has boost the research of Lithium metal-based batteries being Lithium-air and Lithium-sulfur the most promising solutions[14–16]. Although Li-O$_2$ exhibits greater theoretical energy density than Li-S, there is a technological gap between them, being Li-S batteries closer to real market penetration (Figure 0.3 c))[15]. The latter ones have shown up as promising next-generation battery systems due to the exciting properties of sulfur as cathodic material. It presents an outstanding specific capacity of 1672 mAh g^{-1}, and an energy density of 2600 Wh kg^{-1} vs Li/Li^{+}[16–18]. Furthermore, is among the most abundant element in the earth crust what lowers its price dramatically compared with the cathodic materials of lithium ion technology as well as making it environmentally friendly[19].

Although sulfur has been unfairly maligned by being associate with hell and demon by the bible, elemental sulfur is a raw material which uses are known for ages[20]. In the ancient times sulfur was widely used in most of the advanced civilizations such as Egyptian, Greek, Roman and Chinese for several application such as cotton bleaching agent, antimicrobial element and as a component for the gunpowder (Figure 0.4 a)). During the middle age the European alchemists used sulfur in topic application for dermic affections such as, eczema, psoriasis and acne. In the modern ages sulfur and sulfur containing materials were used for several industrial applications such as fertilizers, in rubber industry as vulcanizing agent and as fertilizer (figure 0.4).

Figure 0.4: a) a roman mural depicting a bleaching process of clothes with sulfur and human urine, and the alchemic symbol of sulfur in the middle age. b) digital images of most important sulfur sources, as waste product of desulfuration of oil (sulfur pyramids in Alberta, Canada) and as element produced in volcanic regions (sulfur mine in Java, Indonesia) c) The actual industrial uses of elemental sulfur, as vulcanizer agent for the production of vulcanized rubber, for the production of hydrochloric acid and as fertilizer. d) modern applications of sulfur, such as chalcogen element of the high refractive index lenses, as additive for self-healing polymers and as cathodic material for Na-S batteries.

Sulfur is the 16th most abundant element in earth crust, mainly as a component in several minerals. It can be found in its native form in the soils surrounding volcanic regions, where it is still being mined, and was the principal source of elemental sulfur up to early 1900´s (Figure 0.4 b)). At the beginning of the 20th century and with an increase of the demand for sulfur from the industry, the Frasch process was developed in order to extract large quantities of sulfur from salt dome deposits in North America[21]. This process was predominant up to
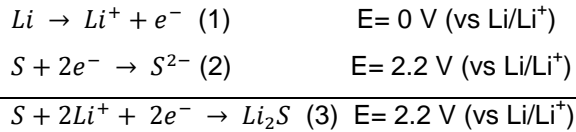
70´s, when the desulfuration of crude oil started to produce elemental sulfur as a byproduct, leading to a production excess. This last process remains nowadays, together with the excess of the production of elemental sulfur. Although most of the produced sulfur is used (nearly the 90%) in industry as commodity chemicals (Sulfuric acid), fungicides and in tire industry, there is still a surplus of 10% that is becoming a storage and environmental problem (Figure 0.4 c)).

Sulfur also has been objective of research due to its interesting properties (Figure 0.4 d))[22]. On one hand, elemental sulfur can perform redox reactions with alkaline elements, making suitable for energy storage systems. Na-S batteries were developed in the 60´s and possess high energy density, efficiency and cycling stability. However, due to the fact that operate at elevated temperatures (300-350 ºC), are limited to stationary energy storage. Li-S batteries, as previously mentioned, are one of the most promising next generation battery system in order to replace the Lithium ion technology. On the other hand, an attractive feature of sulfur is its use as a dopant to increase the refractive index of different materials. The actual IR lenses are comprised of an amorphous semiconductor (Ga, Sb, Ge) doped with a chalcogen element (S, Se, Te). In polymer science, the introduction of a sulfur containing side chains is widely extended in order to increase the refractive index of the films[23]. As a final example of the interest of sulfur, is its covalent dynamic behavior. Due to the relative low dissociation energy of an S-S bond, the introduction of disulfide moieties in polymeric materials have been investigated for self-healing properties[24,25] In this way, materials that can be self-repaired either by pressure or by an external stimulus have been developed during last years.

2. Lithium sulfur batteries: An integral view

2.1 Basics and Mechanism

A conventional lithium sulfur battery comprises a sulfur based cathode, a lithium metal anode and a separator soaked in the electrolyte (figure 0.5 a)). The cathode is the most complex part of the battery. It is composed by the active material (sulfur), conductive additives, such as conductive carbon or polymers, and a binder. As anode, a metallic lithium foil is widely used. The electrolyte is a mixture of ether based solvents, namely, 1,3-dioxolane and dimethoxyethane with lithium bis(trifluorosulfonyl imide) (LiTFSI) salt dissolved on it. During the discharge the oxidation happens in the anode, where the lithium is oxidized releasing lithium ions to the electrolyte and electrons though the external circuit. Both of them travel to the cathode, where the reduction occurs. The elemental sulfur is reduced through the general redox reaction (3):

$$Li \rightarrow Li^+ + e^- \quad (1) \qquad \text{E= 0 V (vs Li/Li}^+)$$
$$S + 2e^- \rightarrow S^{2-} \quad (2) \qquad \text{E= 2.2 V (vs Li/Li}^+)$$
$$\overline{S + 2Li^+ + 2e^- \rightarrow Li_2S \quad (3) \quad \text{E= 2.2 V (vs Li/Li}^+)}$$

Usually elemental sulfur exists as cyclic allotropes of various sizes being the most stable the octasulfur ring S_8, therefore the general redox reaction can be adjusted as the following reaction:

$$S_8 + 16Li^+ + 16e^- \rightarrow 8\,Li_2S \quad (4) \quad \text{E= 2.2 V (vs Li/Li}^+)$$
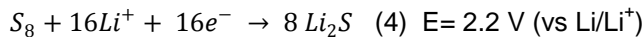
$$Q\left(\frac{mAh}{g}\right) = \frac{n \times F}{3600 \times Mw} \qquad (5)$$

Given the general redox reaction as the reaction (4) and with the formula (5) the theoretical specific capacity of sulfur vs lithium has been calculated to be 1672 mAh g^{-1} and, considering that the average voltage of the redox reaction is around 2.2 V, the theoretical energy density of sulfur vs lithium is around 2500 Wh Kg^{-1}. However, the mechanism of reduction of sulfur is rather more complicated than the general reaction depicted in (4) (Figure 0.5 b). During the discharge, the reduction of sulfur goes through disproportionation reactions of
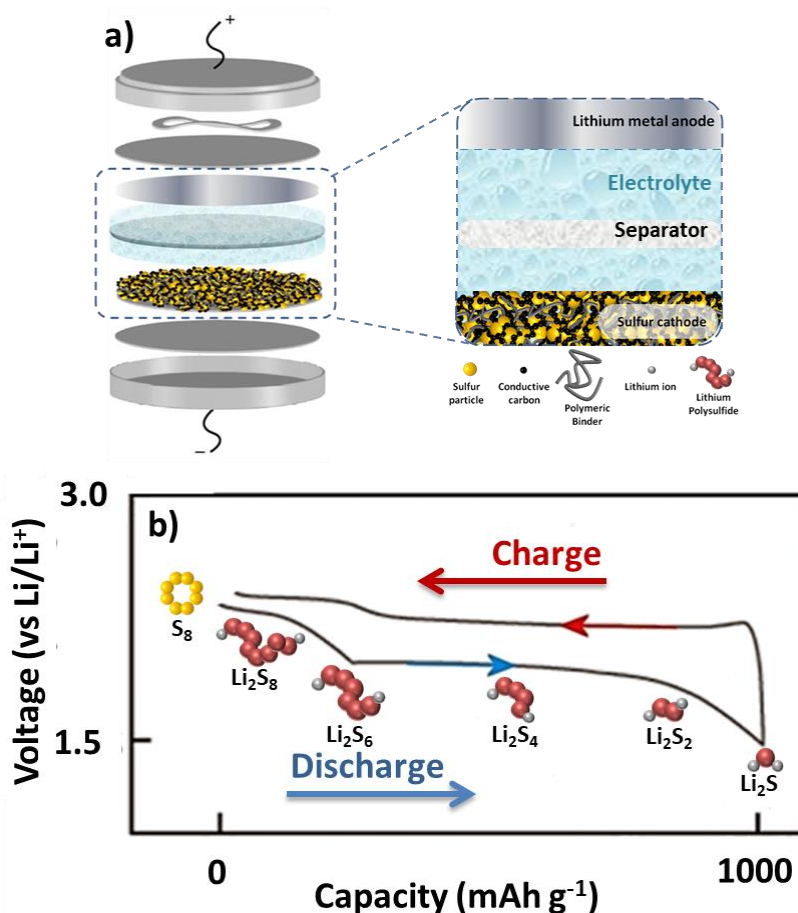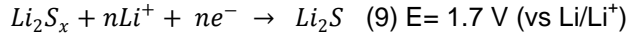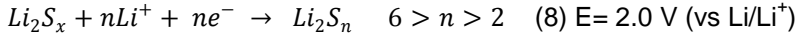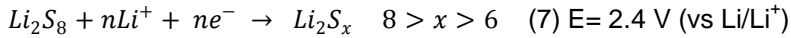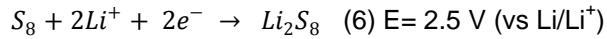
41

Figure 0.5: a) Schematic representation of a lithium-sulfur cell. b) Charge-discharge voltage profiles of sulfur. Inserted drawings of the intermediate formed lithium polysulfide representations.

the octatomic sulfur ring forming high order lithium polysulfides (Li_2S_x with $8 \leq X \leq 6$) at a voltage of 2.5 V (6). The discharge continues via the reduction of Li_2S_x into lower order lithium polysulfides Li_2S_n by different disproportionation reactions (7) and (8). Finally, the discharge finishes with the last products of the oxidation of sulfur with lithium, forming lithium disulfide (Li_2S_2) or lithium sulfide (Li_2S) (9).

$$S_8 + 2Li^+ + 2e^- \rightarrow Li_2S_8 \quad \text{(6) E= 2.5 V (vs Li/Li}^+)$$

$$Li_2S_8 + nLi^+ + ne^- \rightarrow Li_2S_x \quad 8 > x > 6 \quad \text{(7) E= 2.4 V (vs Li/Li}^+)$$

$$Li_2S_x + nLi^+ + ne^- \rightarrow Li_2S_n \quad 6 > n > 2 \quad \text{(8) E= 2.0 V (vs Li/Li}^+)$$

$$Li_2S_x + nLi^+ + ne^- \rightarrow Li_2S \quad \text{(9) E= 1.7 V (vs Li/Li}^+)$$

Many efforts have been done in order to clarify the redox reaction mechanisms that happen during the charge-discharge processes by several advanced characterization techniques[26,27]. Although there is an agreement in the general redox reaction depicted in (6)-(9), the exact species formed during the working of the battery is controversial. The disproponation reactions that take place are strongly dependent of many factors of the battery, such as electrolyte solvent, salts, electrolyte amount, battery configuration, working voltage, etc[28].

2.2 Problems

Despite the exciting theoretical properties of lithium sulfur batteries, there are several factors that affect negatively this battery technology that have to be solved for the success of this battery systems versus the actually implanted lithium ion technology.

On one hand, elemental sulfur is considered an insulator material (conductivity $\approx 10^{-30}$ S cm^{-2}) what hinders the electrochemical utilization of a high percentage of active material. The major strategy is to first confine sulfur in a conductive host (carbonaceous, polymeric or inorganic) and afterwards disperse it in a conductive network. This route, although have been successfully proved that enhances the sulfur utilization and cycle life, brings several limitations of cathode processing, scalability and sulfur loading[29].

On the other hand, as pointed in the previous section, the reduction of sulfur passes through several lithium polysulfide intermediates, that result to be soluble in the electrolyte. These species in solution tend to migrate towards the anode by concentration and potential difference driving forces. In contact with the anode, these species are reduced by the reaction with lithium to lower order lithium polysulfides[30]. Some of these species can be further reduced to Li_2S forming an ionically insulator and irreversible SEI (Solid Electrolyte Interface) that passivates the anode surface. Other reduced species can return to the cathode and be oxidized in the new cycle[19]. This effect leads to self-discharge and low coulombic efficiency as well as the degradation of the cathode, due to the active material loss, and the passivation of the anode.

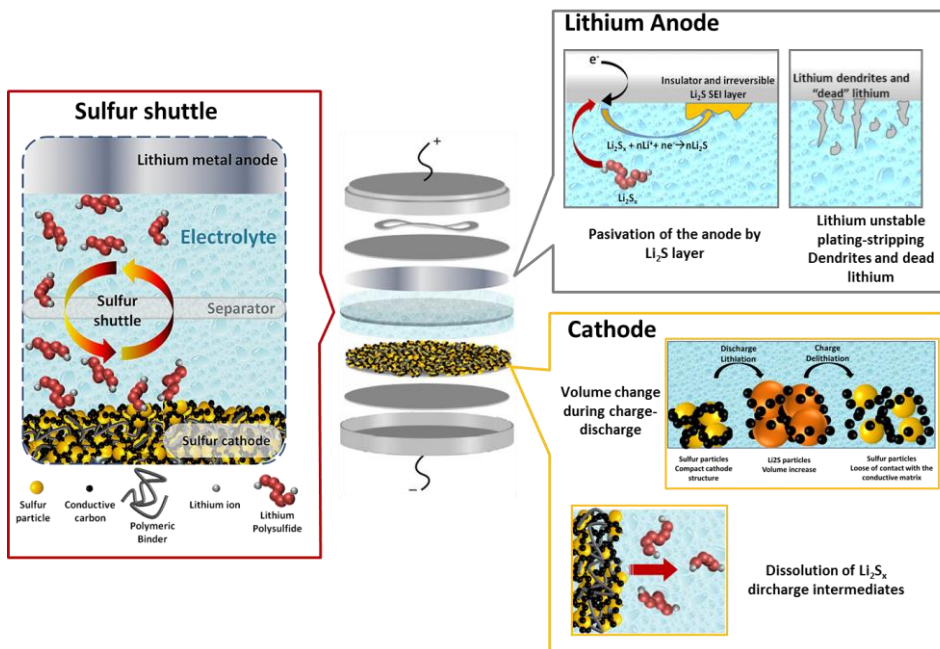Besides, the structural changes during charge-discharge processes of sulfur

Figure 0.6: Schematic representations of the most critical problems in lithium sulfur batteries. With the sulfur shuttle depicted in the left, the problems of the lithium anode in the top right and the issues of the cathode in the bottom right of the figure.

(from solid to liquid to solid) and the density differences between elemental sulfur (2.07 g cm^{-3}) and lithium sulfide (1.66 g cm^{-3}) leads to a mechanical stress to the cathode, that promotes the cracking, delamination and loss of the integrity of the cathode structure that ends in the cell failure[29].

In addition, the use of metallic lithium anode is a challenge itself. As a drawback, lithium metal easily reacts with the solvent used as electrolyte casing a decrease on the coulombic efficiency[31,32]. Furthermore, the inhomogeneous deposition/dissolution (plating/stripping) of lithium during the charge/discharge processes leads to lithium dendrites, that can cause three negative effects on the battery. On one hand, the dendrites can grow along the electrolyte and through the separator up to the cathode, where the physical contact happen causing the short circuit of the battery with safety risks. On the other hand, the non-homogeneous dissolution of can break the lithium crystals formed during the dendrite grow, causing "dead" lithium that reduces the efficiency and stability of lithium anode[33]. Furthermore, this dead lithium can further react with electrolyte that is being consumed what is translated into lower cycle life.

Lithium sulfur batteries have been known since the 60´s and 70´s, however due to the fails in terms of reversibility, safety and performance, together with the irruption of lithium ion batteries in research field, made the researchers to give up with this technology[16,29]. However, promoted by the need of high capacity materials and high energy density cells, the interest on lithium sulfur batteries turned back. In the early 2000´s many research on several factor of the battery such as electrochemical studies of lithium polysulfides in organic solvents, cell fabrication or how the solubility of lithium polysulfides allows improvements in battery performance, but with detrimental shuttling effect and self-discharge, gave an insight of the electrochemistry and mechanism of the battery[34–36]. In 2009 Nazar and coworkers presented the melt diffusion strategy in order to confine sulfur in the pores of a mesoporous carbon[37]. This strategy, together with a polyethylene glycol coating, allowed high utilization of sulfur (80%,1330

mAh g^{-1}) and cycle life of 20 cycles. This work inspired huge research in sulfur-based nanocomposites, achieving high sulfur content cathodes and high sulfur % utilization.

3. Polymers in lithium sulfur batteries

During the last years it has been an intensive research for better understanding and overcoming the aforementioned technological problems for practical viability of lithium sulfur batteries[38]. In overall, four different strategies have been followed[39]. First, there has been plenty of research works focused in the
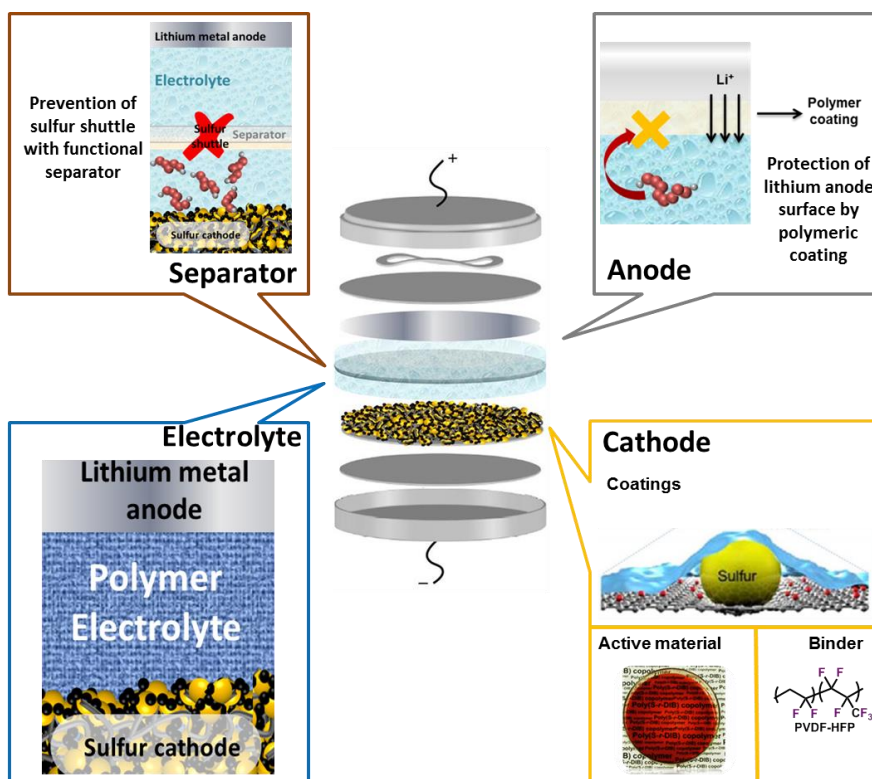

Figure 0.7: Schematic representation of the use of polymers in lithium sulfur batteries in each component of the battery, anode (top right), separator (top left), electrolyte (bottom left) and cathode (bottom right).

design of cathode structure, with the aim to avoid the migration of lithium polysulfides towards the anode. Second, the separator has been objective of different kind of modifications in order to block the polysulfide migration. Third, the use of novel electrolyte systems in order to prevent the polysulfide dissolution have been analyzed. And forth, the protection of the lithium anode interface has been studied in order to have a better control of the SEI layer and avoid the passivation of lithium surface and the grow of lithium dendrites. In this context polymeric materials offer very interesting properties such as excellent mechanical properties, easy processability and chemical tunability, that allow the application of these materials in every component of the battery[40] (Figure 0.7). In the following pages, the use of polymers in lithium sulfur batteries will be shortly reviewed.

3.1. Anode

The failure of most Lithium based batteries comes from the deactivation of the anode due to lithium corrosion promoted by the high reactivity of metallic lithium towards the electrolyte system. Therefore, strategies to protect the anode surface and prevent the parasitic side reaction that decreases the performance of the Lithium sulfur batteries have been studied[31]. Most of the approaches have passed through the addition of additives in the electrolyte in order to form an artificial SEI layer, the use of modified lithium based anodes and the use of coatings onto the surface of the lithium metal anode have been used in order to have a protective physical barrier. The latter strategy allows having a better control over the SEI formed during cycling in addition to the prevention of the reaction of soluble polysulfides with the lithium metal by physical blocking. The coating of the anode should fulfill some requirements, such as high ionic conductivity, as lithium ions have to move through the membrane, non-solubility in the electrolyte and be enough chemically stable towards the anode. PEO containing monomers have been used in order to coat the surface of the lithium metal anode and subsequently polymerize in presence of a crosslinker by UV
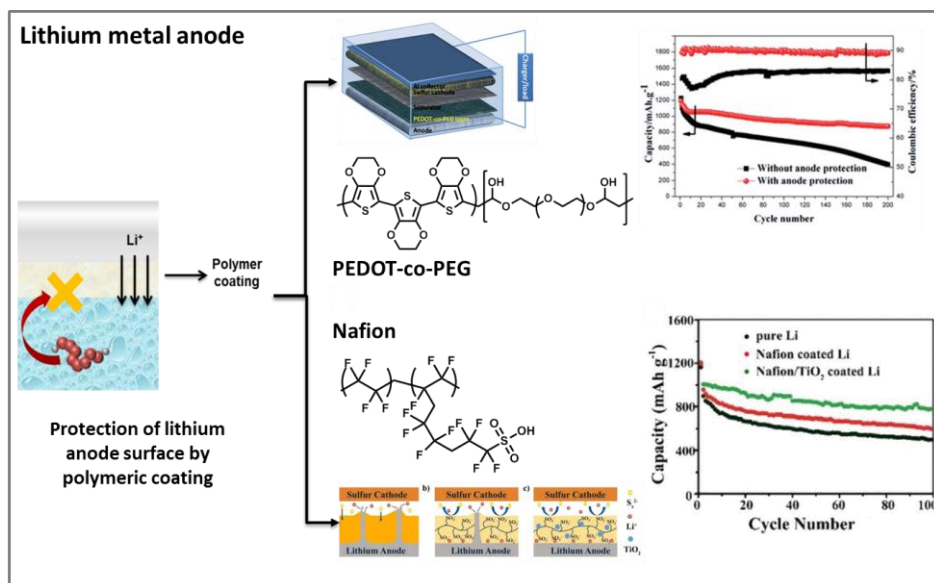
Figure 0.8: Some examples of the application of polymeric coatings on lithium anode surface. Top, an interlayer formed of a ionically conductive PEG and electrically conductive PEDOT (ref 23). Bottom, a protective composite coating composed of Nafion and TiO_2 (ref 23).

curing. In this way, insoluble, chemically stable and ionically conductor membrane can be obtained with controlled thickness[41]. By this strategy the lithium sulfur battery, despite suffer a drop in capacity, extended the life up to 100 cycles vs the 40 without the protective coating as well as reduce significantly the shuttle effect. A similar approach was followed by Wu et al, that coated the lithium metal surface with a copolymer of PEG-co-PEDOT[42] (Figure 0.8 top). The electronically conductive PEDOT enhanced the charge transfer between the anode-electrolyte interface, decreasing the resistance compared with the SEI formed with the ether based electrolyte. A very recent report from Jiang et al described the use of a composite with ionic polymer (Nafion) as host material and TiO_2 as inorganic filler[43] (Figure 0.8 bottom). A combined effect of protecting the lithium anode surface from lithium polysulfides by electrostatic repulsion and prevention of lithium dendrites given by the Nafion coating with

48

the enhanced ionic conductivity and mechanical strength by the presence of TiO_2 could be observed.

3.2. Separator

The separator is an essential component in an electrochemical cell, playing the important role of preventing internal short-circuit by blocking the electron transport and at the same time maintaining the ion diffusion pathways. Porous polyolefin membranes, a heritance from lithium ion technology, are the most extended separators due their availability and low cost. Nevertheless, in lithium sulfur batteries the soluble discharge intermediates lithium polysulfides can easily migrate between the electrodes through this kind of separators, causing the sulfur shuttle. Therefore, an ideal separator for lithium sulfur batteries should present an effective method to inhibit the polysulfide shuttle during cycling presenting good ionic conductivity after absorption of the electrolyte. In this way, two major strategies have been followed in order to prevent the polysulfide shuttle via using functional separators by (1) modifying a commercial polyolefin separator and (2) replace the conventional separator by a functional material designed to provide barrier properties against lithium polysulfide species[44]. Although several strategies can be found in the use of many different compounds, such as carbon materials, inorganic materials and polymeric materials, the following discussion will be exclusively focused in latter one, the use of polymers for functional separators[45].
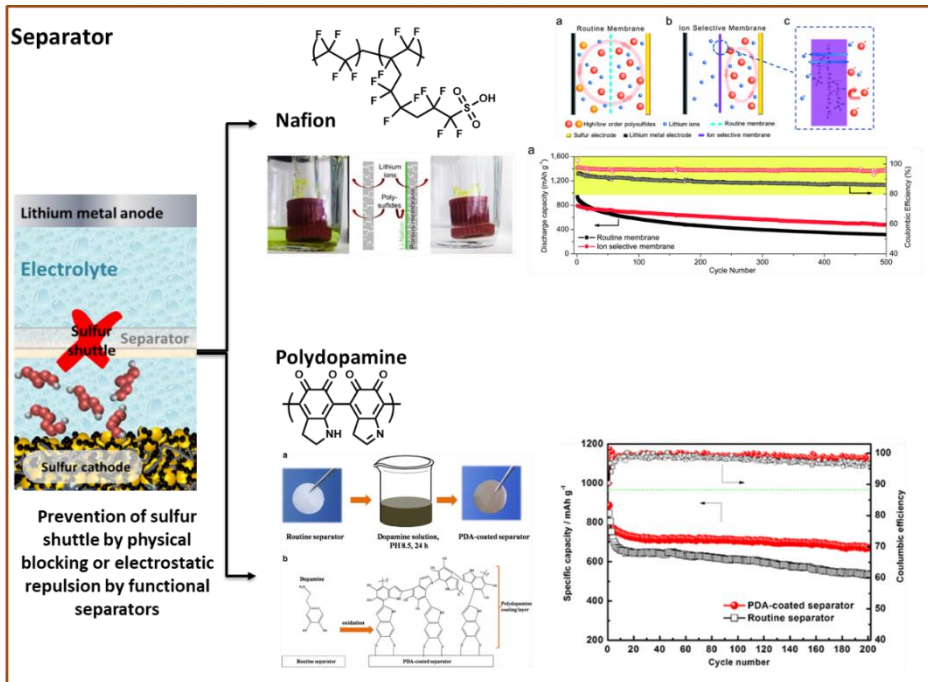
Figure 0.9: Schematic representation on the use of polymers in the separator with the aim of inhibiting the polysulfide shuttle by (top) coating with Nafion and (bottom) with treatment with polydopamine.

Thanks to the ease of coating methods such as drop casting, dip coating or layer-by-layer processes that proved to be effective for the modification of the separator, functional groups coatings have been used as polysulfide shuttle mitigators by physical adsorption, chemical bonding or electrostatic repulsions. Nafion ionomer have been widely used as polymer coating for the separator, as the sulfonated end groups allows both, the diffusion of Li$^+$ ions and the blocking of negatively charged polysulfide species[46–48]. Similar negatively charged polymeric materials have been used as functional separators in lithium sulfur batteries such as poly(Styrene sulfonate) (PSS) or poly(acrylic acid) (PAA)/poly(allylamine hydrochloride) (PAH)[49–51]. Polydopamine have been found to be very attractive as polymeric coating due to its polysulfide affinity. By easy dip-coating method into an aqueous dopamine solution at a pH 8.5 a very

thin layer of PDA was deposited in the surface of the conventional PP separator, demonstrating an enhanced battery performance[52,53].

3.3. Electrolyte

An electrolyte system must own several features, namely, high ionic conductivity (above 10^{-3} S cm^{-1}), stability at the working voltage of the electrochemical system, low surface and low viscosities in order to have a good wettability to present favorable contact between electrolyte and active material together with low interface resistance, among others[54]. In the case of Lithium sulfur batteries, further properties are needed due to the presence of the highly reactive anode and lithium polysulfides. Carbonate based liquid electrolytes are widely used in Li-ion technology, as they fulfill most of the previously mentioned characteristics, however are not suitable for lithium sulfur batteries. The carbonate groups of the solvents commonly used in Li-ion are susceptible to suffer a nucleophilic attack from the lithium polysulfide species, leading to parasitic side reaction resulting in irreversible loss of active material[55]. Ether solvent-based electrolytes have been found to be an appropriate system for lithium sulfur batteries. Nowadays, the most common electrolyte system contains a mixture of 1,3-dioxolane (DOL) and dimethoxyethane (DME) in a 1:1 v:/v ratio with 1M of Lithium vis trifluorosulfonyl imide salt (LiTFSI) and low concentrated Lithium nitrate ($LiNO_3$) salt as has been the end up of plenty of reports on the development of different electrolyte systems that gave a deep insight on which were the desired characteristics of the ideal electrolyte for lithium sulfur technology. This electrolyte system provides high conductivity, high polysulfide solubility and SEI-forming properties, together with low viscosity. Nevertheless, the base solvents of the electrolyte are organic solvents with low boiling point and high flammability, what leads to a safety concern of the battery. Additionally, the low viscosity of liquid electrolytes promotes severe polysulfide shuttle, with all the problems associated with it. Therefore, researchers have moved towards solid state electrolytes to solve the
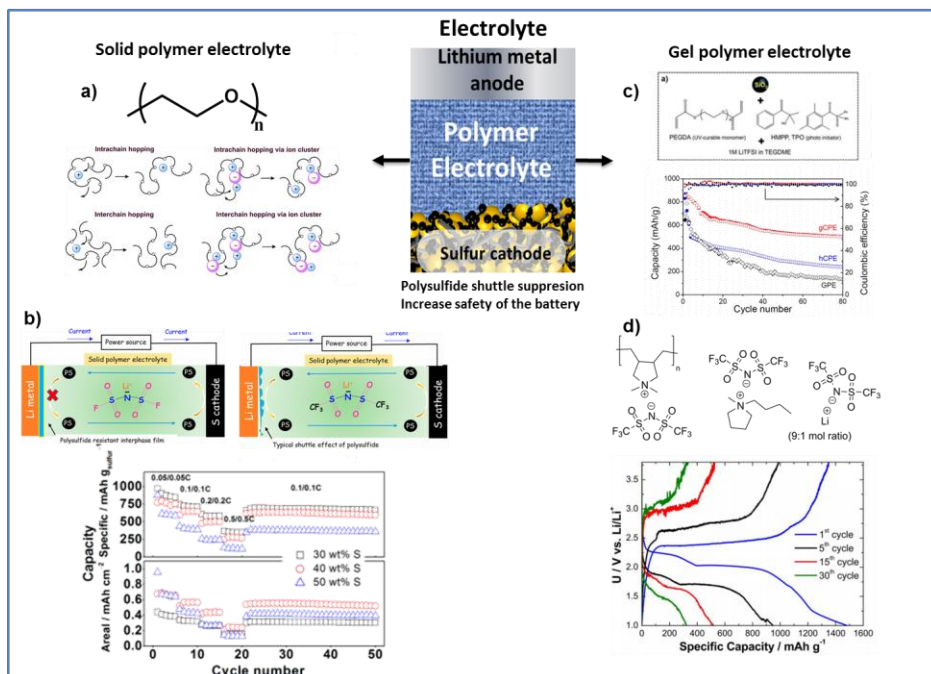
Figure 0.10: Strategies on the use of polymers as an alternative to liquid electrolytes. A) the chemical structure of the most widely used polymer for solid polymer electrolytes, PEO an the ionic conductivity mechanism representations. B) Representation of the effectiveness of the use of LiFSI salt as additive in a solid polymer electrolyte vs LiTFSI (ref 37). C) PEO based gel polymer electrolyte by UV curing a PEGDA difunctional monomer and the battery performance with and without inorganic fillers (ref 38). D) Ion gel polymer electrolyte composed by P(DADMAC) as host material and Pyr$_{14}$ TFSI as plastisizer (ref 44).

fundamental issues of liquid electrolytes, for one side to prevent the lithium polysulfide dissolution and migration towards the anode and for the other side to protect the lithium metal anode and minimize dendrite formation. Following, the use of polymers either as all solid polymer electrolytes or in gel polymer electrolyte will be described.

A solid polymer electrolyte comprises a high molecular weight polymer with a lithium salt dissolved on it. The golden standard of solid polymer electrolytes in lithium sulfur batteries is the Poly(ethylene oxide) (PEO). This polymer

possesses several advantages such as low weight, good interfacial compatibility, excellent electrochemical stability and high lithium transference number. This polymer was firstly tried in lithium sulfur cells by Marmostein and coworkers with good initial capacity but low cycling stability.[56] The major problem of this polymer relies in its semicristalline nature, what makes the operating temperature of the cell beyond room temperature, what is detrimental as increases the polysulfide solubility in the SPE with very similar sulfur shuttle mechanism than in liquid electrolyte. Therefore, researchers have tried to decrease the crystallinity of PEO and enhance the electrochemical behavior of SPE at room temperature from different strategies. The use of inorganic fillers have been a common strategy as they could have several effects such as reducing the crystallinity of PEO, increase the mechanical strength and reduce polysulfide shuttle by adsorbing lithium polysulfides[56–58]. Another strategy presented by Armand and coworkers passed through the crosslinking of Poly(ethylene glycol) diacrylate (PEGDA) with divinylbenzene in a PEO matrix. In this way, the crystallinity of PEO was decreased near to 34% and the melting temperature decreased down to 34 ºC, what leaded to an initial capacity of 1000 mAh/g_s[59]. The lithium salt effect in a solid polymer electrolyte was studied by Rodriguez-Martinez et al, who, inspired by previous studies on the use of LiFSI as a better additive in the electrolyte for lithium metal anode, changed the widely used LiTFSI to LiFSI. This alternative electrolyte improved the battery performance with higher specific discharge capacity of 800 mAh g^{-1} and improved cycling stability[60].

The principal drawback of the aforementioned solid polymer electrolyte is regarding the low conductivity at room temperature. The introduction of a plasticizer component leads to a gel polymer electrolyte, what combines the high ionic conductivity at room temperature of liquid electrolytes with the mechanical strength of the solid polymer electrolytes. Fluoropolymers such as PVDF and PVDF-co-HFP have been widely used as polymer matrix due to their high electrochemical stability, high hardness and porosity[61]. However, they

possess poor polysulfide absorption ability, therefore, structured electrolytes or inorganic fillers have been added in order to diminish polysulfide shuttle[62,63]. Other than fluoropolymer based gel polymer electrolytes, a wide variety of polymers as host matrix for the liquid phase such as PEO, PMMA, PAN and Nafion based crosslinked membraned and poly(ionic liquid) based ion gels[63–67].

3.4. Cathode

Most of the problems of the lithium sulfur batteries come from the direct use of sulfur as cathodic material. The low conductivity of sulfur inhibits the major utilization of the bulk material as well as difficult the electrochemical kinetics, inhibiting high power densities. In addition, the redox activity of sulfur involves the formation of lithium polysulfides, that have resulted to be readily soluble in the electrolyte system. This effect leads to the so-called polysulfide shuttle, that is about the migration of the soluble species from the cathode to the anode causing both, the degradation of the cathode due to the loss of active material and the passivation of the anode, as the result of the reaction of lithium polysulfide with the neat lithium surface, forming an irreversible, insulator and insoluble SEI layer of Li_2S. Additionally phase transition of the cathodic material
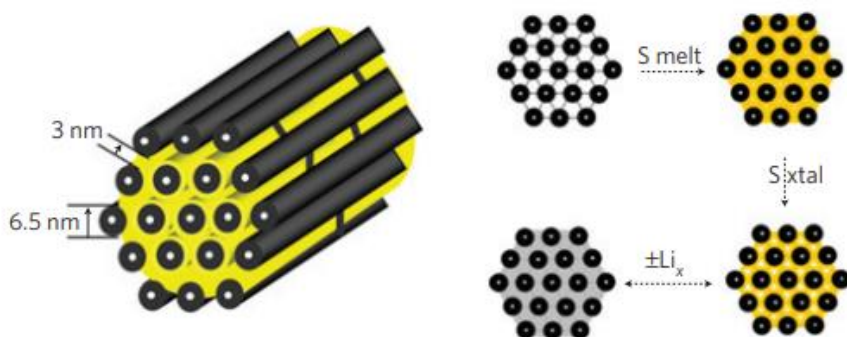

Figure 0.11: Schematic representation of a sulfur/CMK-3 composite after the melt-diffusion treatment (left), and the complete process with the sulfur reduction vs lithium (right) developed by Nazar and coworkers (ref 21).

during redox processes (from solid S_8, to liquid Li_2S_x to solid Li_2S) promotes a mechanical stress to the cathode affecting the structural integrity. All these effects are translated in a wide difference from the theoretical values of capacity and energy density, low coulombic efficiency as well as a poor cycling stability.

In 2009 Nazar and coworkers presented the confinement of sulfur into the pores of a mesoporous carbon (CMK-3), forming a sulfur-carbon nanocomposite (Figure 0.8)[37]. Taking advantage from the low viscosity of sulfur melt at 150 ºC, liquid sulfur is driven into the pores of the mesoporous carbon by capillary effect. This strategy allows an effective sulfur utilization up to 80% (1400 mAh g^{-1}), and together with a Poly(ethylene glycol) coating of the sulfur-carbon nanocomposite, a cycling stability up to 20 cycles with a capacity of 800 mAh g^{-1}. Motivated by this breakthrough report, there has been an intensive research on effective host materials for sulfur, taking carbonaceous materials (mesoporous, carbon nanotubes, carbon spheres, porous hollow carbons and graphene among others) most of the attention, but with noteworthy reports of inorganic and polymeric host materials. Although sulfur-carbon nanocomposites allow very high specific capacity, limited cyclability can be achieved, as the adsorption of soluble lithium polysulfide intermediates is physical and tend to leave the cathode. A different concept of sulfur encapsulation goes through the coating of sulfur nanoparticles with inorganic materials or polymeric materials. This approach can effectively enhance the sulfur utilization, absorb the volume change of sulfur particles during cycling processes as well as prevent the polysulfide migration and the shuttle effect[68].

Polymeric materials have been widely used in the cathode in three major ways. First, in order to process the cathodes as thin films, polymers have been used as binders; a material that is able to accommodate the active material (or the composite) and the conductive network and have enough adhesion to the current collector. Second, coating layers of functional polymers have been used

at every level of the cathode either directly onto the sulfur particle, on the sulfur-carbon nanocomposite or as interface layer onto the cathode surface. And third, redox active polymeric materials have been used as cathodic material in order to replace elemental sulfur. In the following pages, a brief review about how and which polymers have been applied in lithium sulfur batteries will be presented.

3.4.1 Binder:

The binder has to fulfill several requirements in order to be used in batteries. Firstly, to be electrochemically inactive and stable, following by presenting good adhesion towards sulfur, carbon and current collector and finally be able to swell the electrolyte in order to enhance the ionic conductivity in the cathode. Additionally, in LiS good mechanical properties are needed, as, due to the volume change from sulfur to Li_2S and vice versa during cycling processes, the cathode suffers a mechanical stress that can lead to the collapse of the structure[69]. Fluoropolymers, such as PVDF or PTFE, fit in most of the requirements for the ideal binder in LiS system, this is why are the most used polymers by far. However, these family of polymers need the use of toxic and high boiling point solvents (such as NMP) for the cathode processing, what complicates the battery assembly. Furthermore, they do not present the best mechanical properties to face the mechanical stress during charge-discharge. Therefore, researches have moved towards other kind of polymers with additional functionalities in order to enhance the battery performance.

Water soluble binders have been used in order to address the environmental issue of the cathode processing based in NMP. Natural polymers, such as CMC (Carboxymethyl Cellulose) or gelatin, have attracted considerable attention not only for their water solubility but for their mechanical properties. It was proven by Zhang et al that gum Arabic, a natural polymer composed of a mixture of polysaccharides and glycoproteins, improved the mechanical properties of the whole cathode, resulting in a more flexible structure, able to

56

absorb the volume change during cycling leading to a higher capacity retention as well as higher cycling stability(> 800 mAh g^{-1} at cycle 500 at C/5)[70] (Figure 0.12 a)).

Cui et al proved that polar groups, such as groups containing carbonyl moieties, have stronger affinity towards lithium polysulfides than the fluorine containing polymers Poly(Vinylpyrrolidone) have been widely used due to its polar nature, as experimental results confirmed that PVP was able to diminish the lithium
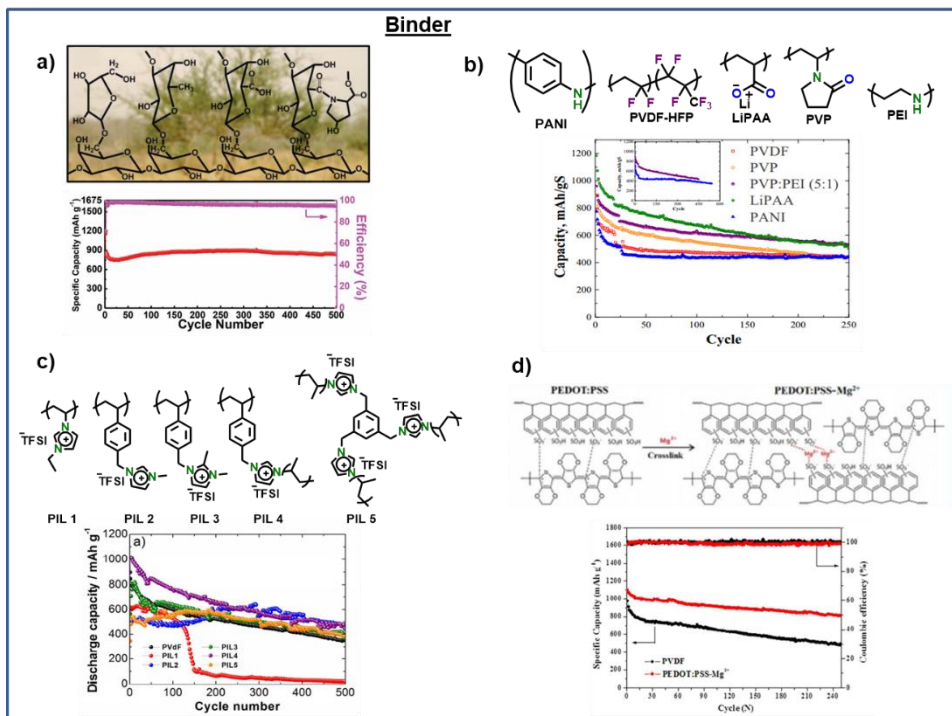

Figure 0.12: Examples of the different polymers used as binders in lithium sulfur batteries; a) top, the molecular structure of gum arabic as water soluble binder, bottom, the battery performance (ref 45). B) A comparison between several polymers as binder in lithium sulfur batteries reported by Golodnitsky and coworkers (ref 47). C) The use of novel cationic poly(ionic liquid)s as binders study presented by Dominko and coworkers (ref 48). D) Li et al presented an ionically crosslinked PEDOT-PSS as a stable conductive binder (ref 49).

57

polysulfides present in the electrolyte, reducing the loss of active material, leading to a higher capacity retention along cycling[71].

Ionic polymers have been applied also as binders in sulfur cathodes. As an example of a poly anionic material, lithiated poly(acrylic acid) have been used with improved result. The strategy passed through the preventing the polysulfide migration by blocking via electrostatic repulsion. Golodnitsky and coworkers presented a comparative study on the use of different binders, being lithium polyacrylate (LiPAA) the material with which the cathode showed enhanced initial capacity and capacity retention (1200 mAh g^{-1} and >600 mAh g^{-1} after 250 cycles, Figure 0.9 b))[72]. Furthermore, a recent report by Dominko and coworkers presented a series of imidazolium based cationic poly(ionic liquids) either as linear or crosslinked binders. In all cases, the poly(ionic liquid)s were superior in performance than widely used PVDF, mostly due to the higher affinity of cationic polymers towards polysulfide species, what is translated into a higher capacity and cycle life (figure 0.12 c))[73]

In order to decrease the resistance due to the charge transfer in the bulk of the cathode, the use of conductive polymeric material as binders have been investigated. Besides, it is known that positively doped conductive polymers have strong attraction towards lithium polysulfide species. Zhan and coworkers presented a water processable binder composed by Poly(acrylic acid) (PAA) and PEDOT/PSS. The cathodes, despite the advantage of avoiding the use of toxic solvents, exhibited an enhanced initial capacity and superior capacity retention. A very recent work from Li and coworkers used a divalent anion (Mg^{2+}) in order to ionically crosslink the PSS, the polymeric counteranion that stabilizes PEDOT in water[74]. In this way, the PEDOT/PSS system exhibit enhanced mechanical strength, what improved the cathode stability during cycling. cycling (Figure 0.12 d))

3.4.2 Coating technologies in the cathode:

With the aim of restricting the redox reactions of sulfur in the cathode, polymer coatings have been used in the cathode interfaces at different levels either at the surface of the sulfur particle, in the composite materials or directly on top of the whole cathode in order to prevent the lithium polysulfide migration out from the cathode.

In the first case, with the aim to restrict the dissolution of lithium polysulfides as well as accommodate the volume change of sulfur, the strategy of the coating of the sulfur particle have been widely chosen. In the case of polymeric materials there have been used either nonconductive polymers, such as PVP, PEO and PSS or conductive polymers such as Polypyrrole, Polythiopyhene, Polyanyiline, Polydopamine and Poly(3,4-ethylenedioxothiophene) (PEDOT) [75–81]. On one hand, the nonconductive polymers not only have good flexibility to absorb the volume changes but also possess polar functional groups that have affinity towards polysulfides. Cui and coworkers presented the preparation of monodisperse PVP-coated sulfur nanoparticles and their use as cathodic materials. They confirmed that the spherical shape was unaltered by cycling processes, what was translated into high coulombic efficiency for up to 1000 cycles[75]. Furthermore, conductive polymers have been widely used as encapsulation materials of sulfur due to both features, electronic conductivity and polysulfide affinity. These interesting properties promote the enhancement of the electron transport from the conductive network to the sulfur particle as well as inhibition of the polysulfide shuttle. Chen and coworkers studied the influence of the conductive polymer in the sulfur surface, concluding that the C-rate capability was enhanced, being PEDOT the best choice as shows the highest conductivity, promoting a faster charge transfer between the conductive network and the sulfur particle[81] (figure 0.11 a)).

The drawback of the coating of sulfur alone is related with the size of sulfur particles, if the particle is too big, the practical utilization of the bulk of the sulfur particle will be lower. For this reason, the coating of sulfur particles has a limited application in term of scalability. Nevertheless, similar strategies have been followed on coating the composite materials with polymers from different nature in order to enhance the ionic conductivity as well as preventing the polysulfide dissolution out from the cathode. Therefore, the aforementioned polymers have
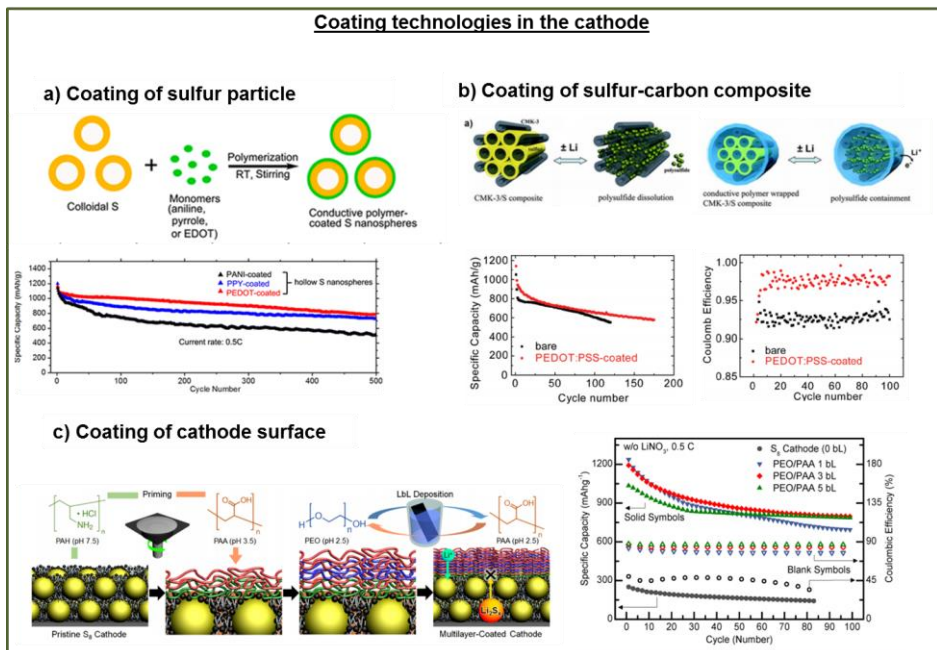

Figure 0.13: Examples of the different polymers used as coatings in the cathode; a) the study of different conductive polymers (Ppy, PANI and PEDOT) as coatings of sulfur particles (ref 56). B) Coating of S/CMK-3 composite with PEDOT-PSS layer to prevent the polysulfide dissolution for higher cycle life (ref 57). C) The use of L-b-L technique as a strategy to deposit thin layers of PAA/PEO onto the surface of the cathode (left); the battery performance of lithium sulfur batteries with $LiNO_3$ (left plot) and without (right plot) (right) (ref 61).

been applied also used in order to coat the sulfur-carbon composite material, decreasing the resistance of the bulk of the cathode, either the polar polymers or the conductive polymers. For instance, the same sulfur/CMK-3 composite have been coated with two polymeric materials from both families. On one hand, Nazar and coworkers in their seminal work of the infiltration of sulfur into CMK-3 pores by melt diffusion, they coated this composite with PEG in order to physically block the diffusion of polysulfides out from the cathode, with the evidence of an increase of the capacity from 1000 mAh g^{-1} to almost 1400 mAh g^{-1}[37]. On the other hand, the same S/CMK-3 composite was coated with a layer of the conductive system PEDOT-PSS with and enhance on the initial capacity, capacity retention and cyclability (figure 0.11 b))[82].

Finally, coating technology have been extended to the surface of the cathode. Further expanding previously mentioned similar approaches, polymers such as PEDOT, PEO or Nafion have been applied in order to prevent the polysulfide dissolution and migration towards the anode[83–85]. In an alternative strategy Pyun and coworkers took advantage of the layer-by-layer deposition of ionic polymers (poly(acrylic acid)/poly(allylamine)) (PAA/PA) in order to prevent the lithium polysulfide diffusion towards the anode through electrostatic interaction maintaining the ionic conductivity of the surface of the anode[86]. This strategy allowed the use of a sulfur cathode without the LiNO$_3$ additive in the electrolyte (figure 0.11 c)).

3.4.3 Active material:

A direct strategy to avoid the sulfur shuttle due to the solubility of lithium polysulfides have been the chemical bond of sulfur to polymeric materials by the use of polymers containing disulfide or polysulfide bonds, what have been baptized as organosulfide polymers. There are different approaches in order to incorporate redox active disulfide or polysulfide bonds in the polymer either in

the main chain or in the side chain (Figure 0.6, middle). Therefore, polymers obtained from these different strategies have been listed in the following points:

Generation I, sulfide bonds in the main chain: The first approaches of sulfur containing polymers were introduced by Visco et al as an alternative cathodic material in the late 80´s. The concept of his of kind of materials relies in the redox activity of disulfide bonds present in the main chain. at. Although the redox activity was proved, this suffer from slow redox kinetic and rapid failure due to the loss of the macromolecular structure and the solubility of the discharge intermediates in liquid electrolyte[87,88]. The strategy of introducing electron rich moieties (such as pyridyl type conjugated cycles) bonded to the redox active disulfide bonds enhanced the electrochemical performance, however the solubility of discharge intermediates was still an issue, what promoted rapid capacity fading, what made the researchers to dismiss this strategy. Nevertheless, in the last years, some reports in the use of hyperbranched disulfide polymers as active material have been presented[89,90]. Seshadri and coworkers reported a hyperbranched polymer based hexadisulfide benzene (figure 0.12 a)). This material showed up stable capacity retention up to 200 cycles[89].

Generation II, sulfide/polysulfide bond in the side chain: The second family of organosulfide polymers have the disulfide bond in the side chain or as pendant group of the main chain, in this way the structure of the cathode is maintained through the cycling processes. Furthermore, the disulfide redox moiety can be bonded to an electronically conductive polymer backbone what enhanced the electron transport to the redox site of the polymer improving the redox reaction rate[91]. However, these kinds of materials suffer from low specific capacity due to the low density of S-S bonds per repeating unit. Nevertheless, recently Shanmukaraj et al presented two different polymers with redox active sulfide
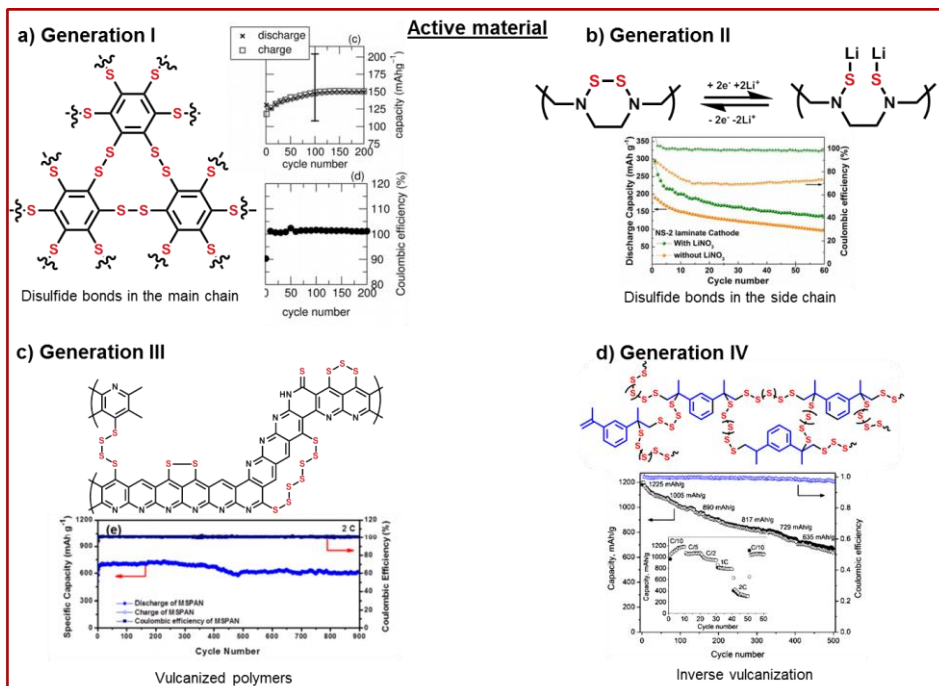
Figure 0.14: Classification of the different generations of organosulfur polymers used for energy storage. a) First generation, with disulfide bonds in the main chain. A recent report in the use of a hyperbranched disulfide polymers with good capacity and reversibility is depicted (ref 64).

bonds in the side chain (figure 0.12 b)). These polymers showed excellent capacity retention up to 100 cycles with good coulombic efficiency above 95%[89].

Generation III, sulfurized polymers: In order to increase the capacity of these organosulfide polymers the post polymerization sulfurization has been studied in several systems. This method is similar to the classical vulcanization method, where polymers with reactive moieties are reacted with sulfur at high temperature. Sulfurized poly(acrylonitrile) have received special attention due to its outstanding results in battery (Figure 0.12 c)). Deep characterization studies revealed that the dehydrogenation ability of sulfur of the cycle structure of PAN leaded to a conjugated backbone with polysulfide linkages as side chains[92]. The

63

conductive backbone of PAN enhanced the electron transport towards the polysulfide redox sites, achieving outstanding battery results. More recently, the post polymerization sulfurization has been extended to other systems such as conductive polymers. Chen and coworkers mixed sulfur with a self-formed polymer from *m*-aminothiophenol at high temperature achieving a hybrid copolymers of sulfur with an electronically conductive polymer[93]. The resulting high sulfur content material exhibited improved capacity, capacity retention and C-rate capability.

Generation IV, inverse vulcanization: Finally, the last group of organosulfide polymers consists in the materials synthesized via inverse vulcanization method. In short, as this process will be deeply described forward, is the bulk copolymerization of elemental sulfur with a low amount of a diene (figure 0.12 d)). In this way, polymers containing up to 90 wt% of sulfur can be synthesized, with very high specific capacity and increased cycle life[94]. In the following pages, the high sulfur content polymers will be reviewed, finishing with a detailed description of the inverse vulcanization process and the application of the resulting polymeric materials as cathodic materials in lithium sulfur batteries.

4. High sulfur content polymers

### 4.1 Polymeric sulfur and high sulfur content polymers

Along the 20th century there has been many research studies in order to understand the different phases of sulfur, either in its crystalline form or in its molten state[95]. From these efforts it has been stated that elemental sulfur exists as cyclic allotropes, being the octatomic sulfur ring the most stable one, that is able to pack in an orthorhombic crystalline structure at room temperature. Above 96 ºC, the crystalline structure changes towards monoclinic, and if the temperature increases up to 120 ºC, sulfur starts to melt into a yellow transparent liquid. The viscosity of the melt decreases with the increase of the

temperature, however, at around 160 ºC, the viscosity increases dramatically, being the maximum of viscosity at 200 ºC. This behavior is related with the self-polymerization of sulfur (Figure 0.13 a)). Above its floor temperature (T=159 ºC), the cyclic allotropes of sulfur break homolitically forming diradical sulfur chains. These radicals tend to react either with sulfur rings, leading to ring opening polymerization, or with other sulfur radicals by free radical polymerization. These both processes result in polymeric sulfur that can be stabilized by quenching the sulfur melt with a drastic decrease of the temperature (dry ice or liquid nitrogen). However, this polymeric sulfur is not stable at temperatures above its glass transition temperature (-30 ºC) and tend
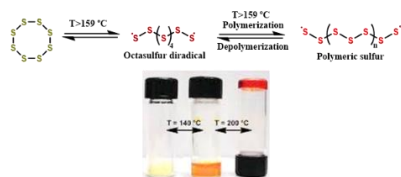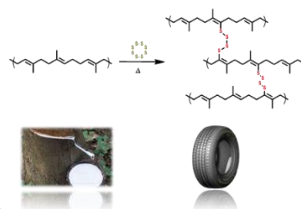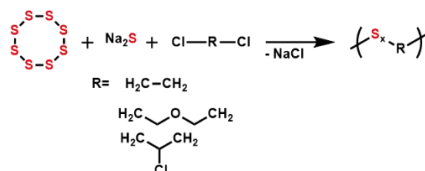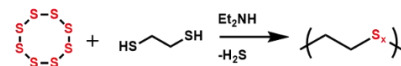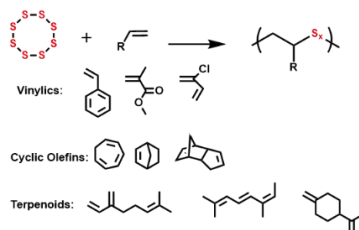

Figure 0.15: Mayor uses of sulfur in polymer science. a) self-polymerization of sulfur mechanism (ref 72). b) schematic representation of the vulcanization process (ref 71). c) typical nucleophilic condensation polymerization of alkyl dihalides with sodium polysulfide in order to obtain poly(alkyl polysulfide) polymers (ref 74). d) Polycondensation reaction of sulfur with ethylene dithiol (ref 75). e) Radical polymerization reaction of sulfur with a series of vinylic, olefinic and terpenoid monomers.

to depolymerize by back-biting from the radical chain ends forming crystalline octatomic sulfur. A way to stabilize the polymeric sulfur, developed by Tobolsky et al, goes through the capping the chain ends, preventing the depolymerization. This material resulted very insoluble and stable only up to 90 ºC, however it was applied in tire industry as a vulcanizing agent [96].

The first application of sulfur in polymer science was accidentally found by Charles Goodyear in 1830´s, when heated a film of natural rubber (composed by poly(isoprene)) in contact with elemental sulfur[22]. By the action of heat sulfur become into diradical species and reacted with the diene moieties of the Poly(isoprene), causing the crosslinking of the resin (Figure 0.13 b)). In this way, the properties of the natural rubber changed from sticky and plastic behavior to a soft and stretchable material. This process remains today, with variations on vulcanizing agent and optimization of the process, to make industrial products like tires and textiles.

Another way to synthesize high sulfur content is taking advantage of the reaction of sodium polysulfides with alkyl dihalides (figure 0.13 c)). This process, developed by Patrick and Moonkin, consist in the condensation emulsion polymerization of Na_2S_x with alkyl dihalides, obtaining good solvent and wear resistance rubbers[97]. This reaction can be easily varied by changing the polysulfide lengths (by changing the sodium sulfide: sulfur ratio) and by changing the organic dihalide. This process has been taken into industrialization, giving sealants like Thiokol rubbers. A different polycondensation reaction passes through the reaction of a dithiol with elemental sulfur, with a kind of thiol-ene reaction[98] (figure 0.14 d)).

In order to produce high sulfur content polymers with a wider variety of monomers, the free radical polymerization reaction have been studied with

sever monomers from different nature, such as vinylic, olefinic as well as terpenoid monomers (figure 0.14 e)). The first approach, by solution polymerization, were unsuccessful as sulfur acts as a radical inhibitor of thermal radical initiators[97]. Therefore, bulk polymerization of sulfur with monomers have been widely studied, especially in the 60´s and 70´s.

4.2 Inverse vulcanization reaction

In 2013 Pyun and coworkers presented new kind of polymeric materials using elemental sulfur as the major component (Figure 0.15 a)). The process was termed inverse vulcanization as, differently from classical vulcanization where sulfur acts as the crosslinker of an organic polymer, the main chain is composed of polymeric sulfur "crosslinked" by an organic comonomer. The reaction goes through the bulk copolymerization of sulfur with an organic divinylic comonomer. During the self-polymerization of sulfur at elevated temperatures, when sulfur exists as long polysulfide diradical species, the organic comonomer is added and the copolymerization occurs. The challenge of this technique was to find a high boiling point comonomer with enough controlled kinetic. The monomer 1,3-diisopropenyl benzene (DIB) showed to be readily miscible with sulfur and give very controlled reaction with 100% yield. The final materials resulted to be red, opaque and brittle at high sulfur content and transparent with the increase of the organic comonomer. The polymers with high amount of organic monomer were soluble in commonly used organic solvents what allowed to deep studies on molecular weight, molecular weight kinetic analysis (Figure 0.15 b)) and NMR analysis (Figure 0.15 c)) DSC studies determined that crystalline materials were obtained with sulfur feed ratios of < 85 wt%, whereas completely amorphous polymers could be obtained with at lower sulfur: DIB weight ratios. In this way, simply by varying the sulfur – DIB feed ratios different composition as well as thermomechanical properties could be obtained. Interestingly, the glass transition temperature of the amorphous copolymers was increasing with the increase of the organic comonomer
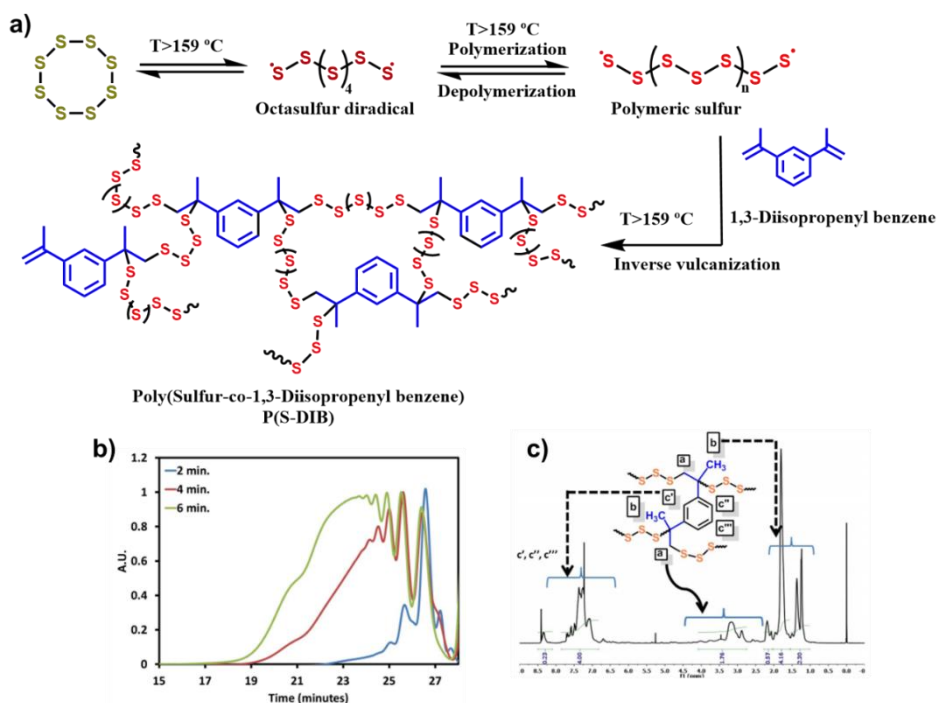
Figure 0.16: Description of inverse vulcanization reaction. a) polymerization reaction mechanism of inverse vulcanization process. b) Study of molecular weight growth of the P(S-co-DIB) polymer with reaction time. c) ^{1}H NMR spectrum of P(S-co-DIB) polymer.

suggesting a more rigid structure; however extensive thermomechanical and rheological analyses pointed out a behavior that was not crosslinked, but hyperbranched like.

The polymers made by inverse vulcanization reaction present very interesting features, combining the physicochemical properties of sulfur (such as high refractive index, high specific capacity and heavy metal trap ability) with the mechanical properties and processability of polymeric materials. Therefore, the poly(Sulfur-*co*-1,3-diisopropenyl benzene) (P(S-DIB)) have been applied in a wide range of sustainable and technological research areas. For instance, it is
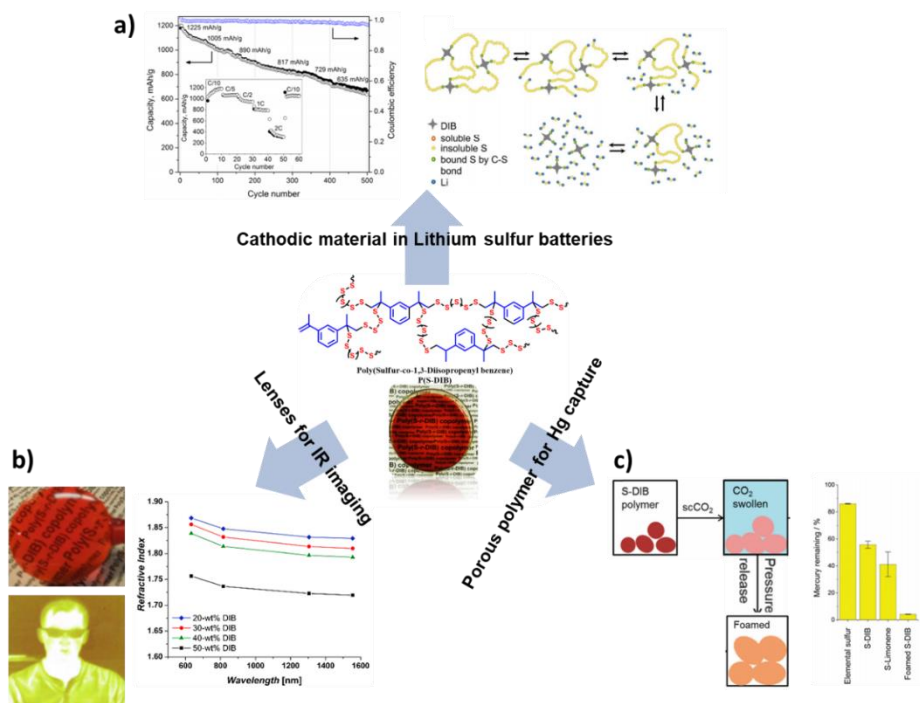
Figure 0.17: Advanced application of inverse vulcanized polymers: a) as cathodic material in lithium sulfur batteries. b) as polymeric high refractive index lenses for MRI optic devices. c) as porous polymers for water treatment and cleaning from heavy metals.

known that sulfur can capture heavy metals, such as mercury, from water solutions, however it´s bad processability and poor chemical stability hinders it´s possible application[99]. The inverse vulcanization process allows the synthesis of polymers that can be processed into advanced structures with very high sulfur content, obtaining very high heavy metal capture capacity. Another example for the application of P(S-DIB) polymers in advanced technologies is their use as IR imaging lenses[100]. Sulfur has been used as the chalcogen element for metallic chalcogen high refractive index lenses for IR imaging applications. However, these inorganic complexes have glassy behavior, that is, they are brittle and difficult to manufacture, besides of using expensive transition metals

like germanium. The P(S-DIB) polymers showed very high refractive index, as well as easy manipulation, and by easy melt impregnation procedure, high quality lenses could be obtained. Furthermore, due to the S-S bonds along the macromolecular structure, these lenses proved to be self-healing behavior, recovering the total of the transmittance of a scratched lens after a thermal treatment[101].

In addition, due to the high sulfur content in the macromolecular structure, inverse vulcanized polymers have been widely applied as cathodic material in lithium sulfur batteries[94,102]. Electrochemical tests revealed that P(S-DIB) polymer possess high capacity and similar electrochemistry towards lithium that elemental sulfur. These materials proved to have high initial capacity and higher cycling stability compared to elemental sulfur. This enhanced behavior as cathodic material has not been perfectly understood yet; nevertheless, the presence of the branching point of the polymer has a beneficial effect during the charge – discharge processes. Pyun and coworkers suggested that the organosulfide species formed during the discharge step are able to trap the lithium polysulfide intermediates and at the same time, have a "plasticizer" effect on the cathode during charge-discharge processes[94]. Furthermore, in deep studies of the cathodes with sulfur polymers revealed that the aromatic moieties from the organic comonomer made the material more compatible with the carbonaceous network, promoting the better distribution in the cathode, enhancing the electrochemical performance[103]. Theatho et al presented innovative solid-state NMR studies of cathodes formed with P(S-DIB) polymers as active material in order to characterize the redox processes during the different cycling steps[104].
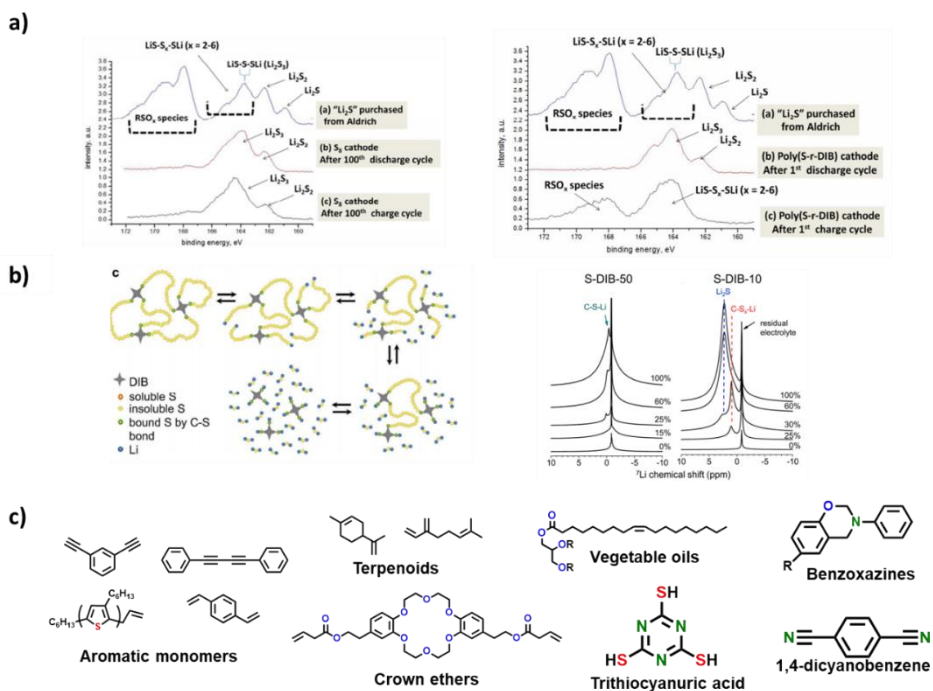
Figure 0.18: a) XPS spectra of: Left: sulfur cathodes at 100th cycle at charge and discharge state (left) and right: P(S-co-DIB) cathodes at 1st cycle at charge and discharge state. b) Schematic representation of the redox processes mechanism of P(S-co-DIB) as cathodic material (left) and solid state Li NMR of P(S-co-DIB) polymers of 10 and 50 wt% of DIB cathodes at different DOD (Deep of Discharge, right) (ref 101). c) Summary of monomers used in inverse vulcanization reaction for the synthesis of cathodic materials for lithium sulfur batteries.

The seminal work of Pyun and coworkers with the P(S-co-DIB) encouraged many researchers towards the development of novel high sulfur content polymer by inverse vulcanization with a wide range of monomers. Firsts reports were focused on monomers with similar chemical structure than the firstly reported 1,3-diisopropenyl benzene, with an aromatic core and low polarity such as 1,3-diethynylbenzene, diphenylbutadiyne, allyl functionalized polythiophene and divinylbenzene among other examples[105–108]. The inverse vulcanization process of sulfur has been extended towards other kind of monomers such as

71

natural terpenes (limonene, myrcene), vegetable oils (triglycerides) and allyl functionalized crown ethers[109–111]. This kind of monomers were found to be suitable for the reaction with sulfur radicals generated from the homolytic cleavage of the S_8 molecules at high temperature. In addition, monomers with different functionalities rather than unsaturated Carbon-carbon bonds have been spotted as alternative feedstock of comonomers for inverse vulcanization such as benzoxazines, trithiocyanuric acid (TTCA) or dicyanobenzene[112–114].

5. Objective of the PhD.

As illustrated before, lithium sulfur battery technology is a promising alternative to the actual lithium ion technology. However, new materials and battery
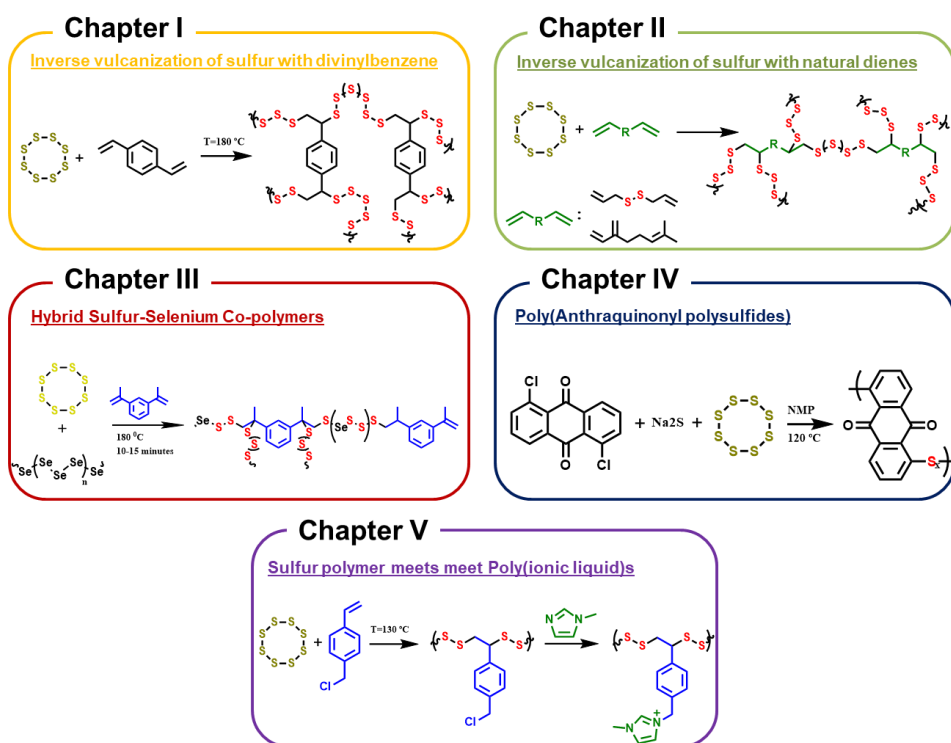

Figure 0.19: Summary of the chapters of this thesis, whit the general polymerization reactions of each chapter.

configurations are needed to overcome some critical drawbacks and technical limitations. Among the different materials being investigated, polymers offered interesting solutions and opportunities in different parts of the battery as illustrated in the previous sections. In this context, the general goal of this PhD thesis was the development of novel high sulfur content polymeric materials which can be used mostly in the cathode of lithium sulfur batteries. Five different strategies to synthesize new polymers will be presented in this manuscript as summarized in figure 0.19.

In the first chapter the inverse vulcanization reaction of sulfur with divinylbenzene was studied and optimized. This monomer, a widely used crosslinker in polymer science, was similar to the reference 1,3-Diisopropenyl benzene described by Pyun and coworkers, therefore it was a good starting point for the thesis. The reaction resulted to be faster than with 1,3-diisopropenyl benzene, yielding to amorphous and yellow materials. These materials resulted to be more rigid what eases the processability of the active material what enhances the electrochemical performance.

In the second chapter, in order to move towards more sustainable chemistry, the reaction of sulfur with natural sourced monomers was explored. Taking into account that the compatibility with molten sulfur is limited to relatively flat and apolar molecules, two natural sourced monomers susceptible to have good miscibility with sulfur were studied. Diallyl sulfide, coming from garlic and onion, and Myrcene, a molecule present in the essential oil of aromatic plants, like thyme. Additionally, Dicyclpentadiene, a olefinic insaturated cyclic monomer coming from the cracking of naphta for the obtention of ethylene, was used. The inverse vulcanization reaction was optimized yielding polymeric materials with different properties. The final battery application proved that the inverse vulcanization method can be further extended to more sustainable monomers

with similar improvement in the cyclability than the classical reaction of sulfur with organic aromatic monomers.

In the third chapter, the inverse vulcanization method was applied to the sulfur-selenium system. Selenium proved to be another interesting candidate as cathodic material, as it has comparable values of capacity than elemental sulfur and similar electrochemistry towards lithium with the advantage of being a semiconductor material. Our proposed strategy was the use of Sulfur-Selenium binary system in order to synthesize novel hybrid materials with enhanced electrochemical performance. In this chapter, the hybrid Sulfur-Selenium mixture preparation together with the inverse vulcanization process, were used in order to synthesize hybrid inorganic/organic sulfur-selenium copolymers. These materials were chemically characterized with advanced analyses prior to their study in batteries, where they proved their synergetic performance of good cycle life of an inverse vulcanized polymer and a higher C-rate capability of sulfur-selenium materials.

In the fourth chapter, a different sulfur chemistry than the inverse vulcanization used in the previous chapters was studied. The principal drawback of the inverse vulcanization process is the limited compatibility of sulfur with wide range of potential monomers in particular redox active ones. In this chapter, the combination of the ability of sulfur to form long polysulfide dianionic species in organic solvents along with the step growth polymerization reaction of alkyl or benzyl dihalides with sodium sulfide is studied. Furthermore, a commonly used organic redox molecule, anthraquinone, was used as organic comonomer. The synthesis yield to new sulfur containing polyanthraquinone polymers PAQSn that were characterized by different solid-state methods. The electrochemical characterization showed the redox combination of polysulfide segments with the anthraquinone moieties.

In the last chapter, new polymers combining the chemistry and properties of sulfur containing polymers and poly(ionic liquid)s were synthesized. The synthesis was carried out by inverse vulcanization of sulfur with a functional styrenic monomer followed by a post-polymerization modification reaction. The final materials showed the redox properties of sulfur containing polymers combined with ionic conductivity and tunable chemistry of Poly(ionic liquid)s. This chapter shows the first combination of these two polymer families which are having important applications in energy, leading to new polymeric materials with unique combination of properties.

5. References

1. Panwar, N. L., Kaushik, S. C. & Kothari, S. Role of renewable energy sources in environmental protection: A review. *Renewable and Sustainable Energy Reviews* **15,** 1513–1524 (2011).

2. Owusu, P. A. & Asumadu-Sarkodie, S. A review of renewable energy sources, sustainability issues and climate change mitigation. *Cogent Engineering* **3,** (2016).

3. Burke, M. J. & Stephens, J. C. Political power and renewable energy futures: A critical review. *Energy Research and Social Science* (2018). doi:10.1016/j.erss.2017.10.018

4. Abbasi, T., Premalatha, M. & Abbasi, S. A. The return to renewables: Will it help in global warming control? *Renewable and Sustainable Energy Reviews* (2011). doi:10.1016/j.rser.2010.09.048

5. Amponsah, N. Y., Troldborg, M., Kington, B., Aalders, I. & Hough, R. L. Greenhouse gas emissions from renewable energy sources: A review of lifecycle considerations. *Renewable and Sustainable Energy Reviews* **39,** 461–475 (2014).

6. Yang, Z. *et al.* Electrochemical energy storage for green grid. *Chemical Reviews* (2011). doi:10.1021/cr100290v

7. Larcher, D. & Tarascon, J. M. Towards greener and more sustainable batteries for electrical energy storage. *Nature Chemistry* (2015). doi:10.1038/nchem.2085

8. Ibrahim, H., Ilinca, A. & Perron, J. Energy storage systems-Characteristics and comparisons. *Renewable and Sustainable Energy Reviews* (2008). doi:10.1016/j.rser.2007.01.023

9.   Dunn, B., Kamath, H. & Tarascon, J. M. Electrical energy storage for the grid: A battery of choices. *Science* (2011). doi:10.1126/science.1212741

10.   Goodenough, J. B. & Park, K. S. The Li-ion rechargeable battery: A perspective. *Journal of the American Chemical Society* (2013). doi:10.1021/ja3091438

11.   Thackeray, M. M., Wolverton, C. & Isaacs, E. D. Electrical energy storage for transportation—approaching the limits of, and going beyond, lithium-ion batteries. *Energy & Environmental Science* (2012). doi:10.1039/c2ee21892e

12.   Armand, M. & Tarascon, J. M. Building better batteries. *Nature* (2008). doi:10.1038/451652a

13.   Mauger, A. & Julien, C. M. Critical review on lithium-ion batteries: are they safe? Sustainable? *Ionics* **23,** 1933–1947 (2017).

14.   Choi, J. W. & Aurbach, D. Promise and reality of post-lithium-ion batteries with high energy densities. *Nature Reviews Materials* (2016). doi:10.1038/natrevmats.2016.13

15.   Carbone, L., Greenbaum, S. G. & Hassoun, J. Lithium sulfur and lithium oxygen batteries: new frontiers of sustainable energy storage. *Sustainable Energy Fuels* (2017). doi:10.1039/C6SE00124F

16.   Bruce, P. G., Freunberger, S. A., Hardwick, L. J. & Tarascon, J.-M. Li–O2 and Li–S batteries with high energy storage. *Nature Materials* **11,** 19–29 (2012).

17.   Zhang, H., Li, X. & Zhang, H. in *SpringerBriefs in Molecular Science* 1–48 (2017). doi:https://doi-org.ez.library.latrobe.edu.au/10.1007/978-981-10-0746-0_1

18.   Chou, S. & Yu, Y. Next Generation Batteries: Aim for the Future. *Advanced Energy Materials* **7,** (2017).

19.   Nazar, L. F., Cuisinier, M. & Pang, Q. Lithium-sulfur batteries. *MRS Bulletin* (2014). doi:10.1557/mrs.2014.86

20.   Kutney, G. in (ed. Kutney, G. B. T.-S. (Second E.) 1–4 (ChemTec Publishing, 2013). doi:https://doi.org/10.1016/B978-1-895-19867-6.50004-8

21.   Kutney, G. in (ed. Kutney, G. B. T.-S. (Second E.) 5–41 (ChemTec Publishing, 2013). doi:https://doi.org/10.1016/B978-1-895-19867-6.50005-X

22.   Boyd, D. A. Sulfur and Its Role In Modern Materials Science. *Angewandte Chemie - International Edition* (2016). doi:10.1002/anie.201604615

23. Lim, J., Pyun, J. & Char, K. Recent approaches for the direct use of elemental sulfur in the synthesis and processing of advanced materials. *Angewandte Chemie - International Edition* (2015). doi:10.1002/anie.201409468

24. Rekondo, A. *et al.* Catalyst-free room-temperature self-healing elastomers based on aromatic disulfide metathesis. *Materials Horizons* (2014). doi:10.1039/c3mh00061c

25. Martín, R. *et al.* Room temperature self-healing power of silicone elastomers having silver nanoparticles as crosslinkers. *Chemical Communications* (2012). doi:10.1039/c2cc32030d

26. Tonin, G. *et al.* Multiscale characterization of a lithium/sulfur battery by coupling operando X-ray tomography and spatially-resolved diffraction. *Scientific Reports* (2017). doi:10.1038/s41598-017-03004-4

27. Zhao, E. *et al.* Advanced Characterization Techniques in Promoting Mechanism Understanding for Lithium-Sulfur Batteries. *Advanced Functional Materials* (2018). doi:10.1002/adfm.201707543

28. Wild, M. *et al.* Lithium sulfur batteries, a mechanistic review. *Energy and Environmental Science* (2015). doi:10.1039/c5ee01388g

29. Chung, S. H., Chang, C. H. & Manthiram, A. Progress on the Critical Parameters for Lithium-Sulfur Batteries to be Practically Viable. *Advanced Functional Materials* (2018). doi:10.1002/adfm.201801188

30. Li, G. *et al.* Revisiting the Role of Polysulfides in Lithium–Sulfur Batteries. *Advanced Materials* **30,** 1705590 (2018).

31. Tao, T. *et al.* Anode Improvement in Rechargeable Lithium–Sulfur Batteries. *Advanced Materials* (2017). doi:10.1002/adma.201700542

32. Cheng, X.-B., Huang, J.-Q. & Zhang, Q. Review—Li Metal Anode in Working Lithium-Sulfur Batteries. *Journal of The Electrochemical Society* (2018). doi:10.1149/2.0111801jes

33. Judez, X. *et al.* Review—Solid Electrolytes for Safe and High Energy Density Lithium-Sulfur Batteries: Promises and Challenges. *Journal of The Electrochemical Society* (2018). doi:10.1149/2.0041801jes

34. Yamin, H. & Peled, E. Electrochemistry of a nonaqueous lithium/sulfur cell. *Journal of Power Sources* **9,** 281–287 (1983).

35. Shim, J., Striebel, K. A. & Cairns, E. J. The Lithium/Sulfur Rechargeable Cell - Effects of Electrode Composition and Solvent on Cell Performance. *J. Electrochem. Soc.* **149,** A1321 (2002).

36. Mikhaylik, Y. V. & Akridge, J. R. Low Temperature Performance of Li/S Batteries. *Journal of The Electrochemical Society* **150,** A306 (2003).

77

37.   Ji, X., Lee, K. T. & Nazar, L. F. A highly ordered nanostructured carbon-sulphur cathode for lithium-sulphur batteries. *Nature Materials* **8,** 500–506 (2009).

38.   Kumar, R., Liu, J., Hwang, J.-Y. & Sun, Y.-K. Recent research trends in Li–S batteries. *Journal of Materials Chemistry A* **6,** 11582–11605 (2018).

39.   He, Y., Chang, Z., Wu, S. & Zhou, H. Effective strategies for long-cycle life lithium-sulfur batteries. *Journal of Materials Chemistry A* (2018). doi:10.1039/c8ta01115j

40.   Dirlam, P. T., Glass, R. S., Char, K. & Pyun, J. The use of polymers in Li-S batteries: A review. *Journal of Polymer Science, Part A: Polymer Chemistry* (2017). doi:10.1002/pola.28551

41.   Lee, Y. M., Choi, N. S., Park, J. H. & Park, J. K. Electrochemical performance of lithium/sulfur batteries with protected Li anodes. in *Journal of Power Sources* (2003). doi:10.1016/S0378-7753(03)00300-8

42.   Ma, G. *et al.* Enhanced cycle performance of a Li-S battery based on a protected lithium anode. *Journal of Materials Chemistry A* (2014). doi:10.1039/c4ta04172k

43.   Shuang, J. *et al.* Nafion/Titanium Dioxide-Coated Lithium Anode for Stable Lithium–Sulfur Batteries. *Chemistry – An Asian Journal* **13,** 1379–1385 (2018).

44.   He, Y., Qiao, Y. & Zhou, H. Recent advances in functional modification of separators in lithium-sulfur batteries. *Dalton Transactions* (2018). doi:10.1039/c7dt04717g

45.   Fan, W., Zhang, L. & Liu, T. Multifunctional second barrier layers for lithium–sulfur batteries. *Materials Chemistry Frontiers* (2018). doi:10.1039/C7QM00405B

46.   Huang, J. Q. *et al.* Ionic shield for polysulfides towards highly-stable lithium-sulfur batteries. *Energy and Environmental Science* (2014). doi:10.1039/c3ee42223b

47.   Cai, W. *et al.* A novel laminated separator with multi functions for high-rate dischargeable lithium–sulfur batteries. *Journal of Power Sources* (2015). doi:10.1016/j.jpowsour.2015.03.085

48.   Hao, Z. *et al.* High performance lithium-sulfur batteries with a facile and effective dual functional separator. *Electrochimica Acta* (2016). doi:10.1016/j.electacta.2016.03.166

49.   Conder, J., Urbonaite, S., Streich, D., Novák, P. & Gubler, L. Taming the polysulphide shuttle in Li-S batteries by plasma-induced asymmetric functionalisation of the separator. *RSC Advances* (2015). doi:10.1039/c5ra13197a

50.   Conder, J. *et al.* Performance-Enhancing Asymmetric Separator for Lithium-Sulfur Batteries. *ACS Applied Materials and Interfaces* (2016). doi:10.1021/acsami.6b04662

51.   Gu, M. *et al.* Inhibiting the shuttle effect in lithium-sulfur batteries using a layer-by-layer assembled ion-permselective separator. *RSC Advances* (2014). doi:10.1039/c4ra09718a

52.   Li, G. C. *et al.* A hydrophilic separator for high performance lithium sulfur batteries. *Journal of Materials Chemistry A* **3,** 11014–11020 (2015).

53.   Zhang, Z., Zhang, Z., Li, J. & Lai, Y. Polydopamine-coated separator for high-performance lithium-sulfur batteries. *Journal of Solid State Electrochemistry* (2015). doi:10.1007/s10008-015-2797-8

54.   Zhang, S., Ueno, K., Dokko, K. & Watanabe, M. Recent Advances in Electrolytes for Lithium-Sulfur Batteries. *Advanced Energy Materials* (2015). doi:10.1002/aenm.201500117

55.   Manthiram, A., Fu, Y., Chung, S.-H., Zu, C. & Su, Y.-S. Rechargeable Lithium–Sulfur Batteries. *Chemical Reviews* **114,** 11751–11787 (2014).

56.   Marmorstein, D. *et al.* Electrochemical performance of lithiumrsulfur cells with three different polymer electrolytes. *Journal of Power Sources* (2000). doi:10.1016/S0378-7753(00)00432-8

57.   Jeong, S. S. *et al.* Electrochemical properties of lithium sulfur cells using PEO polymer electrolytes prepared under three different mixing conditions. *Journal of Power Sources* (2007). doi:10.1016/j.jpowsour.2007.06.108

58.   Croce, F., Appetecchi, G. B., Persi, L. & Scrosati, B. Nanocomposite polymer electrolytes for lithium batteries. *Nature* (1998). doi:10.1038/28818

59.   Ben youcef, H., Garcia-Calvo, O., Lago, N., Devaraj, S. & Armand, M. Cross-Linked Solid Polymer Electrolyte for All-Solid-State Rechargeable Lithium Batteries. *Electrochimica Acta* (2016). doi:10.1016/j.electacta.2016.10.122

60.   Judez, X. *et al.* Lithium Bis(fluorosulfonyl)imide/Poly(ethylene oxide) Polymer Electrolyte for All Solid-State Li-S Cell. *Journal of Physical Chemistry Letters* (2017). doi:10.1021/acs.jpclett.7b00593

61.   Shin, J. H., Jung, S. S., Kim, K. W., Ahn, H. J. & Ahn, J. H. Preparation and characterization of plasticized polymer electrolytes based on the PVdF-HFP copolymer for lithium/sulfur battery. *Journal of Materials Science: Materials in Electronics* (2002). doi:10.1023/A:1021521207247

62.   Gao, S. *et al.* Poly(vinylidene fluoride)-based hybrid gel polymer electrolytes for additive-free lithium sulfur batteries. *Journal of Materials*

Chemistry A (2017). doi:10.1039/c7ta05145j

63.   Yang, W., Yang, W., Feng, J., Ma, Z. & Shao, G. High capacity and cycle stability Rechargeable Lithium-Sulfur batteries by sandwiched gel polymer electrolyte. *Electrochimica Acta* (2016). doi:10.1016/j.electacta.2016.05.087

64.   Rao, M., Geng, X., Li, X., Hu, S. & Li, W. Lithium-sulfur cell with combining carbon nanofibers-sulfur cathode and gel polymer electrolyte. *Journal of Power Sources* (2012). doi:10.1016/j.jpowsour.2012.03.111

65.   Choi, I. Y., Kim, H. & Park, M. J. Making a better organic-inorganic composite electrolyte to enhance the cycle life of lithium-sulfur batteries. *RSC Advances* (2014). doi:10.1039/c4ra12657b

66.   Gao, J. *et al.* Lithiated Nafion as polymer electrolyte for solid-state lithium sulfur batteries using carbon-sulfur composite cathode. *Journal of Power Sources* (2018). doi:10.1016/j.jpowsour.2018.01.063

67.   Baloch, M. *et al.* Application of Gel Polymer Electrolytes Based on Ionic Liquids in Lithium-Sulfur Batteries. *Journal of The Electrochemical Society* **163,** A2390–A2398 (2016).

68.   Zhang, J. *et al.* Nanostructured Host Materials for Trapping Sulfur in Rechargeable Li-S Batteries: Structure Design and Interfacial Chemistry. *Small Methods* (2017). doi:10.1002/smtd.201700279

69.   Liu, J., Zhang, Q. & Sun, Y.-K. Recent progress of advanced binders for Li-S batteries. *Journal of Power Sources* **396,** 19–32 (2018).

70.   Li, G. *et al.* Acacia Senegal-Inspired Bifunctional Binder for Longevity of Lithium-Sulfur Batteries. *Advanced Energy Materials* (2015). doi:10.1002/aenm.201500878

71.   Seh, Z. W. *et al.* Stable cycling of lithium sulfide cathodes through strong affinity with a bifunctional binder. *Chemical Science* (2013). doi:10.1039/c3sc51476e

72.   Peled, E. *et al.* The Effect of Binders on the Performance and Degradation of the Lithium/Sulfur Battery Assembled in the Discharged State. *Journal of The Electrochemical Society* (2017). doi:10.1149/2.0161701jes

73.   Vizintin, A., Guterman, R., Schmidt, J., Antonietti, M. & Dominko, R. Linear and Crosslinked Ionic Liquid Polymers as Binders in Lithium-Sulfur Battery. *Chemistry of Materials* (2018). doi:10.1021/acs.chemmater.8b02357

74.   Yan, L. *et al.* Ionically cross-linked PEDOT:PSS as a multi-functional conductive binder for high-performance lithium–sulfur batteries. *Sustainable Energy & Fuels* **2,** 1574–1581 (2018).

75. Li, W. *et al.* High-performance hollow sulfur nanostructured battery cathode through a scalable, room temperature, one-step, bottom-up approach. *Proceedings of the National Academy of Sciences* (2013). doi:10.1073/pnas.1220992110

76. Sun, Z. *et al.* Electrostatic shield effect: An effective way to suppress dissolution of polysulfide anions in lithium-sulfur battery. *Journal of Materials Chemistry A* (2014). doi:10.1039/c4ta03570d

77. Li, L. *et al.* PEO-coated sulfur-carbon composite for high-performance lithium-sulfur batteries. *Journal of Solid State Electrochemistry* **19,** 3373–3379 (2015).

78. Xiao, L. *et al.* A soft approach to encapsulate sulfur: Polyaniline nanotubes for lithium-sulfur batteries with long cycle life. *Advanced Materials* (2012). doi:10.1002/adma.201103392

79. Chen, H. *et al.* Ultrafine Sulfur Nanoparticles in Conducting Polymer Shell as Cathode Materials for High Performance Lithium/Sulfur Batteries. *Scientific Reports* (2013). doi:10.1038/srep01910

80. Deng, Y. *et al.* Durable polydopamine-coated porous sulfur core–shell cathode for high performance lithium–sulfur batteries. *Journal of Power Sources* **300,** 386–394 (2015).

81. Li, W. *et al.* Understanding the role of different conductive polymers in improving the nanostructured sulfur cathode performance. *Nano Letters* (2013). doi:10.1021/nl403130h

82. Yang, Y. *et al.* Improving the performance of lithium-sulfur batteries by conductive polymer coating. *ACS Nano* (2011). doi:10.1021/nn203436j

83. Li, Y. *et al.* Improving the electrochemical performance of a lithium–sulfur battery with a conductive polymer-coated sulfur cathode. *RSC Advances* **5,** 44160–44164 (2015).

84. Huang, J. Q. *et al.* Aligned sulfur-coated carbon nanotubes with a polyethylene glycol barrier at one end for use as a high efficiency sulfur cathode. *Carbon* (2013). doi:10.1016/j.carbon.2013.02.037

85. Song, J., Choo, M. J., Noh, H., Park, J. K. & Kim, H. T. Perfluorinated ionomer-enveloped sulfur cathodes for lithium-sulfur batteries. *ChemSusChem* (2014). doi:10.1002/cssc.201402789

86. Kim, E. T. *et al.* Conformal Polymeric Multilayer Coatings on Sulfur Cathodes via the Layer-by-Layer Deposition for High Capacity Retention in Li-S Batteries. *ACS Macro Letters* (2016). doi:10.1021/acsmacrolett.6b00144

87. Liu, M., Visco, S. J. & De Jonghe, L. C. Electrochemical Properties of Organic Disulfde/thiolate Redox Couples. *J. Electrochem. Soc.* (1989).

doi:10.1149/1.2097478

88. Doeff, M. M., Visco, S. J. & De Jonghe, L. C. The use of redox polymerization electrodes in lithium batteries with liquid electrolytes. *Journal of Applied Electrochemistry* **22,** 307–309 (1992).

89. B., P. M., Bernd, O., J., H. C., Ram, S. & Fred, W. High Sulfur Content Material with Stable Cycling in Lithium-Sulfur Batteries. *Angewandte Chemie International Edition* **56,** 15118–15122

90. Liu, X. *et al.* A Hyperbranched Disulfide Polymer as Cathode Material for Lithium-Ion Batteries. *Journal of The Electrochemical Society* **165,** A1297–A1302 (2018).

91. Baloch, M. *et al.* New Redox Polymers that Exhibit Reversible Cleavage of Sulfur Bonds as Cathode Materials. *ChemSusChem* (2016). doi:10.1002/cssc.201601032

92. Fanous, J., Wegner, M., Grimminger, J., Andresen, Ä. & Buchmeiser, M. R. Structure-related electrochemistry of sulfur-poly(acrylonitrile) composite cathode materials for rechargeable lithium batteries. *Chemistry of Materials* (2011). doi:10.1021/cm202467u

93. Zeng, S. *et al.* Conducting Polymers Crosslinked with Sulfur as Cathode Materials for High-Rate, Ultralong-Life Lithium–Sulfur Batteries. *ChemSusChem* **10,** 3378–3386 (2017).

94. Simmonds, A. G. *et al.* Inverse Vulcanization of Elemental Sulfur to Prepare Polymeric Electrode Materials for Li–S Batteries. *ACS Macro Letters* **3,** 229–232 (2014).

95. Tobolsky, A. V. Polymeric Sulfur and Related Polymers*. *Journal of Polymer Science: Part C* (1966). doi:10.1002/polc.5070120107

96. Tobolsky, A. V, MacKnight, W., Beevers, R. B. & Gupta, V. D. The glass transition temperature of polymeric sulphur. *Polymer* **4,** 423–427 (1963).

97. Griebel, J. J., Glass, R. S., Char, K. & Pyun, J. Polymerizations with elemental sulfur: A novel route to high sulfur content polymers for sustainability, energy and defense. *Progress in Polymer Science* **58,** 90–125 (2016).

98. Bordoloi, B. K. & Pearce, E. M. Kinetics of the base-catalyzed reactions of cyclo-octameric and catenapolymeric sulfur with dithiol. *Journal of Applied Polymer Science* (1979). doi:10.1002/app.1979.070230920

99. Hasell, T., Parker, D. J., Jones, H. A., McAllister, T. & Howdle, S. M. Porous inverse vulcanised polymers for mercury capture. *Chem. Commun.* **52,** 5383–5386 (2016).

100. Griebel, J. J. *et al.* New Infrared Transmitting Material via Inverse

Vulcanization of Elemental Sulfur to Prepare High Refractive Index Polymers. *Advanced Materials* **26,** 3014–3018 (2014).

101. Griebel, J. J. *et al.* Dynamic Covalent Polymers via Inverse Vulcanization of Elemental Sulfur for Healable Infrared Optical Materials. *ACS Macro Letters* **4,** 862–866 (2015).

102. Chung, W. J. *et al.* The use of elemental sulfur as an alternative feedstock for polymeric materials. *Nat Chem* **5,** 518–524 (2013).

103. Oleshko, V. P. *et al.* Multimodal Characterization of the Morphology and Functional Interfaces in Composite Electrodes for Li-S Batteries by Li Ion and Electron Beams. *Langmuir* (2017). doi:10.1021/acs.langmuir.7b00978

104. Hoefling, A. *et al.* Mechanism for the Stable Performance of Sulfur-Copolymer Cathode in Lithium-Sulfur Battery Studied by Solid-State NMR Spectroscopy. *Chemistry of Materials* (2018). doi:10.1021/acs.chemmater.7b05105

105. Sun, Z. *et al.* Sulfur-rich polymeric materials with semi-interpenetrating network structure as a novel lithium–sulfur cathode. *Journal of Materials Chemistry A* **2,** 9280 (2014).

106. Oschmann, B. *et al.* Copolymerization of Polythiophene and Sulfur to Improve the Electrochemical Performance in Lithium-Sulfur Batteries. *Chemistry of Materials* **27,** 7011–7017 (2015).

107. Dirlam, P. T. *et al.* Inverse vulcanization of elemental sulfur with 1,4-diphenylbutadiyne for cathode materials in Li–S batteries. *RSC Advances* **5,** 24718–24722 (2015).

108. Gomez, I. *et al.* Inverse vulcanization of sulfur with divinylbenzene: Stable and easy processable cathode material for lithium-sulfur batteries. *Journal of Power Sources* (2016). doi:10.1016/j.jpowsour.2016.08.046

109. Crockett, M. P. *et al.* Sulfur-Limonene Polysulfide: A Material Synthesized Entirely from Industrial By-Products and Its Use in Removing Toxic Metals from Water and Soil. *Angewandte Chemie - International Edition* **55,** 1714–1718 (2016).

110. Behr, A. & Johnen, L. Myrcene as a natural base chemical in sustainable chemistry: A critical review. *ChemSusChem* **2,** 1072–1095 (2009).

111. Worthington, M. J. H. *et al.* Laying Waste to Mercury: Inexpensive Sorbents Made from Sulfur and Recycled Cooking Oils. *Chemistry - A European Journal* (2017). doi:10.1002/chem.201702871

112. Shukla, S. *et al.* Cardanol benzoxazine-Sulfur Copolymers for Li-S batteries: Symbiosis of Sustainability and Performance. *ChemistrySelect*

1, 594–600 (2016).

113. Je, S. H. *et al.* Rational Sulfur Cathode Design for Lithium-Sulfur Batteries: Sulfur-Embedded Benzoxazine Polymers. *ACS Energy Letters* (2016). doi:10.1021/acsenergylett.6b00245

Chapter I

Inverse vulcanization of sulfur with divinyl benzene: Stable and easy processable cathode materials for lithium sulfur batteries
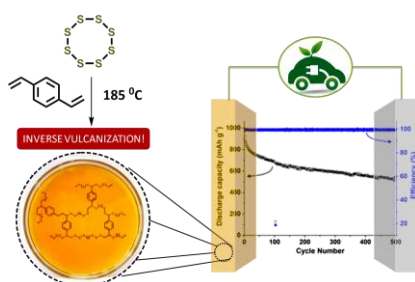
1 Introduction

Lithium-Sulfur (Li-S) battery technology is one of the promising candidates for next generation energy storage systems with low cost and high energy density. According to the complete reduction from elemental sulfur to lithium sulfide (Li_2S), sulfur is expected to deliver a specific capacity of 1675 A h Kg^{-1}. At the cell level, the best Li-S batteries offer specific energies on the order of 500-600 Wh Kg^{-1} [1–5]. Furthermore, the elemental sulfur is naturally abundant, has low toxicity and it is a cheap raw material for chemical and petrochemical industry[6]. Beyond its interesting intrinsic properties, namely the high electrochemical capacity and refractive indexes, sulfur possesses a very low conductivity and complex electrochemistry[6–8]. These two characteristics lead to a series of limitations on its performance as an active cathode material in batteries. Firstly, the cathodes need a large amount of conductive carbon additives to improve the low conductivity of sulfur which limits the real capacity of the batteries. Secondly, the chemical reactions involved in the Li-S cells generate several intermediates (lithium polysulfides (PS)), which subsequently form insoluble precipitate of Li_2S_2 and Li_2S[9,10]. Long chains PS, (Li_2S_8 and Li_2S_6) are dissolved in liquid electrolyte and cause parasitic reactions when they migrate towards the Li anode (loss of active materials, formation of insulating layer)[10]. This phenomenon, so called polysulfide shuttle, leads to very low battery efficiency, reduced cyclability and short cycle life[10,11].

To tackle the different problems related to the Li-S technology, different paths have been investigated and highlighted in recent reviews of Li-S batteries[5,10,12]. Most of the approaches were directed toward the protection of Li anode; the use of porous separators and development of new electrolytes; the use of structured microporous carbons, metal oxides and new binders in order to reduce the polysulfide shuttle problem[13–23].

In our opinion, a few efforts have been focused on modifying the chemistry of elemental sulfur itself as key parameter in Li-S batteries. Recently, Pyun and coworkers have proposed the inverse vulcanization of molten sulfur using low amount of dienes as route to prepare new sulfur polymers cathode[6]. The concept was demonstrated by crosslinking of elemental sulfur using 1,3-diisopropenylbenzene (DIB) which is an expensive crosslinker agent with slow copolymerization kinetics (alpha methyl group in the vinyl group). Other similar studies also have involved the use of expensive chemicals as cross-linkers. For instance, diethynylbenzene was used by Meng et al. to copolymerize sulfur at high temperature, 1,4-Diphenylbutadiyne was used to prepare high sulfur content polymers as cathodic materials or a thiophene monomer having allyl groups[24–26].

In this work we propose the inverse vulcanization of sulfur using divinylbenzene (DVB) to create a sulfur/organic polymer network with good chemical stability and easy processability. DVB is a well-known relatively cheap chemical commonly used as crosslinker in polymer industry. Compared to most inverse vulcanization reports that show reaction times between 1 and 2 h, the high reactivity of DVB monomer makes possible to prepare copolymers in a very fast way 5 min at low DVB contents and 15 min at high DVB content[24–27]. This is even faster than the inverse vulcanization of sulfur using DIB, which was the fastest inverse vulcanization reaction reported so far, taking place between 10 and 20 min. In this paper, we report the synthesis and characterization of sulfur-DVB copolymers (poly (S-DVB)), together with its promising electrochemical performance and long term testing as cathodes in Li-S batteries.

2. Experimental

2.1 Materials and methods

Elemental sulfur (purum p. a.; 99.5%) and divinylbenzene (DVB) (technical grade 80%; Sigma-Aldrich) were used as received.

The general reaction of inverse vulcanization of sulfur with DVB was performed as follows. In a round bottom flask equipped with a magnetic stir bar elemental sulfur (9 g, 0.281 mol) was added under argon atmosphere. Then the flask was placed in an oil bath preheated at 185 ^{0}C. When the liquid sulfur showed a cherry red color DVB (1 g, 0.0077 mol) was added. Two phases were observed but they became a single one with the reaction time. The solution was stirred until the vitrification of the media. Then the flask was placed in a liquid nitrogen bath in order to quench the reaction as well as to break the solid block. Yellow transparent crystals were obtained. It is worth pointing out that for the copolymers with DVB content superior to 20 wt% an additional step was done. In this case, the reaction was allowed to stir until a rise in the viscosity was observed and then the reaction was quenched in a liquid nitrogen bath. In this case, opaque and soft material was obtained. In order to promote all the reaction of the DVB with free sulfur a curing step at 120 ^{0}C during 3 h in the oven was performed and the result was a hard and transparent copolymer. The composition of the synthesized solids was determined via FTIR spectroscopy using a Vertex 70 (Bruker) FTIR System spectrometer with the ATR setup which allowed for sample examination in the form of powder. The molecular composition was elucidated by ^{1}H NMR. The NMR measurements of the DVB monomer and poly (S-DVB) 50 wt% of DVB were carried out on a Bruker AVANCE 400 spectrometer with $CDCl_3$-d^6 as solvent. The thermal characterization of the poly (S-DVB) was carried out in the DSC (Q2000, TA instruments) from -40 ^{0}C to 140 ^{0}C with a heating rate of 10 ^{0}C/min. Two cycles of heating were carried out. The thermogravimetric analyses (TGA) of the elemental sulfur and the poly (S-DVB) were determined on a Netsch STA with a heating rate of 10 ^{0}C/min under N_2.

2.1 Electrochemical characterization

Positive electrodes were prepared using 60% in weight of the selected sulfur copolymers in the final cathode. The selected sulfur copolymers were dry ball milled prior to the cathode preparation, turning into a fine pale yelowish powder. Afterwards, a mixture of Ketjen Black 600JD (AkzoNobel) and the selected copolymer was wet dry milled in ethanol for 3 h. The mixture was dried and added to a solution of polyvinylidene fluoride 5130 (SOLVAY) in Nmethylpyrrolidone to form the cathodic slurry. Slurries with a final solid content of 30% were prepared by using mechanical mixer (RW 20 digital, IKA) at 600 rpm. These slurries were blade cast onto a carbon-coated aluminum foil (MTI Corp.) and dried at 60 ⁰C under dynamic vacuum during 12 h before cell assembly. The cathodes were prepared for a theoretical capacity of 2.7 mAh cm-2. One layer of commercial polyolefin separator (Celgard 2501) soaked with 50 µL of 0.38 M solution of bis(trifluoromethane)sulfonamide lithium salt (LiTFSI; Sigma–Aldrich) and 0.32 M of LiNO3 (Sigma–Aldrich) as additive in a 1:1 (v/v) mixture of dimethoxyethane (BASF) and dioxolane (BASF), was placed between electrodes. Lithium metal (0.05 mm, Rockwood Lithium) was used as the anode in coin half cells (2025, Hohsen). Vacuum drying of electrodes and cell crimping was performed in a dry room with a dew point below -50 0C. Thereafter, assembled cells were aged during 20 h and then cycled using a BaSyTec Cell Test System (Germany) at 25:1 ⁰C under air. The electrochemical behavior of the obtained sulfur copolymer electrodes was evaluated at different C rates considering the theoretical capacity of elemental sulfur (1672 mAh g-1). The cyclability of coin cells was investigated within a 1.7–2.6 V interval at C/5 charge and discharge current rates. Cyclic voltammetry experiments were performed in a coin cell at a scan rate of 10 mV s-1 from 2.8 to 1.5 V.*3.*

Results and discussion

3.1 Synthesis

In this work a series of copolymers with varying compositions of DVB between 5 and 50 wt% were synthesized. The inverse vulcanization reaction was conducted through the melting of sulfur above its floor temperature (T>160 ºC) where the stable cyclic allotropes of sulfur suffer from homolytic cleavage forming diradical polysulfanes. Afterwards the organic commoner DVB is added. It is worth to note that DVB is a very reactive diene and allows the inverse vulcanization of sulfur in a very fast time (Figure 1.1). Compared to other inverse vulcanization reports that show reaction times between 1 and 2 h the synthesis with DVB lasts between 5 and 15 min (depending the amount of DVB), even faster than the reaction of sulfur with DIB, that was the fastest inverse vulcanization reaction reported so far[6,24–27].

3.2 Physicochemical characterization

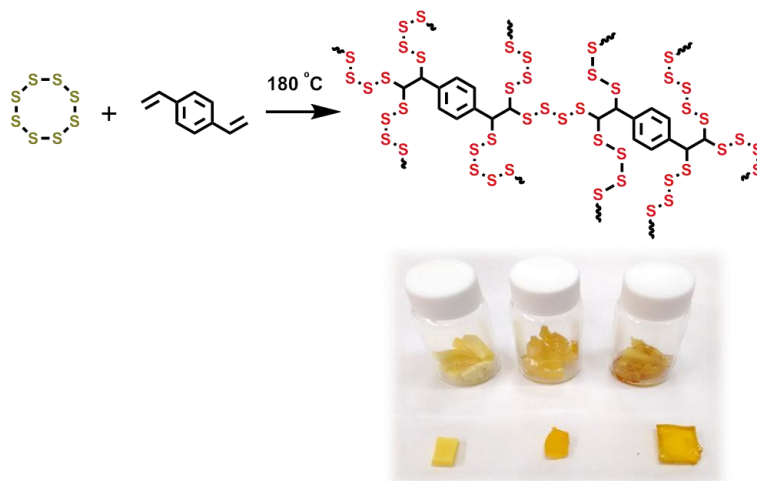In order to elucidate the chemical nature of the poly (S-DVB), the FTIR-ATR

Figure 1.1: Schematic representation of the inverse vulcanization reaction of sulfur with Divinylbenzene with digital images of each step of the reaction.

spectrum was first carried out and compared to the spectra of elemental sulfur (Figure 1.2). It is clear that the peak appearing at 465 cm^{-1} is attributed to the S-S bond which is visible in both the sulfur and poly (S-DVB). The C-S stretching peak is appearing at 648 cm^{-1}, while the different peaks appearing in the region between 700 cm^{-1} and 900 cm^{-1} are attributed to the C-H bond of the DVB isomers. Moreover, the FTIR spectra show the existence of the C=C stretch (Aromatic; appearing at 1600 cm^{-1} attributed to the aromatic benzylic ring). It is to be noted here that the used DVB is 80% grade, which is a mixture of 2 isomers (p-DVB and m-DVB), whereas the remaining 20% are the non-crosslinking isomers, namely, 3-ethylvinylbenzens and 4-ethylvinylbenzene. The para- and meta-species can be distinguished by distinct positions of some of their respective absorption peaks. Indeed, distinct and unique bands at 1484 cm^{-1} and 1512 cm^{-1} are assigned for meta-disubstituted benzene and para-disubstituted benzene, respectively.

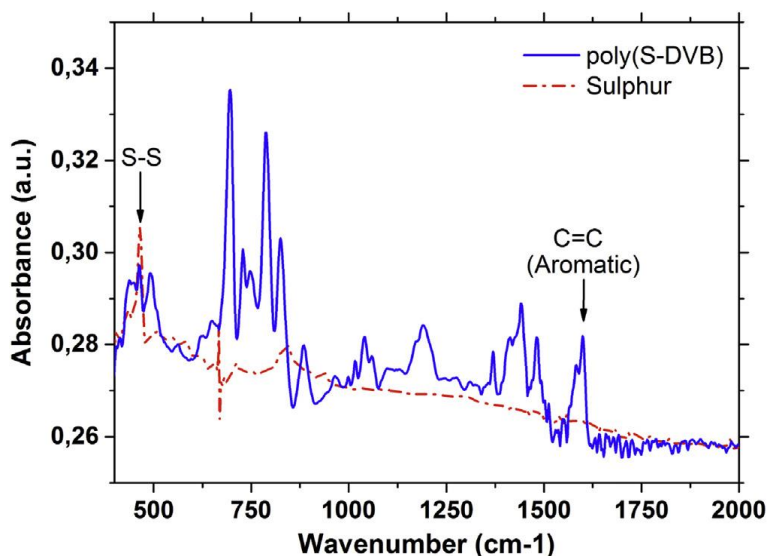It was observed that the solubility of poly (S-DVB) copolymers in organic

Figure 1.2: FTIR-ATR spectrum of the obtained P(S-DVB) copolymer compared with the spectrum of bare sulfur

solvents increases with the DVB content. At low contents (<20 wt%) in the organic comonomer DVB, the obtained copolymers tend to behave as elemental sulfur in the physical properties such as solubility and crystallinity. However, at high DVB contents (>40 wt%), the nature of the material tends to change and it behaves similar as an organic polymer becoming soluble in common non-polar solvents such as chloroform and toluene. This allows to further characterization of the chemical composition of the copolymers by liquid ^{1}H NMR spectroscopy. The ^{1}H NMR spectrum of divinylbenzene and poly (S-DVB) having 50 wt% of DVB are depicted in Figure 1.3. The spectrum shows the disappearance of the signals from vinyl protons, which indicates the total reaction of all the vinyl groups of the DVB cross-linker. Furthermore, two different sets of new signals appeared in the NMR spectrum. The peaks between 1 and 2 ppm (labelled as "a" protons) indicated the presence of alkyl protons which may be due to the copolymerization of the vinyl with other vinyl groups. The second set of signals between 2.5 and 4.5 ppm (labelled as "b" protons) are assigned to the protons of methylene groups near to a polysulfide chain. Interesting the integration between the signals coming from vinyl-vinyl
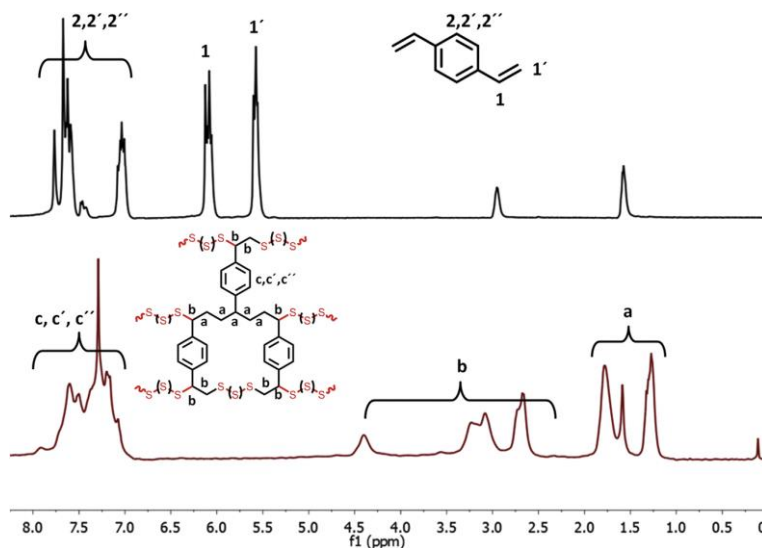

Figure 1.3: ^{1}H NMR spectra of the obtained P(S-DVB) (50 %wt of S, bottom part) compared with the spectrum of the organic monomer Divinyl bezene

bonds or vinyl-sulfur bonds is equilibrated. These results are similar to those presented in previous inverse vulcanization reports using other organic dienes such as 1,3-diisopropenylbenzene as cross-linkers which indicates that sulfur and DVB are randomly distributed in the final poly (S-DVB) materials.

Next the thermal properties of the copolymers were characterized by Differential Scanning Calorimetry (DSC) (Figure 1.4, a)). Elemental sulfur is a yellow crystalline material with a Tm of 107 ^{0}C for the monoclinic sulfur and a Tm of 120 ^{0}C for the orthorhombic sulfur. Interestingly, the poly (S-DVB) copolymers were glassy without showing crystallization due to the presence of unreacted sulfur. Thus, a gradual increase in the glass transition of the poly (S-DVB) copolymers is observed with the increase of the DVB content, which varies from
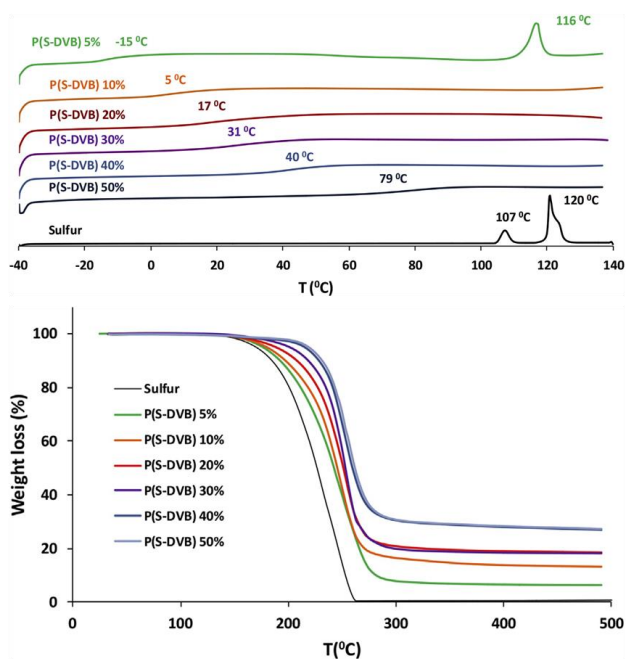

Figure 1.4: Top, DSC thermograms of the obtained P(S-DVB) polymers changing the initial feed ratios (from 95 to 50 wt% of sulfur). Bottom, TGA thermograms of the obtained P(S-DVB) polymers changing the initial feed ratios (from 95 to 50 wt% of sulfur).

-15 ^{0}C to 79 ^{0}C. (-15 ^{0}C for the copolymer with 5 wt% of DVB, 5 ^{0}C for 10 wt% of DVB,17 ^{0}C for 20 wt% DVB, 31 ^{0}C for 30 wt% DVB, 40 ^{0}C for 40 wt% DVB and 79 ^{0}C for the highest ratio of 50 wt% DVB). Only the copolymers resulting from the copolymerization with the low amounts of DVB (5 wt%) turn to opaque and brittle upon storage and their DSC thermograms show a melting peak at 116 ^{0}C. This may be associated to the crystallization of long polysulfide chains or unreacted sulfur. Altogether, the poly (S-DVB) copolymers are amorphous and show a gradual increase of the glass transition that further indicates the random nature of the copolymerization between elemental sulfur and DVB. In order to determine the thermal stability of the poly (S-DVB) copolymers, thermal gravimetric analysis (TGA) were carried out under Nitrogen atmosphere (Figure 1.4, b)). In all cases, it can be seen a single degradation step, which is related with the loss of sulfur and volatile sulfides of the polymer. It is worth pointing out that the onset of the degradation is delayed with the increase of the DVB crosslinker content in the copolymers. The TGA of the elemental sulfur shows a complete degradation and weight loss up to 100% after 280 ^{0}C, while the poly (S-DVB) copolymers show in all cases some residue which increases with the DVB content. It is worth noting that the residue of the copolymers with lowest amount of DVB is comparable and directly related with the added comonomer weight in the reaction feed.

3.2 Electrochemical characterization

The galvanostatic cycling were performed on electrodes containing 90 wt% of S and 10% of DVB in poly (S-DVB) as active material. It is well known that the higher the sulfur content the higher the theoretical capacity. 2032 type coin cells vs. Li/Li$^+$ were tested at C/10, C/5, C/2.5 and 1C (Figure 5 a)). The capacity decreases to about 400 mAh g^{-1} at fast charge/discharge current density (1C).

The initial specific discharge capacity exhibited at C/4 exceeded 950 mAh g^{-1}, and after 500 cycles the capacity obtained is around 700 mAh g^{-1} (Figure 1.5
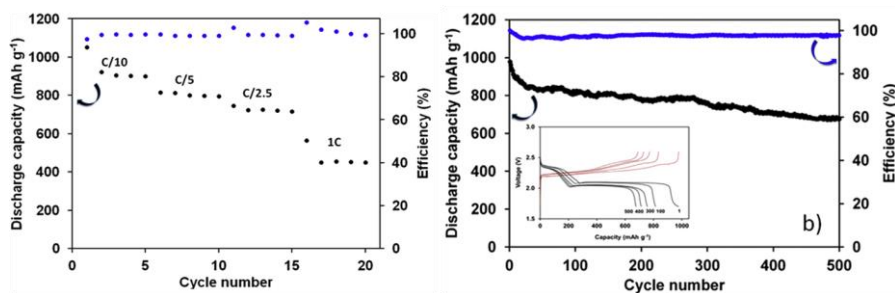
95

Figure 1.5: a) Effect of current density in the discharge capacity of the cathodes containing P(S-DVB) with 90 wt% of sulfur. b) Long term cycling stability of of the cathodes containing P(S-DVB) with 90 wt% of sulfur, inset, charge discharge profiles at different cycles of the experiment.

b)). Discharge/charge profiles at different cycles (inserted figure in Figure 1.5 b)) were similar to that observed with cathodes containing elemental sulfur in classical Li-S batteries. Both the lower and upper plateaus are shortened with the increase of cycle number. It is assumed that the practical active materials and the soluble polysulfides are gradually decreasing as cycling proceeds[28]. The determined value of degradation rate per cycle for the galvanostatic cycling experiments at C/4 rate was 0.11%. This value is comparable with those reported by Su et al. with elemental sulfur but using complicated and multi-steps approaches (e.g., S-TiO yolk-shell nanocomposite, mesoporous carbons). Here, a successful long term cycling at C/4 without cell failure is demonstrated.

It is worth to remark that these results are superior to previous reports of Li-S coin cells using sulfur copolymers obtained by Inverse Vulcanization. In this work, the poly (S-DVB) copolymers showed a capacity of 700 mAh g^{-1} after 500 cycles at moderate rate C/4. In previous works, other copolymers such as the well known P(S-DIB) showed an inferior value of 635 mAh g^{-1} at the cycle 500 but at slow C-rate of C/10. Even the engineered copolymer synthesized by the inverse vulcanization of elemental sulfur with a synthetic monomer (1,4-diphenylbutadiine) reached only 600 mAh g^{-1} in the 500th cycle at C/5. So, the new copolymer material shows promising results and characteristics, indicating

its huge potential for commercial cells application (easy scalability, processability, versatility and cost effectiveness).

4. Conclusion

In this work we show that the inverse vulcanization of sulfur with divinylbenzene (DVB) leads to a series of poly (S-DVB) copolymers. The inverse vulcanization process is particularly fast using DVB which is a cheap and common chemical in the polymer industry. The chemical characterization of the poly (S-DVB) copolymers by FTIR and NMR demonstrated the random copolymerization between sulfur and DVB. The copolymers were amorphous yellow-red glassy materials with improved thermal stability with respect to elemental sulfur. The glass transition temperature of the copolymers depended in the copolymer composition (S/DVB ratio) and varied between -5 and 79 ^{0}C. These copolymers could be processed in a simple and effective way as a powder and used as cathode material for Li-S batteries. The poly (S-DVB) showed comparable electrochemical activity than that of elemental sulfur but with improved capacity retention and cyclability at several C/rates. These copolymers are very attractive due to their low cost, easy and fast synthesis, chemical stability and compatibility.

5. References

1.   Bouchet, R. *et al.* Single-ion BAB triblock copolymers as highly efficient electrolytes for lithium-metal batteries. *Nature Materials* **12,** 452–457 (2013).

2.   Dunn, B., Kamath, H. & Tarascon, J. M. Electrical energy storage for the grid: A battery of choices. *Science* **334,** 928–935 (2011).

3.   Bruce, P. G., Freunberger, S. A., Hardwick, L. J. & Tarascon, J.-M. Li–O2 and Li–S batteries with high energy storage. *Nature Materials* **11,** 19–29 (2012).

4.   Song, M. K., Zhang, Y. & Cairns, E. J. A long-life, high-rate lithium/sulfur cell: A multifaceted approach to enhancing cell performance. *Nano Letters* **13,** 5891–5899 (2013).

5.   Hagen, M., Fanz, P. & Tübke, J. Cell energy density and electrolyte/sulfur ratio in Li-S cells. *Journal of Power Sources* **264,** 30–34 (2014).

6.   Chung, W. J. *et al.* The use of elemental sulfur as an alternative feedstock for polymeric materials. *Nature Chemistry* (2013). doi:10.1038/nchem.1624

7.   Armand, M. & Tarascon, J. M. Building better batteries. *Nature* (2008). doi:10.1038/451652a

8.   Zhang, S. S. Liquid electrolyte lithium/sulfur battery: Fundamental chemistry, problems, and solutions. *Journal of Power Sources* (2013). doi:10.1016/j.jpowsour.2012.12.102

9.   Wujcik, K. H. *et al.* Fingerprinting Lithium-Sulfur Battery Reaction Products by X-ray Absorption Spectroscopy. *Journal of the Electrochemical Society* **161,** A1100–A1106 (2014).

10. Adams, B. D. *et al.* Towards a stable organic electrolyte for the lithium oxygen battery. *Advanced Energy Materials* **5,** (2015).

11. Akridge, J. R., Mikhaylik, Y. V. & White, N. Li/S fundamental chemistry and application to high-performance rechargeable batteries. in *Solid State Ionics* **175,** 243–245 (2004).

12. Song, M.-K., Cairns, E. J. & Zhang, Y. Lithium/sulfur batteries with high specific energy: old challenges and new opportunities. *Nanoscale* **5,** 2186 (2013).

13. Zheng, M. Sen, Chen, J. J. & Dong, Q. F. The Enhanced Electrochemical Performance of Lithium/Sulfur Battery with Protected Lithium Anode. *Advanced Materials Research* **476–478,** 676–680 (2012).

14. Xin, S. *et al.* Smaller sulfur molecules promise better lithium'sulfur batteries. *Journal of the American Chemical Society* (2012). doi:10.1021/ja308170k

15. Wu, F. *et al.* Sulfur/Polythiophene with a Core/Shell Structure: Synthesis and Electrochemical Properties of the Cathode for Rechargeable Lithium Batteries. *The Journal of Physical Chemistry C* **115,** 6057–6063 (2011).

16. Evers, S., Yim, T. & Nazar, L. F. Understanding the nature of absorption/adsorption in nanoporous polysulfide sorbents for the Li-S battery. *Journal of Physical Chemistry C* **116,** 19653–19658 (2012).

17. Ai, W. *et al.* A novel graphene-polysulfide anode material for high-performance lithium-ion batteries. *Scientific Reports* **3,** (2013).

18. Xiao, L. *et al.* A soft approach to encapsulate sulfur: Polyaniline nanotubes for lithium-sulfur batteries with long cycle life. *Advanced*

Materials **24,** 1176–1181 (2012).

19. Shi Chao, Z., Lan, Z. & Jinhua, Y. Preparation and electrochemical properties of polysulfide polypyrrole. *Journal of Power Sources* **196,** 10263–10266 (2011).

20. Liang, X. *et al.* A nano-structured and highly ordered polypyrrole-sulfur cathode for lithium-sulfur batteries. *Journal of Power Sources* **196,** 6951–6955 (2011).

21. Fu, Y. & Manthiram, A. Enhanced cyclability of lithium-sulfur batteries by a polymer acid-doped polypyrrole mixed ionic-electronic conductor. *Chemistry of Materials* **24,** 3081–3087 (2012).

22. Fu, Y. & Manthiram, A. Core-shell structured sulfur-polypyrrole composite cathodes for lithium-sulfur batteries. *RSC Advances* **2,** 5927 (2012).

23. Wu, F., Wu, S., Chen, R., Chen, J. & Chen, S. Sulfur–Polythiophene Composite Cathode Materials for Rechargeable Lithium Batteries. *Electrochemical and Solid-State Letters* **13,** A29 (2010).

24. Sun, Z. *et al.* Sulfur-rich polymeric materials with semi-interpenetrating network structure as a novel lithium–sulfur cathode. *Journal of Materials Chemistry A* **2,** 9280 (2014).

25. Dirlam, P. T. *et al.* Inverse vulcanization of elemental sulfur with 1,4-diphenylbutadiyne for cathode materials in Li–S batteries. *RSC Advances* **5,** 24718–24722 (2015).

26. Oschmann, B. *et al.* Copolymerization of Polythiophene and Sulfur to Improve the Electrochemical Performance in Lithium-Sulfur Batteries. *Chemistry of Materials* **27,** 7011–7017 (2015).

27. Wei, Y. *et al.* Solution processable hyperbranched inverse-vulcanized polymers as new cathode materials in Li-S batteries. *Polymer Chemistry* **6,** 973–982 (2015).

28. Su, Y. S., Fu, Y., Cochell, T. & Manthiram, A. A strategic approach to recharging lithium-sulphur batteries for long cycle life. *Nature Communications* **4,** (2013).

29. Yang, Z. *et al.* Electrochemical energy storage for green grid. *Chemical Reviews* (2011). doi:10.1021/cr100290v

30. Choi, J. W. & Aurbach, D. Promise and reality of post-lithium-ion batteries with high energy densities. *Nature Reviews Materials* (2016). doi:10.1038/natrevmats.2016.13

31. Griebel, J. J., Glass, R. S., Char, K. & Pyun, J. Polymerizations with elemental sulfur: A novel route to high sulfur content polymers for sustainability, energy and defense. *Progress in Polymer Science* **58,** 90–

125 (2016).

32. Rybarczyk, M. K. *et al.* Porous carbon derived from rice husks as sustainable bioresources: insights into the role of micro-/mesoporous hierarchy in hosting active species for lithium–sulphur batteries. *Green Chem.* **18,** 5169–5179 (2016).

33. Rosenman, A. *et al.* Review on Li-Sulfur Battery Systems: An Integral Perspective. *Advanced Energy Materials* **5,** (2015).

34. Wild, M. *et al.* Lithium sulfur batteries, a mechanistic review. *Energy and Environmental Science* (2015). doi:10.1039/c5ee01388g

35. Manthiram, A., Fu, Y., Chung, S. H., Zu, C. & Su, Y. S. Rechargeable lithium-sulfur batteries. *Chemical Reviews* (2014). doi:10.1021/cr500062v

36. Ding, B. *et al.* Nanospace-confinement copolymerization strategy for encapsulating polymeric sulfur into porous carbon for lithium-sulfur batteries. *ACS Applied Materials and Interfaces* **7,** 11165–11171 (2015).

37. Pang, Q., Liang, X., Kwok, C. Y. & Nazar, L. F. Review—The Importance of Chemical Interactions between Sulfur Host Materials and Lithium Polysulfides for Advanced Lithium-Sulfur Batteries. *Journal of The Electrochemical Society* **162,** A2567–A2576 (2015).

38. Lin, Y. *et al.* Unique starch polymer electrolyte for high capacity all-solid-state lithium sulfur battery. *Green Chem.* **18,** 3796–3803 (2016).

39. Simmonds, A. G. *et al.* Inverse vulcanization of elemental sulfur to prepare polymeric electrode materials for Li-S batteries. *ACS Macro Letters* (2014). doi:10.1021/mz400649w

40. Kim, H., Lee, J., Ahn, H., Kim, O. & Park, M. J. Synthesis of three-dimensionally interconnected sulfur-rich polymers for cathode materials of high-rate lithium-sulfur batteries. *Nature Communications* **6,** (2015).

41. Gomez, I. *et al.* Inverse vulcanization of sulfur with divinylbenzene: Stable and easy processable cathode material for lithium-sulfur batteries. *Journal of Power Sources* (2016). doi:10.1016/j.jpowsour.2016.08.046

42. Shukla, S. *et al.* Cardanol benzoxazine-Sulfur Copolymers for Li-S batteries: Symbiosis of Sustainability and Performance. *ChemistrySelect* **1,** 594–600 (2016).

43. Crockett, M. P. *et al.* Sulfur-Limonene Polysulfide: A Material Synthesized Entirely from Industrial By-Products and Its Use in Removing Toxic Metals from Water and Soil. *Angewandte Chemie - International Edition* **55,** 1714–1718 (2016).

44. Hasell, T., Parker, D. J., Jones, H. A., McAllister, T. & Howdle, S. M.

Porous inverse vulcanised polymers for mercury capture. *Chem. Commun.* **52,** 5383–5386 (2016).

45. Wang, K., Groom, M., Sheridan, R., Zhang, S. & Block, E. Liquid sulfur as a reagent: Synthesis of polysulfanes with 20 or more sulfur atoms with characterization by UPLC-(Ag+)-coordination ion spray-MS. *Journal of Sulfur Chemistry* **34,** 55–66 (2013).

46. Block, E. Fifty years of smelling sulfur. *Journal of Sulfur Chemistry* **34,** 158–207 (2013).

47. Behr, A. & Johnen, L. Myrcene as a natural base chemical in sustainable chemistry: A critical review. *ChemSusChem* **2,** 1072–1095 (2009).

48. BLIGHT, L., CURRELL, B. R., NASH, B. J., SCOTT, R. A. M. & STILLO, C. in *New Uses of Sulfur—II* **165,** 2–13 (AMERICAN CHEMICAL SOCIETY, 1978).

Chapter II

Inverse Vulcanization of Sulfur using Natural Dienes as Sustainable Materials for Lithium–Sulfur Batteries
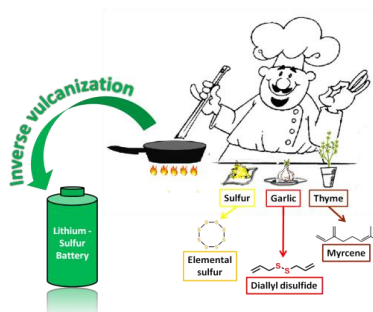
1. Introduction

Sustainable materials for energy production are searched to mitigate environmental problems such as the increase of the pollution and global warming. Thus, the application of renewable energy sources such as tidal, solar, and wind energy will be crucial in the near future to maintain the modern lifestyle. One limitation of these renewable energy sources is the fact that they are intermittent. For their economic competitiveness in comparison to the currently implemented energy production, energy storage systems are critical[1]. Lithium-ion batteries are the predominant energy storage systems used over the past two decades, but due to the increasing demand of energy this technology is reaching its limit[2,3]. Among the next-generation batteries under development, lithium–sulfur batteries are attracting considerable attention.

Elemental sulfur is a raw material that has several advantages compared to transition-metal oxides used as cathode materials. Sulfur is one of the most abundant elements in the earth crust, which makes it an inexpensive material. Furthermore, it is readily available owing to excess production during the desulfuration of petroleum[4]. On the other hand, it has high theoretical energy-storage properties (1762 mAh g^{-1} and 2567 Wh kg^{-1}). Beyond its interesting intrinsic properties, sulfur has a very low electronic conductivity and a complex electrochemistry, which involves the high solubility of lithium sulfides in the electrolyte[5]. These two characteristics are the source for a series of limitations on its performance as an active cathode material, which leads to batteries with low capacity retention and cyclability[6–11]. Recently, Pyun and coworkers presented a new synthetic method to obtain high-sulfur polymers called inverse vulcanization[12]. This reaction allows stabilizing the polymeric sulfur with a low amount of a diene, inversely to the conventional vulcanization process where a polydiene is stabilized by a low amount of sulfur. Interestingly, sulfur copolymers presented excellent enhanced capacity retention and cyclability in Li–S batteries compared to elemental sulfur. In the last two years, a large

amount of research dealt with the identification of the-best performing and cheapest diene for this reaction. Initially, inverse vulcanization of sulfur was demonstrated by cross-linking of elemental sulfur using 1,3-diisopropenylbenzene (DIB) which is a synthetic cross-linking agent with slow copolymerization kinetics[13]. Further studies involved the use of other non-natural and/or expensive chemicals as crosslinkers. For example, diethynylbenzene was used by Sun et al. to copolymerize sulfur at high temperature, 1,4-diphenylbutadiyne was used to prepare high-sulfur polymers, and a thiophene monomer having allyl groups was copolymerized with elemental sulfur to give a high-capacity cathodic materials[14–16]. Another example of high-temperature synthesis of sulfur polymers is the method reported by Park and coworkers in which sulfur was polymerized with trithiocyanuric acid to form a three-dimensionally interconnected polymer that showed good performance at high C rates[17]. Only recently has the inverse vulcanization method been extended to the use of the more common divinylbenzene cross-linkers or natural molecules[18]. Lochab and co-workers reported the inverse vulcanization using a natural lipid molecule, Cardanol[19]. However, an additional step in modifying Cardanol into a reactive benzoxazine was required. Chalker and co-workers studied the polymerization of sulfur with limonene directly without using any prior modification step, but no battery tests were performed[20]. In parallel, different efforts were made to carry out the inverse vulcanization process in green solvents such as supercritical CO_2[21].

In this work the inverse vulcanization of sulfur is investigated using two natural dienes, diallyl disulfide (DAS) and 7-methyl-3-methylene-1,6-octadiene (myrcene, Myr) and a molecule coming from industrial waste, dicyclpentadiene (DPCD). On one hand, DAS is present in garlic and onions and is responsible for their characteristic strong odor and on the other hand Myrcene is a natural terpene coming from the essential oil of different plants, especially from thyme[22–24]. Additionally, dicyclopentadiene (DPCD), a monomer coming from

the waste of the industrial process of naphta craking to obtain ethylene, is used[25].

Herein, a facile, one-pot copolymerization of sulfur with these three monomers and their application in Li–S batteries as cathodic materials is presented. The obtained copolymers were physicochemically characterized. Finally, a Li–S cell using these copolymers was characterized electrochemically and its performance was measured; the cell showed promising results with a long lifetime of 200 cycles at a moderate discharge rate of C/5 and 80% retention of the initial capacity.

2. Experimental

2.1 Materials and methods

Diallyl sulfide (+80% FG), myrcene (technical grade), dicyclopentadiene (purum, > 95%) and sulfur (99.5–100.5%) were purchased from Sigma–Aldrich and used as received.

The synthesis of the high-sulfur polymers was carried out as follows. In a 50 mL flask equipped with a magnetic stir bar sulfur (9 g, 0.28 mol) was added. The flask was placed in an oil bath preheated at 185 ºC. When the sulfur was molten and showing cherry red color, the respective monomer (1 g, 7 mmol) was added batch wise. The reaction mixture showed two immiscible phases at the beginning, but it turned into a single one during reaction (between 5 and 20 min). The reaction was stirred until an increase of the viscosity was observed. Then the flask was placed in a liquid nitrogen bath to quench the reaction. A curing step at 120 ^{0}C was applied for 24 h to promote the reaction of all reactive groups with the free sulfur imbibed in the solid. After this step, the reaction was cooled to room temperature and the solid was recovered. It is worth pointing out that in the case of myrcene the temperature was decreased to 170 ^{0}C to avoid

rapid decomposition and evolution of gas during the polymerization due to the self-acceleration and self-heating of the reaction. This synthesis route was followed to synthesize various series of polymers at various sulfur/monomer weight ratios. The molecular composition was elucidated by ^{1}H NMR and FTIR attenuated total reflectance (ATR) spectroscopy. The NMR measurements of the natural monomers and their polymers were carried out on a Bruker AVANCE 400 spectrometer. The poly(sulfur–DAS) and poly(sulfur-DCPD) polymer was dissolved in anhydrous carbon disulfide, and a capillary with deuterated chloroform was immersed into the solution. The spectra of myrcene and poly(sulfur–myrcene) were carried out in deuterated chloroform. The thermal characterization of the high-sulfur polymers was carried out in the DSC (Q2000, TA instruments) from -40 to 140 ^{0}C at a heating rate of 10 ^{0}C min^{-1}. Two cycles of heating were performed with a fast cooling step. TGA of elemental sulfur and the polymers were recorded on Q500 (TA instruments) using a heating rate of 10 ^{0}C min^{-1} under N_2 atmosphere.

2.2 Electrochemical characterization

Positive electrodes were prepared using 60% in weight of the selected sulfur copolymers in the final cathode. The selected sulfur copolymers were dry ball milled prior to the cathode preparation, turning into a fine pale brownish powder. Afterwards, a mixture of Ketjen Black 600JD (AkzoNobel) and the selected copolymer was wet dry milled in ethanol for 3 h. The mixture was dried and added to a solution of polyvinylidene fluoride 5130 (SOLVAY) in Nmethylpyrrolidone to form the cathodic slurry. Slurries with a final solid content of 30% were prepared by using mechanical mixer (RW 20 digital, IKA) at 600 rpm. These slurries were blade cast onto a carbon-coated aluminum foil (MTI Corp.) and dried at 60 ºC under dynamic vacuum during 12 h before cell assembly. The cathodes were prepared for a theoretical capacity of 2.7 mAh cm^{-2}. One layer of commercial polyolefin separator (Celgard 2501) soaked with 50 µL of 0.38 M solution of bis(trifluoromethane)sulfonamide lithium salt

(LiTFSI; Sigma–Aldrich) and 0.32 M of $LiNO_3$ (Sigma–Aldrich) as additive in a 1:1 (v/v) mixture of dimethoxyethane (BASF) and dioxolane (BASF), was placed between electrodes. Lithium metal (0.05 mm, Rockwood Lithium) was used as the anode in coin half cells (2025, Hohsen). Vacuum drying of electrodes and cell crimping was performed in a dry room with a dew point below -50 ^{0}C. Thereafter, assembled cells were aged during 20 h and then cycled using a BaSyTec Cell Test System (Germany) at 25:1 ºC under air. The electrochemical behavior of the obtained sulfur copolymer electrodes was evaluated at different C rates considering the theoretical capacity of elemental sulfur (1672 mAh g^{-1}). The cyclability of coin cells was investigated within a 1.7–2.6 V interval at C/5 charge and discharge current rates. Cyclic voltammetry experiments were performed in a coin cell at a scan rate of 10 mV s^{-1} from 2.8 to 1.5 V.

3. Results and discussion

3.1 Synthesis

High-sulfur polymers were obtained by copolymerizing sulfur with DAS, myrcene and DCPD. The general inverse vulcanization method is depicted in Figure 2.1. The synthesis of the high sulfur polymers starts with the melting of sulfur at high temperature (185 ^{0}C). Under these conditions the cyclic allotropes of sulfur are homolytically cleaved at one of the S-S bonds to form linear biradical polysulfides. These polysulfides can react with other reactive sulfur chains to form polymeric sulfur. At this point the natural monomer is added. Initially, two phases can be observed during the synthesis of both polymers (Figure 2.3). However, depending on the added monomer the reaction showed different behaviors. In the case of DAS the reaction mixture became homogeneous or miscible after 1 min (Figure 2.3, left). Afterwards, the color of the reaction media turns dark red and the viscosity increases. After 10 min, the reaction is quenched by introducing liquid nitrogen to avoid self-acceleration and self-heating. Next, a curing step at 120 ^{0}C is needed to allow the free sulfur to react with the remaining double bonds of DAS. After curing for 24 h, the

reaction medium was solidified, forming a rubbery-like self-standing film. In the case myrcene, the reaction with sulfur was slightly different. The reaction mixture showed two phases until 10 min reaction (Figure 2.3, right). After this extended initial mixing time, the reaction proceeded similarly to the DAS case, after which the viscosity of the solution increased rapidly; the reaction was quenched after 15 min. Then, the product was cured for 24 h at 130 ^{0}C, yielding a dark brown brittle solid. Finally, in the case of DCPD the reaction was slightly different. Although the behavior of the reaction was similar (increase of the viscosity within 10-15 minutes and darkening of the mixture) the reaction never became homogeneous. Nevertheless, the same proceeding reaction method was followed for this system, with a step at high temperature until the reaction viscosity increased until a maximum point, then the quenching of the reaction and the further curing at 120 ºC for overnight, Using this method, a series of
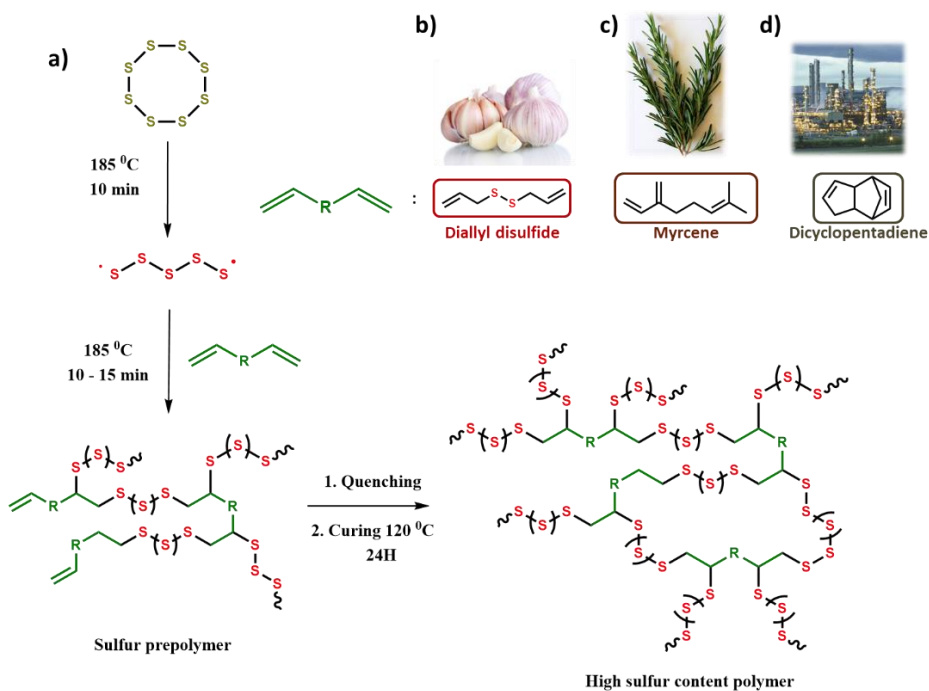

Figure 2.1: Schematic representation of the inverse vulcanization of sulfur with dienes coming from natural sources (DAS and Myr) and from industrial wastes (DCPD).

sulfur copolymers with varying contents of natural dienes between 10–50 wt% were synthesized. These copolymers were termed poly(sulfur–DAS) with 10–40 wt% of the natural diene, poly(sulfur–myrcene) with 10–50 wt% of the natural diene and poly(sulfur-DCPD) with 10-50% of the waste monomer in the reaction mixture. After the reaction, the resulting materials from the inverse vulcanization of sulfur with these two natural monomers showed different characteristics. In the case of poly(sulfur–DAS) the materials were rubbery like and black reddish whereas poly(sulfur–myrcene) showed dark brown color and brittle, similar to poly(sulfur-DCPD) that resulted to be black and brittle materials. The polymers showed poor solubility in commonly used organic solvents, even at a high amount of the organic comonomer. Only the materials with the highest amount of the natural diene showed solubility. In the case of poly(sulfur– DAS) 40% wt% the polymers could be dissolved in CS_2, and the poly(sulfur–myrcene) copolymer with 50 wt% myrcene content was soluble in chloroform. In the case of poly(sulfur-DCPD) materials they did not show total solubility in any solvent at
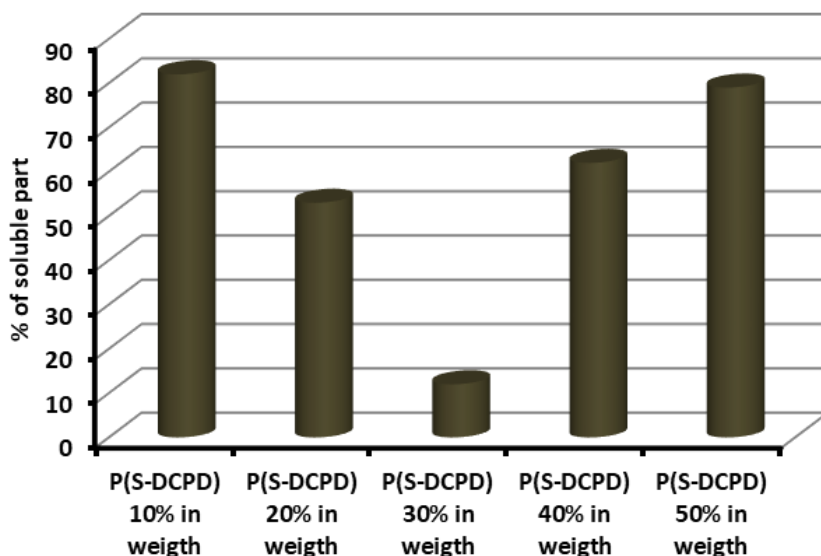

Figure 2.2: Solubility study by Soxhlet extraction with CS_2 of the series of poly(sulfur-DCPD) polymers.

any composition. Therefore, Soxhlet extraction was performed with CS_2 which was reported to be the best solvent for this system. As can be observed in figure 2.2, the soluble fraction of poly(sulfur-DCPD) decreases until a composition of 30:70 of DPCD and sulfur (wt %), and it increases again with the increase of the organic comonomer.

3.2 Physicochemical characterization

The chemical nature of the polymers was studied by means of ^{1}H NMR spectroscopy. In Figure 2.4 a), in the upper part the ^{1}H NMR spectrum of DAS is depicted as an example. The signals related to the protons of the allyl bonds (labeled as a and b) are located at 6.2 and 5.5 ppm. The signal at 3.7 corresponds to the methyne protons near to the disulfide bond (labeled c). The spectrum of the copolymer poly(sulfur–DAS) 40% (Figure 2.4 a, lower spectrum) reveals the disappearance of the allyl protons a and b. The set of signals between 1.0 and 2.5 ppm (labeled 2) is related to protons of an alkyl group not bonded to polysulfide chains. The next set of signals between 2.5 and 4 (labeled 1) ppm is very broad. In previous reports of high sulfur polymers these signals were assigned to protons that are near to a polysulfide chain. Interestingly, the integration of both sets of signals gives a ratio between protons of the alkyl chain and the protons linked to a polysulfide chain of 1:1. This could suggest that there is a structure of hyperbranched polymer in which
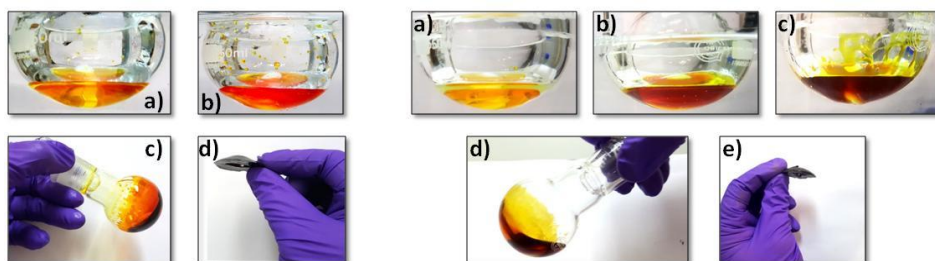

Figure 2.3: Digital images of the different steps during the inverse vulcanization reactions. Left, the inverse vulcanization of sulfur with diallyl disulfide (DAS), right the inverse vulcanization of sulfur with myrcene (Myr).
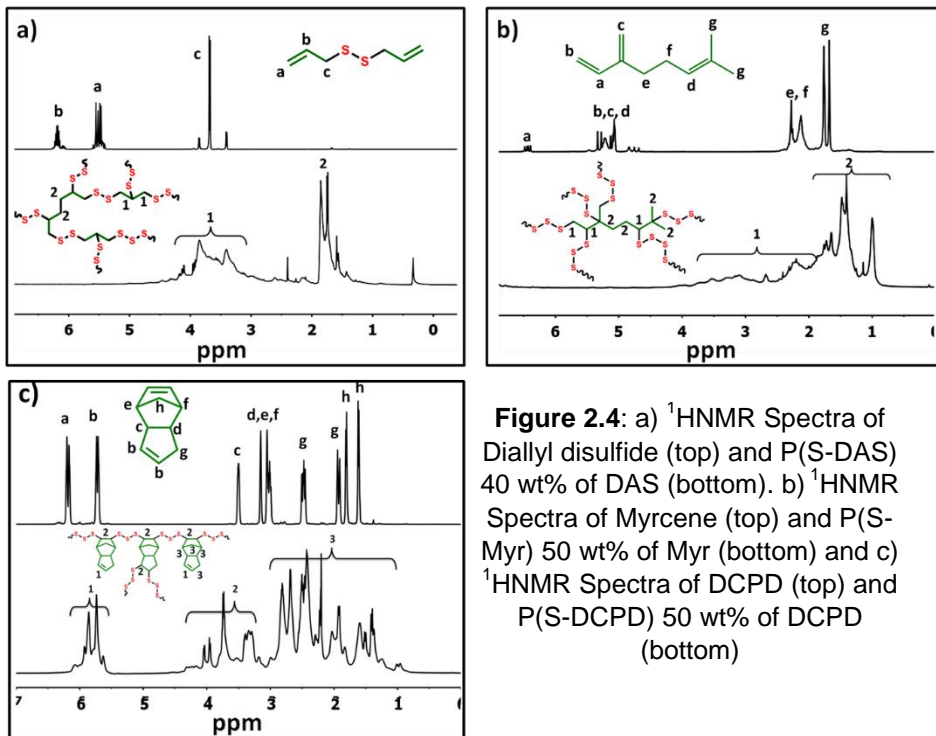
Figure 2.4: a) ^{1}HNMR Spectra of Diallyl disulfide (top) and P(S-DAS) 40 wt% of DAS (bottom). b) ^{1}HNMR Spectra of Myrcene (top) and P(S-Myr) 50 wt% of Myr (bottom) and c) ^{1}HNMR Spectra of DCPD (top) and P(S-DCPD) 50 wt% of DCPD (bottom)

polysulfide chains are bonded to polyalkyl chains. Similarly, the myrcene and poly(sulfur–myrcene) 50% NMR spectra are compared in Figure 2.4 b). The signals of the double bonds of myrcene, the quartet at 6.5 ppm, and the multiplet of 5.2 ppm (signals a, b, c, and d) disappear in the spectrum of the polymer. As in the previous case, two new sets of signals appear that could correspond to protons near to a polysulfide chain (labeled 1) and protons related to aliphatic chains (labeled 2). The integration of the sets of signals indicates that the ratio between the protons near to a polysulfide chain and alkyl protons is approximately 6:10. This is similar to the ratio of methyne and methyline protons. This supports the previous supposition that homopolymerization of myrcene does not occur and that the stabilization of polymeric sulfur is achieved through the predominant copolymerization of sulfur with myrcene molecules. Finally, the spectra of dicyclopentadiene and poly(sulfur-DCPD) is shown in figure 2.4 c). As can be observed, only the signals related to the norbonyl double bond (signals a in the upper spectrum)
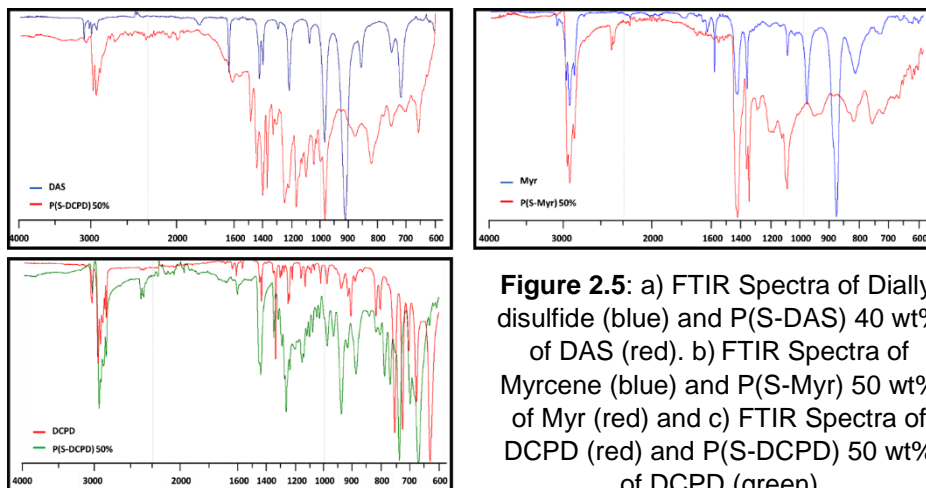
Figure 2.5: a) FTIR Spectra of Diallyl disulfide (blue) and P(S-DAS) 40 wt% of DAS (red). b) FTIR Spectra of Myrcene (blue) and P(S-Myr) 50 wt% of Myr (red) and c) FTIR Spectra of DCPD (red) and P(S-DCPD) 50 wt% of DCPD (green)

are totally consumed, whereas the signals of the cyclopentene double bond do not disappear. New signals can be detected in the poly(sulfur-DCPD) spectrum at 3-4.5 ppm region, what can be related with protons near to a polysulfide chain. The aliphatic signals of the dicyclopentadiene, from 1 to 3 ppm, get broader in the spectrum of the polymer, what is a classical behavior. It is worth to point that, due to overlapping of new signals of the protons near to a polysulfide chains and the protons near to the cyclopentene double bond in the 3-5 ppm region, the assignation of the signals becomes very difficult, therefore is not possible to analyze the integrals and elucidate a possible structure as in the previous cases.

The chemical nature of the sulfur–diene copolymers was also investigated by FTIR. The spectra of the polymers with the highest organic monomer content were compared with the spectra of their corresponding monomers. In Figure 2.5 a) the FTIR spectra of poly(sulfur–DAS) 50% and DAS are compared. The vibrations of the allyl moiety (3100 cm^{-1} =C-H stretching, 1660 cm^{-1} C=C stretching, 1380 cm^{-1} =C-H bending, and 990 and 910 cm^{-1} =C-H out-of-plane bending vibrations) is absent in the spectrum of the copolymer. Furthermore, new bands related to alkyl groups appear below 3000 cm^{-1} and between 1360

and 1500 cm^{-1}, which further indicates that the double bonds had reacted. On the other hand, the FTIR spectrum of myrcene (Figure 2.5 b)) shows the usual bands of double bonds at 3100 (C-H stretching), 1600 (C-H bending), and 990 and 890 cm^{-1} (out-of-plane vibrations). The vibrations of methyl carbons are also present between 2800 and 3000 cm^{-1} for C-H stretching, at 1400 cm^{-1} for the C-H bending of the -CH2- group, and at 1350 cm^{-1} for the umbrella vibration of methyl groups. The spectrum of the poly(sulfur–myrcene) again reveals the
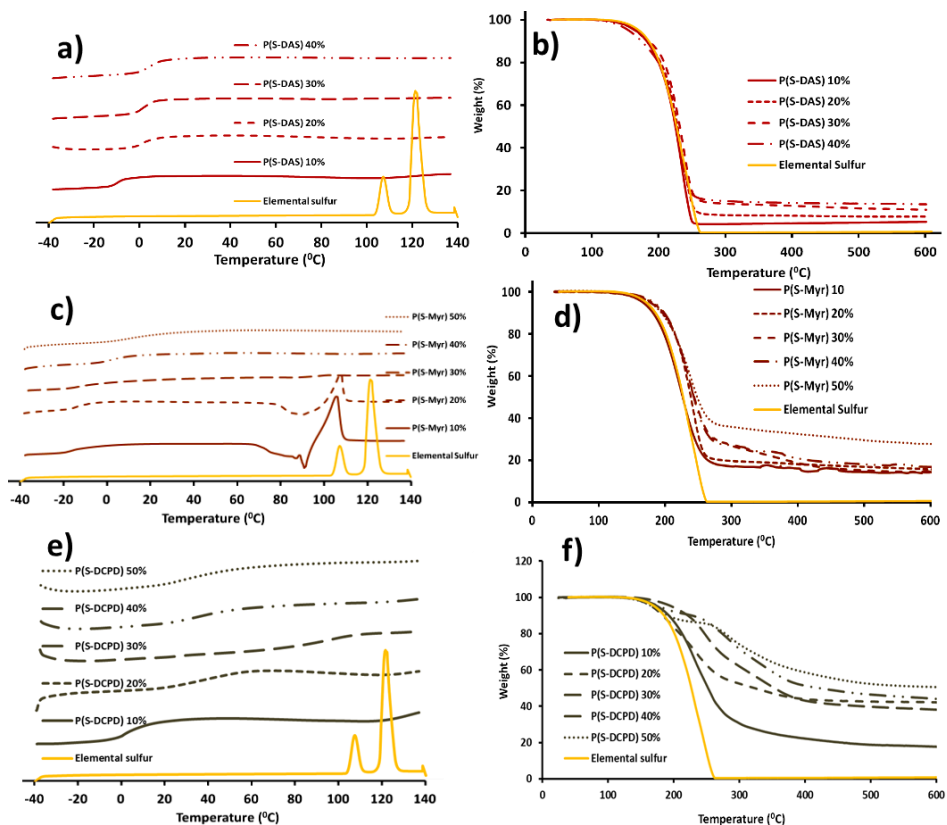

Figure 2.6: Thermal analysis of the series of polymers obtained by inverse vulcanization of sulfur with Diallyl disulfide, Myrcene and dicyclopentadiene. a) Thermogrmas of the 2nd scan of the DSC of the P(S-DAS) polymers. b) TGA curves of the P(S-DAS) polymers c) Thermogrmas of the 2nd scan of the DSC of the P(S-Myr) polymers, d) TGA curves of the P(S-Myr) polymers. e) Thermogrmas of the 2nd scan of the DSC of the P(S-DCPD) polymers, f) TGA curves of the P(S-DCPD) polymers.

disappearance of the bands related to the double bonds, but no new significant bands appear. Similarly to the ^{1}H NMR analysis, the assignation of new bands of the FTIR spectrum of poly(sulfur-DCPD) is complicated. Nonetheless, the signals in the range of the out of plane (o.o.p.) vibrations (between 600 and 1000 cm^{-1}) are completely altered, what indicates, that the reaction has occurred.

Next, the thermal properties of the polymers were investigated by differential scanning calorimetry (DSC) and thermogravimetric analysis (TGA). The DSC thermograms of all polymers are shown in Figure 2.6 a) and b), revealing that these polymers are amorphous at high contents of the organic comonomer (in all cases, a glass-transition temperature (Tg) is observed). Comparing the thermal properties with the composition of the different polymers, a similar behavior is observed for both series of polymers with natural dienes. The poly(sulfur–DAS) polymers do not show any crystallinity above a DAS content of 10 wt%. Also, Tg increases gradually on increasing the organic comonomer content. The Tgs observed were -9.2 ^{0}C for the poly(sulfur–DAS) with 10 wt% DAS, 0.5 ^{0}C for 20 wt%, 2.2 ^{0}C for 30 wt%, and 4.4 ^{0}C for 40 wt% DAS. A similar trend is observed for the poly(sulfur–myrcene) polymers, which show a gradual increase of the Tg with the amount of myrcene: -17.6 ^{0}C for a myrcene content of 10 wt%, -13.5 ^{0}C for 20 wt%, -8.7 ^{0}C for 30 wt%, 3.2 ^{0}C for 40 wt%, and 9.8 ^{0}C for 50 wt% myrcene. In contrast with the previous two polymers, P(S-DCPD) materials do not show a direct relation between Tg and the polymer composition. As can be observed in figure 2.6 c) the DSC data shows that the Tg increases from 1.3 ºC of 10% in weight of DCPD to 39.3 ºC of 20% to 96.5 ºC of 30%. But at this point the Tg of the 40% drops to 50.0 ºC as the polymer with a composition of 50% to 26.8. Interestingly this behavior is similar to the previously observed in solubility (figure 2.2). Bordoloi and Pearce studied deeply this polymerization in the 70´s by following the increase rate of the viscosity during the polymerization[26]. It was found that with an equimolecular feed of dicyclopentadiene and sulfur (which is approximately 30% in weight of

Poly(Sulfur-Diallyl sulfide)		
Composition (wt% in Diallyl sulfide)	Crystallinity 1º cycle (J/g)	% of crystallinity
10	13,61	23,5
20	0	0,0
30	0	0,0
40	0	0,0

Table 2.1: Crystallinity degree of P(S-DAS) polymers calculated from the 1st cycle of the DSC.

Poly (Sulfur-Myrcene)		
Composition (wt% of Myrcene)	Crystallinity 1º cycle (J/g)	% of crystallinity
10	27,76	48,0
20	26,18	45,2
30	13,92	24,1
40	2,21	3,8

Table 2.2: Crystallinity degree of P(S-Myr) polymers calculated from the 1st cycle of the DSC.

Poly(sulfur-Dicyclopentadiene)		
Composition (wt% in dicyclopentadiene)	Cristalllinity 1º cycle (J/g)	% of crystallinity
10	14,23	24,6
20	0	0,0
30	0	0,0
40	0	0,0

Table 2.3: Crystallinity degree of P(S-DCPD) polymers calculated from the 1st cycle of the DSC.

dicyclopentadiene) the increasing rate in the viscosity was the maximum, suggesting that the molecular weight of the polymer formed was the highest with this feed ratio due to the step growth polymerization mechanism proposed.

Similar to other inverse vulcanized copolymers, a small melting peak at around 106 ^{0}C (Table 2.1, 2.2 and 2.3) in the first cycle disappears in the second heating scan. The melting temperature is around the melting of monoclinic sulfur (107 ^{0}C). This characteristic may be due to one of two possible facts the presence of unreacted sulfur, as was proposed in earlier investigations of these systems or polysulfide chains long enough to crystallize as suggested by Pyun et al[27,12]. In the case of the poly(sulfur–DAS) and poly(sulfur-DCPD) copolymers the crystallization peak is only observed at low 10 wt% of organic monomer. In the case of poly(sulfur-DAS) the absence of melting peaks for the rest of the polymers could suggest that elemental sulfur has a strong random character as reported before by Block and coworkers with their investigation of the reaction of elemental sulfur with some organodisulfide molecules, and its reaction through free-radical polymerization with the allyl moieties of the monomer[22]. However, crystallization is observed until a high myrcene content of 40 wt%. It can be observed that by varying the composition of the copolymer the crystallization temperature decreases as does the crystallization degree (Table 2.2). This would suggest that in the case of myrcene, the polysulfide chains can crystallize due to a less random character of the copolymers.

The thermal stability of the polymers was studied by TGA. Elemental sulfur shows a single-step decomposition with an onset at around 200 ^{0}C. As can be observed in Figure 2.6 b, d and f, the polymers show similar decomposition curves. This could suggest that the decomposition occurs due to the cleavage of S-S bonds in the polymer. This leads to formation of small sulfur molecules and volatile organic sulfides that can sublimate. In every case there is always a waste product. For poly(sulfur–DAS) polymers the waste product weights are very low but increase directly with the amount of monomer added. Similar trend is followed by the poly(sulfur-DCPD) materials, but with increased waste percentage. However, the polymers obtained from myrcene show a different

trend. The weight loss percentage is very similar in all cases, but the onset of the decomposition is delayed.

3.3 Electrochemical characterization

Poly(sulfur–DAS), poly(sulfur–myrcene) and poly(sulfur-DCPD) were then investigated as active materials in Li–S batteries. It is well known that the higher the sulfur content the higher the theoretical capacity. For this reason, the galvanostatic cycling was performed on electrodes containing polymers with 10 wt% of the monomer to achieve the maximum sulfur content in the copolymer.

First, we performed cyclic voltammetry (CV) experiments for the copolymers (Figure 2.7 a) and b)). The CV results for both poly(sulfur–DAS) and poly(sulfur– myrcene) were very similar as signified by peaks at 2.3–2.4 V, which are associated with sulfur reduction generating higher order linear polysulfides, along with a second peak at 2.0–2.1 V assigned to the formation of lower-order sulfides down to Li_2S. These CV experiments confirmed that these copolymers exhibited electrochemical behavior very similar to results previously reported for inverse vulcanized sulfur copolymers and elemental sulfur[12].
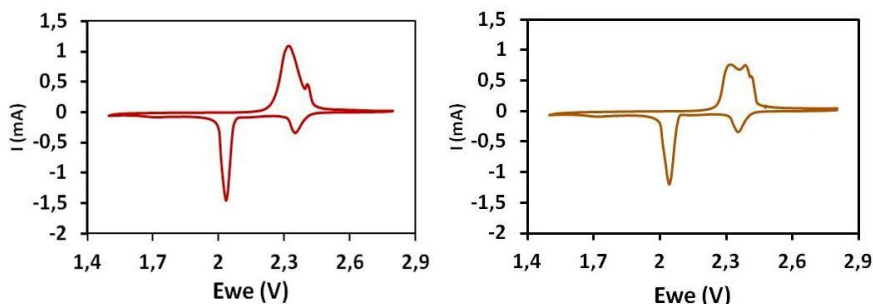

Figure 2.7: Cyclic voltagrams of polymers P(S-DAS) (left) and P(S-Myr) (right) both with 10 wt% of the organic comonomer.

Next, the polymers were tested as cathodes in coin cells versus Li/Li$^+$ at C/10, C/5, C/2.5, and 1C using a conventional liquid electrolyte (Figure 2.8 a)). The poly(sulfur–DAS) polymer showed the best performance with capacities of 860 mAh g^{-1} at C/10, 770 mAh g^{-1} at C/5, 710 mAh g^{-1} at C/2.5, and even 405 mAh g^{-1} at the high rate of 1C. Poly(sulfur–myrcene) shows a very similar behavior with slightly lower discharge capacities at moderate and high C rates. Differently, poly(sulfur-DCPD) shows similar capacities than the previous two materials at C/10, however the capacity decreases dramatically at C/2.5 and it almost completely fails at 1C, showing poorer battery performance.

The principal feature of the high-sulfur polymers as cathodic materials for Li–S batteries is the enhanced capacity retention during cycling. In Figure 2.8 b), the long-term cycling profiles of poly(sulfur–DAS), poly(sulfur–myrcene) and poly(sulfur-DCPD) at a moderate C rate of C/5 are shown. It is worth to mention that an activation process was performed for the cells, which consisted of ten charge–discharge cycles at C/20, to stabilize the capacity. As can be seen, these polymers exhibited initial discharge capacities of 600 mAh g^{-1} for poly(sulfur–DAS) and for poly(sulfur–myrcene) and 750 mAh g^{-1} for poly(sulfur-DCPD) and the afore-mentioned characteristic of high sulfur content polymers
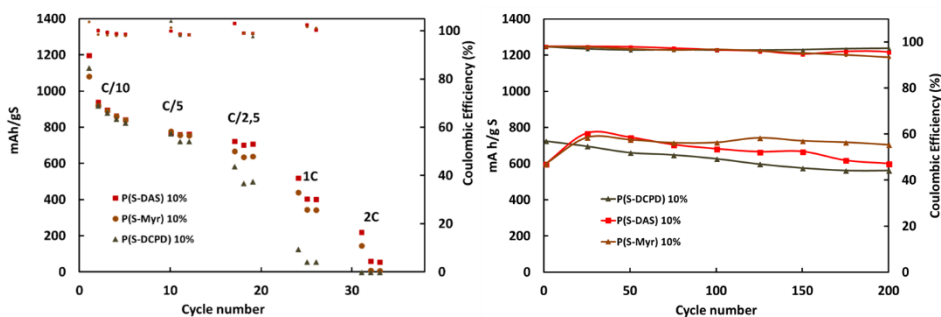

Figure 2.8: Electrochemical characterization in coin cell of P(S-DAS) (red) and P(S-Myr) (brown) and P(S-DCPD) (dark brown). A) C-rate capability of the polymers at C/10, C/5, C/2.5, 1C and 2C current densities (1C=1672 mAh). B) long cycle life stability at C/5.

as cathodic materials was proven, showing a capacity retention higher than 80% of the initial capacity.

4. Conclusion

In this work, inverse vulcanization of sulfur with abundant, inexpensive, and natural diene monomers such as diallyl sulfide (DAS), myrcene and dicyclopentadiene (DCPD) is reported for the first time. The chemical characterization of the poly(sulfur–natural diene) copolymers by FTIR and NMR spectroscopy demonstrated the random copolymerization typical of inverse vulcanization processes. Also, the investigation of the thermal properties of the final poly(sulfur–DAS) poly(sulfur–myrcene) and poly(sulfur-DCPD) showed differences in the glass-transition temperatures and crystallinity. These copolymers could be processed in a simple and effective way as a powder and used as cathode material for lithium–sulfur batteries. The sulfur–natural diene copolymers consisting of cheap and abundant chemicals are an excellent option of sustainable materials for electrochemical energy storage due to their good capacity retention (at a moderate C rate of C/5) being higher than 80% of the initial capacity even after 200 cycles.

5. References

1.   Yang, Z. *et al.* Electrochemical energy storage for green grid. *Chemical Reviews* **111,** 3577–3613 (2011).

2.   Armand, M. & Tarascon, J. M. Building better batteries. *Nature* **451,** 652–657 (2008).

3.   Choi, J. W. & Aurbach, D. Promise and reality of post-lithium-ion batteries with high energy densities. *Nature Reviews Materials* **1,** (2016).

4.   Griebel, J. J., Glass, R. S., Char, K. & Pyun, J. Polymerizations with elemental sulfur: A novel route to high sulfur content polymers for

sustainability, energy and defense. *Progress in Polymer Science* **58,** 90–125 (2016).

5.   Rybarczyk, M. K. *et al.* Porous carbon derived from rice husks as sustainable bioresources: insights into the role of micro-/mesoporous hierarchy in hosting active species for lithium–sulphur batteries. *Green Chem.* **18,** 5169–5179 (2016).

6.   Rosenman, A. *et al.* Review on Li-Sulfur Battery Systems: An Integral Perspective. *Advanced Energy Materials* **5,** (2015).

7.   Wild, M. *et al.* Lithium sulfur batteries, a mechanistic review. *Energy Environ. Sci.* **8,** 3477–3494 (2015).

8.   Manthiram, A., Fu, Y., Chung, S. H., Zu, C. & Su, Y. S. Rechargeable lithium-sulfur batteries. *Chemical Reviews* **114,** 11751–11787 (2014).

9.   Ding, B. *et al.* Nanospace-confinement copolymerization strategy for encapsulating polymeric sulfur into porous carbon for lithium-sulfur batteries. *ACS Appl. Mater. Interfaces* **7,** 11165–11171 (2015).

10.   Pang, Q., Liang, X., Kwok, C. Y. & Nazar, L. F. Review—The Importance of Chemical Interactions between Sulfur Host Materials and Lithium Polysulfides for Advanced Lithium-Sulfur Batteries. *J. Electrochem. Soc.* **162,** A2567–A2576 (2015).

11.   Lin, Y. *et al.* Unique starch polymer electrolyte for high capacity all-solid-state lithium sulfur battery. *Green Chem.* **18,** 3796–3803 (2016).

12.   Chung, W. J. *et al.* The use of elemental sulfur as an alternative feedstock for polymeric materials. *Nat. Chem.* **5,** 518–524 (2013).

13.   Simmonds, A. G. *et al.* Inverse vulcanization of elemental sulfur to prepare polymeric electrode materials for Li-S batteries. *ACS Macro Lett.* **3,** 229–232 (2014).

14.   Oschmann, B. *et al.* Copolymerization of Polythiophene and Sulfur to Improve the Electrochemical Performance in Lithium-Sulfur Batteries. *Chem. Mater.* **27,** 7011–7017 (2015).

15.   Dirlam, P. T. *et al.* Inverse vulcanization of elemental sulfur with 1,4-diphenylbutadiyne for cathode materials in Li–S batteries. *RSC Adv.* **5,** 24718–24722 (2015).

16.   Sun, Z. *et al.* Sulfur-rich polymeric materials with semi-interpenetrating network structure as a novel lithium–sulfur cathode. *J. Mater. Chem. A* **2,** 9280 (2014).

17.   Kim, H., Lee, J., Ahn, H., Kim, O. & Park, M. J. Synthesis of three-dimensionally interconnected sulfur-rich polymers for cathode materials of high-rate lithium-sulfur batteries. *Nat. Commun.* **6,** (2015).

18.   Gomez, I. *et al.* Inverse vulcanization of sulfur with divinylbenzene: Stable and easy processable cathode material for lithium-sulfur batteries. *J. Power Sources* **329,** 72–78 (2016).

19.   Shukla, S. *et al.* Cardanol benzoxazine-Sulfur Copolymers for Li-S batteries: Symbiosis of Sustainability and Performance. *ChemistrySelect* **1,** 594–600 (2016).

20.   Crockett, M. P. *et al.* Sulfur-Limonene Polysulfide: A Material Synthesized Entirely from Industrial By-Products and Its Use in Removing Toxic Metals from Water and Soil. *Angew. Chemie - Int. Ed.* **55,** 1714–1718 (2016).

21.   Hasell, T., Parker, D. J., Jones, H. A., McAllister, T. & Howdle, S. M. Porous inverse vulcanised polymers for mercury capture. *Chem. Commun.* **52,** 5383–5386 (2016).

22.   Wang, K., Groom, M., Sheridan, R., Zhang, S. & Block, E. Liquid sulfur as a reagent: Synthesis of polysulfanes with 20 or more sulfur atoms with characterization by UPLC-(Ag$^+$)-coordination ion spray-MS. *J. Sulfur Chem.* **34,** 55–66 (2013).

23.   Block, E. Fifty years of smelling sulfur. *Journal of Sulfur Chemistry* **34,** 158–207 (2013).

24.   Behr, A. & Johnen, L. Myrcene as a natural base chemical in sustainable chemistry: A critical review. *ChemSusChem* **2,** 1072–1095 (2009).

25.   Blight, L., Currel, B. R., Nash, B. J., Scott, R. A. M. & Stillo, C. in *New Uses of Sulfur—II* **165,** 2–13 (American Chemical Society, 1978)

Chapter III

Hybrid SulfurSelenium Co-polymers as Cathodic Materials for Lithium Batteries
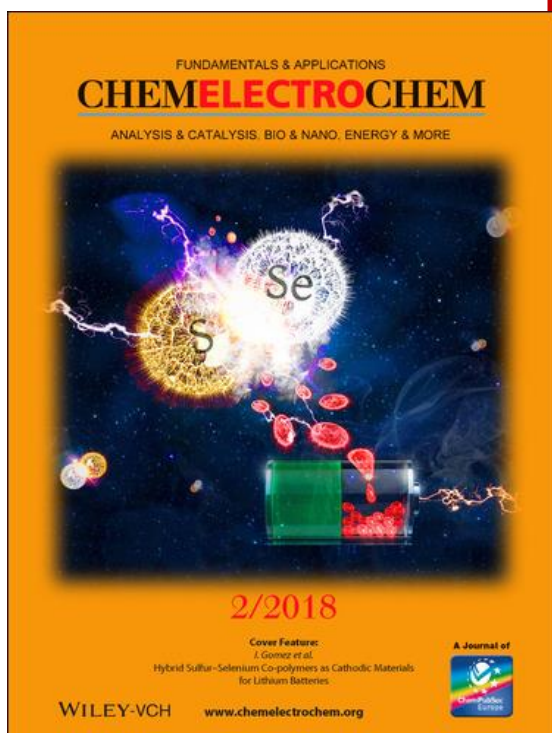
1. Introduction

Lithium-sulfur batteries is one of the most promising next generation electrochemical energy storage technologies due to the intrinsic properties of sulfur, namely, superior electrochemical properties (1672 mAh g^{-1} and 2500 Wh kg^{-1} vs Li/Li^{+}), low price and availability[1-5]. However, this battery technology has several and critical drawbacks that limit its performance directly caused by the use of elemental sulfur, such as low electrical conductivity, solubility of discharge intermediates in the cathode and large volume changes during cycling[2, 6-8]. The intensive research in all aspects of lithium sulfur cells like the cathode fabrication, host materials, electrolytes, separators or cell configuration has promoted a significant improvement in the performance of this battery system[9-12]. However, new cathode materials are needed in order to diminish the carbon content of the sulfur cathodes and to be able to use scalable electrode processing methods[13].

Selenium has shown up as a promising chalcogen element alternative to sulfur for lithium batteries. Its high electrically conductive nature and the redox active ability of their discharge products (Li$_2$Se$_2$ and Li$_2$Se) have attracted great attention in the last years[14-15]. However, its lower abundance and lower specific capacity hinders the research of elemental selenium vs elemental sulfur as cathodic material. In 2012, the use of a sulfur-selenium mixed chalcogenide system was first introduced by Amine et al. as a new suitable material for Li and Na batteries[16]. Mixed Se$_x$S$_y$ systems allow for tunable electrodes, combining the high capacities of S-rich systems with the high electrical conductivity of the d-electron containing Se. A deep and extensive study in the (de)lithiation mechanism of different SeS mixtures was presented proving that the redox process in ether based electrolytes was very similar to the one of sulfur[17-19]. More recently, in 2015 Quian et al. reported a SeS/Carbon composites showing an impressive capacity of 1000 mAh g^{-1} at 500 cycles with negligible capacity loss. In this case, the addition of a low proportion of selenium to sulfur helped to the polysulfide solubility suppression, contributing to the enhanced

electrochemical performance. However the preparation route of the composite involved non-scalable carbon porous materials where the Se-S alloy was immobilized and a high energy and time consuming step at 260 ^{0}C during 24 h[20].

In a pioneering work, in 2013 Pyun and coworkers presented the inverse vulcanization of sulfur with 1,3-diisopropenyl benzene (DIB) to obtain high sulfur content hybrid copolymers[21]. These co-polymers as cathodic materials showed a higher capacity than elemental sulfur at high C-rates and enhanced capacity retention showing more than 600 mAh g^{-1} at 500 cycles at C/10 C-rate[22]. As a consequence, the low energy and fast inverse vulcanization method became a very popular route to a wide variety of new sulfur co-polymers for energy and sustainability[23-28]. Very recently, the inverse vulcanization method has been extended to the synthesis of hybrid organic-inorganic sulfur-selenium co-polymers[29-30]. These materials were named CHIPS as Chalcogenide Hybrid Inorganic/Organic glasses and are being investigated for the preparation of ultrahigh refractive index materials. Combining the ease and scalability of the inverse vulcanization process and the sulfur-selenium system advantages versus bare sulfur in battery performance, we report for the first time the use of hybrid chalcogenide polymers in Lithium-sulfur batteries. In this way a synergetic effect of the high cycling stability due to the presence of organic moieties in the polymer and the high Crate cycling capability of the SeS system can be obtained. In this article we extend and optimize the low energy inverse vulcanization method to poly(Sulfur-r-Selenium-r-DIB) terpolymers to be used as cathode materials in lithium-sulfur batteries.

2. Experimental section

2.1 Materials and methods

Sulfur (Sigma, 99.5–100.5 %), Selenium (Acros, 99.5 %), 1,3-Diisopropenylbenzene (TCI, >97.0%) were used as received.

As a general synthesis method, Sulfur and Selenium (amounts in table 3.1 and 3.2) were physically mixed in a 25 ml vial and inserted in an oil bath preheated at 180 ^{0}C. After the melting of the solids, which showed a reddish black color, DIB (0.5 g, 3.16 mmol) was added via syringe. The reaction media was homogenous after 1 minute of stirring and showed vitrification after 10–15 minutes. The vial was kept in the oil bath further 5 minutes in order to promote the reaction of most of the vinyl groups. Afterwards the vial was inserted into a liquid nitrogen bath and broken in order to obtain the dark red crystals. These

	Sulfur		Selenium	
	Mol	**Mass (g)**	**Mol**	**Mass (g)**
P(S-DIB) 10%	0.14	4.5	---	----
P(Se$_{0.025}$S$_{0.975}$-DIB) 10%	0.136	4.368	0.0035	0.276
P(Se$_{0.05}$S$_{0.95}$-DIB) 10%	0.133	4.256	0.007	0.553
P(Se$_{0.075}$S$_{0.925}$-DIB) 10%	0.1295	4.144	0.0105	0.829
P(Se$_{0.1}$S$_{0.9}$-DIB) 10%	0.126	4.032	0.014	1.106

Table 3.1: Masses and mol for different feed ratios of sulfur and selenium for hybrid polymers with 10 wt% of DIB.

	Sulfur		Selenium		DIB	
	Mol	**Mass (g)**	**Mol**	**Mass (g)**	**Mol**	**Mass (g)**
P(S-DIB) 50%	0.078	2.5	---	----	0.016	2.5
P(Se$_{0.1}$S$_{0.9}$-DIB) 50%	0.070	2.25	0.0078	0.6162	0.016	2.5

Table 3.2: Masses and mol for different feed ratios of sulfur and selenium for hybrid polymers with 50 wt% of DIB.

materials showed a change in the color when cooling, becoming transparent light red. For NMR analysis, polymers with 50% in organic co-monomer were synthesized, in order to have $CDCl_3$ soluble polymers. The reaction procedure was the same as previously explained but with longer homogenization (5 minutes) and reaction times (20 minutes). It is worth to mention that high speed rate and slow addition of DIB is needed.

Raman spectra were recorded in a DXR2 Raman Microscope from Thermo Scientific with a 780 nm excitation laser. Bruker AVANCE 400 spectrometer was used to obtain ^{1}H NMR and the AVANCE 500 spectrometer for the ^{77}SeNMR. The samples were dissolved in $CDCl_3$ (Deutero GmbH). The DSC thermograms were obtained in a Q2000 from TA instruments with two heating scans from -40 ^{0}C to 140 ^{0}C at 10 ^{0}C/min rate with a cooling scan of 50 ^{0}C min$^-$^{1}. The thermogravimetric analyses (TGA) were done in a Q500 from TA instruments in a heating rate of 10 ^{0}C min^{-1} under N_2 atmosphere.

2.2 Electrochemical characterization

Positive electrodes were elaborated using 60% of poly(Se_xS_{1-x}-DIB). The selected sulfur and sulfur-selenium co-polymers were dry ball milled prior to the cathode preparation, turning into a fine deep orange powder. Afterwards, a mixture of Ketjen Black 600JD (AkzoNobel) and the selected co-polymer was wet ball milled in ethanol during 3 h. The mixture was dried and added to a solution of PVDF 5130 (SOLVAY) in NMP to form the cathodic slurry. The final solid content 30% slurries were prepared by mechanical mixer (RW 20 digital, IKA) at 600 rpm agitation rate. These slurries were blade cast onto a carbon coated aluminum foil (MTI Corp.) and dried at 60 ^{0}C under dynamic vacuum during 12 hours before cell assembling. The cathodes were prepared with theoretical capacity of 2.7 mAh cm^{-2}, from theoretical capacity of elemental Sulfur and Selenium (S=1672 mAh g^{-1}; $Se_{0.025}S_{0.975}$=1647 mAh g^{-1}; $Se_{0.05}S_{0.95}$=

1622 mAh g^{-1}; $Se_{0.075}S_{0.925}$=1597 mAh g^{-1}; $Se_{0.1}S_{0.9}$=1573 mAh g^{-1}), taking this into account, the current applied to each cell depends on the polymer used. For the P(S-DIB) 1 C corresponds to 1672 mA g^{-1}; for P($Se_{0.025}S_{0.975}$-DIB) 1 C corresponds to 1647 mA g^{-1}; for P($Se_{0.05}S_{0.95}$-DIB) 1 C corresponds to 1622 mA g^{-1}; for P($Se_{0.075}S_{0.925}$-DIB) 1 C corresponds to 1597 mA g^{-1} and for P($Se_{0.1}S_{0.9}$-DIB) 1 C corresponds to 1573 mA g^{-1}. One layer of commercial polyolefin separator Celgard 2500 separation soaked with 50 µL of 0.38 M solution of Bis(trifluoromethane)sulfonimide lithium salt (LiTFSI) (Sigma-Aldrich) and 0.32 M of lithium nitrate ($LiNO_3$) (Sigma-Aldrich) as additive, in 1/1 (v/v) mixture of dimethoxyethane (DME) (BASF) and dioxolane (DOL) (BASF), was placed between electrodes. Lithium metal (0.05 mm, Rockwood Lithium) was used as the anode in coin half cells (2025, Hohsen). Vacuum drying of electrodes and cell crimping has been performed in a dry room with dew point below -50 ^{0}C. Thereafter assembled cells were aged during 20 hours and then cycled by BaSyTec Cell Test System (Germany) at 25 ± 1 ^{0}C by air conditioning.

3. Results and discussion

3.1 Synthesis

The inverse vulcanization reaction of different sulfur-selenium compositions was carried out starting with the elemental forms of the chalcogenides, as depicted in Figure 3.1. The physical mixtures of sulfur and selenium at different molar ratio were melted together at 180 ^{0}C. Instead of the cherry red color showed by elemental sulfur in the conventional inverse vulcanization reaction, the melt S-Se mixtures were black liquids. Once sulfur and selenium were melted the commonly used diallyl DIB organic co-monomer was added. The reaction became homogeneous in short time and was stirred until the vitrification of the reaction media which occurs in approximately 15 minutes. Dark-reddish glassy materials were obtained after 15 minutes of reaction which became clear red after cooling. Using this synthetic method, different copolymers were synthesized varying the sulfur-selenium molar ratio while maintaining low the

organic content (10 wt% of DIB). Thus, five different hybrid co-polymers with compositions poly(Se_xS_{1-x}-DIB) with x=0, 0.25, 0.05, 0.075 and 0.1 in mol were produced and characterized.

3.2 Physicochemical characterization

The chemical characterization of the hybrid co-polymers was carried out by Raman spectroscopy, ^{77}Se NMR and ^{1}H NMR[31-32]. In Figure 3.2 a) the Raman spectra of obtained materials with different selenium ratios is compared. The spectrum of the co-polymer without selenium poly(Se_0S_1-DIB) shows three main peaks at 467 cm^{-1}, 220 cm^{-1} and 150 cm^{-1}. These bands are related to stretching, bending and deformation vibrations of S-S bonds respectively. In the case of all the co-polymers which contain selenium new peaks at 375 cm^{-1} and 194 cm^{-1} can be observed. As previously demonstrated, the new bands are related with Se-S stretching and Se-Se s tretching respectively. As it can be seen, the bands grow in intensity with the selenium content. Furthermore, within 360 and 340 cm^{-1} and 260 and 240 cm^{-1} new bands related with Se-S stretching
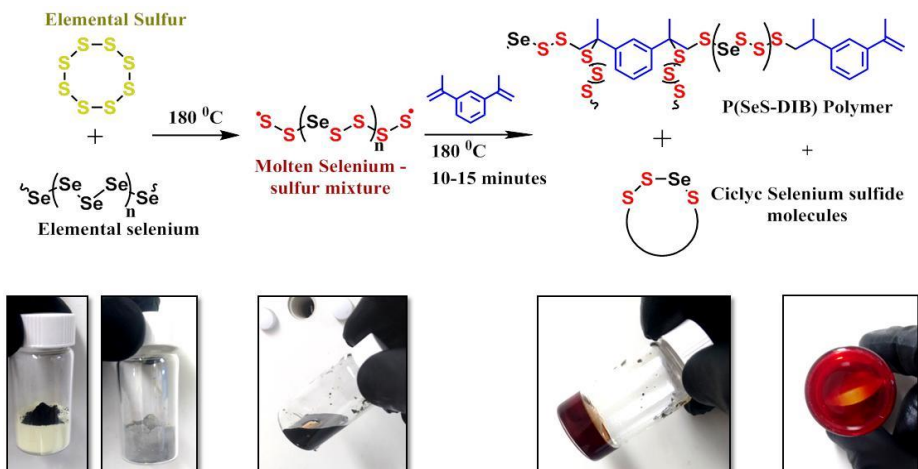

Figure 3.1: Reaction scheme of the synthesis of the hybrid Selenium-Sulfur polymeric materials by inverse vulcanization. Bottom part, digital images of each step of the reaction
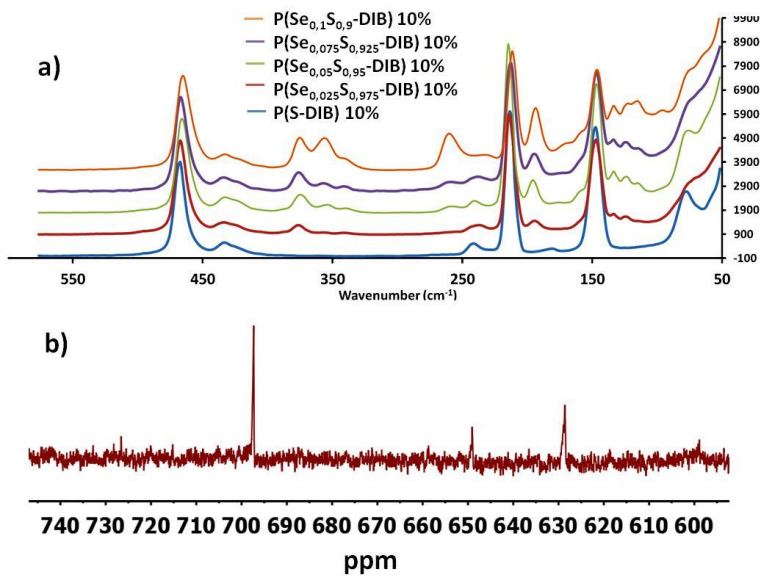
Figure 3.2: a) Raman spectra of the series of P(Se$_x$S$_{1-x}$-DIB) with different Se-S ratios with 10 wt% of the organic comonomer DIB. b) ^{77}SeNMR of P(Se$_{0.1}$S$_{0.9}$-DIB) with 50 wt% of the organic comonomer DIB.

appear. According to the literature the first set of bands, in the region of 360–340 cm^{-1}, has been identified as the stretching of Se-S bond within a sulfur environment, that is, -S-Se-S-. The second set of signals is related again with Se-S stretching but with a Se-Se bond, a region of –S-Se-Se-S- bonds. Altogether, the Raman Spectroscopy demonstrates the incorporation of selenium between the sulfur sequences of the hybrids. As previously reported, the co-polymers obtained by inverse vulcanization are soluble in commonly used organic solvents only when high amount of organic co-monomer is used (approx. >40 wt%). So in order to investigate the co-polymers by solution NMR, poly(Se$_x$S$_{1-x}$-DIB) with y=0 and 0.1 with 50% in weight of DIB were synthesized leading to co-polymers soluble in deuterated chloroform. First, the atomi c combination between Se and S was investigated by ^{77}Se NMR. In the NMR spectrum, Figure 3.2 b), tree singlets can be observed. These signals are related to different Se-S combinations further confirm the incorporation of selenium into sulfur sequences previously observed by Raman spectroscopy.

133

However the interpretation of the Sulfur-Selenium combination by ^{77}Se NMR is ambiguous as the combination possibilities is very broad with very small differences in the shift of the NMR signals. Further studies of the P(SeS-DIB) co-polymers would be crucial to better understand the molecular structure of the chalcogenide part of these sulfur-selenium polymers.

On the other hand, the ^{1}H NMR was used to characterize the organic part of the hybrid co-polymers. As shown in Figure 3.3 all the co-polymers show very similar sets of signals at 7.3 ppm, 4.5–3.5 ppm and 2.2–1.8 ppm. These signals were assigned respectively as the aromatic protons, the protons directly linked to a polysulfide chain and the protons of the methylene group of the DIB. The comparison between the different polymers shows that the chemical environment of the DIB moieties did not significantly change with the selenium addition. The absence of decoupling in ^{77}Se NMR and the same signals in ^{1}H NMR point that the selenium atoms are not bonded to the organic cross-linker
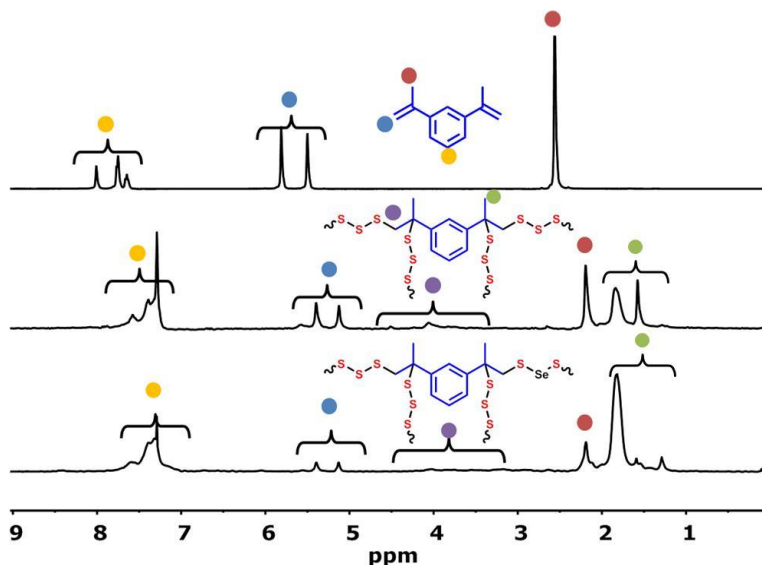

Figure 3.3: ^{1}HNMR spectra of DIB (top part), P(S-DIB) 50 wt% (middle part) of DIB and P(Se$_{0.1}$S$_{0.9}$-DIB) with 50 wt% of DIB (bottom part).

and

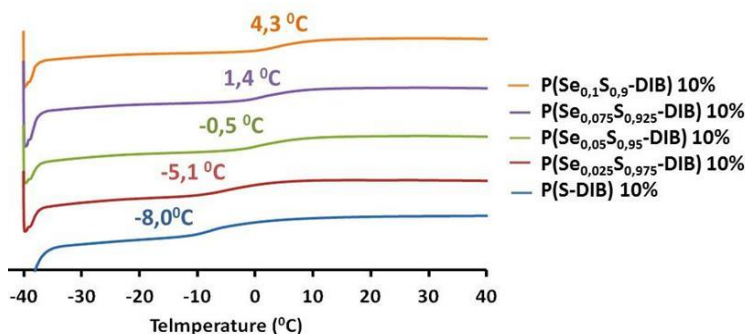
DSC 2nd Scan 10% wt of DIB

are

Figure 3.4: DSC curves of the 2nd scan of the series of P(Se$_x$S$_{1-x}$-DIB) with different Se-S ratios with 10 wt% of the organic comonomer DIB.

homogeneously dispersed in the sulfur matrix. However it is worth to mention that in the ^{1}H NMR, in the spectrum of the material with selenium the protons between 5 and 5.5 (methylene protons of the double bond) have lower intensity and the signal of 1.8 is higher (methyl protons of the isopropyl). This may be due to a slightly lower conversion of DIB in the presence of selenium.

The hybrid sulfur-selenium co-polymers were then characterized by differential scanning calorimetry (DSC) and thermogravimetric analysis (TGA). The DSC data (Figure 3.4) reveals that the addition of selenium has affected the glass transition temperature of the hybrids. As it can be observed, amorphous co-polymers are obtained and the glass transition increases with the selenium content. The glass transition temperature for neat poly(S-DIB) co-polymer having 10 wt% of DIB is -8 ^{0}C whereas the glass transition increases up to 4.3 ^{0}C in the case of the co-polymer of 10 mol% selenium with respect to sulfur, poly(Se$_{0,1}$S$_{0,9}$-DIB). Even though this Tg result in the DSC suggest that this co-polymers should be rubbery or even fluids the materials resulted in brittle solids that can be grounded to fine powders. The recent report of Pyun and coworkers about P(S-DIB) co-polymers proved by mechanicals tests that the DSC underestimates the real Tg of the polymers by almost 30 ^{0}C. On the other hand,
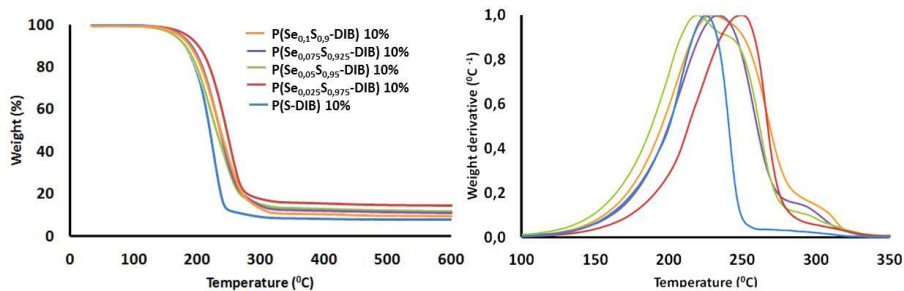
Figure 3.5: TGA curves (left) and the weight derivative (right) of the series of P(Se$_x$S$_{1-x}$-DIB) with different Se-S ratios with 10 wt% of the organic comonomer DIB.

the TGA curves shows that the degradation profile is very similar for all of the materials showing an onset of degradation around 200 ^{0}C and a single degradation step with a weight loss of 85–90% (Figure 3.5 a)). All of them also show a residual 10–15% in weight, which is associated to the organic DIB part. On the other hand, in all the selenium containing polymers it can be seen a little shoulder in between 270 ^{0}C and 310 ^{8}C. The derivative TGA (Figure 3.5 b)) indicates a new degradation step which growths with the selenium content.

3.3 Electrochemical characterization

Interestingly, the hybrid S-Se co-polymer can be processed using conventional methods used to obtain sulfur cathodes. Thus hybrid co-polymer powders were mixed by ball-milling with commercially available conductive carbon additives, and subsequently added to a PVDF binder solution in NMP. Good quality cathodes were obtained in large scale by blade-casting the resulting slurry onto aluminum foil current collector with an average loading of polymer of 1.8 mg cm^{-2}. It is worth to mention that is one of the highest loadings reported for inverse vulcanized sulfur polymers applied in lithium sulfur polymers. Then, the electrochemical behavior of the co-polymers was investigated in coin-cells having lithium metal as anode and a typical ether based electrolyte.
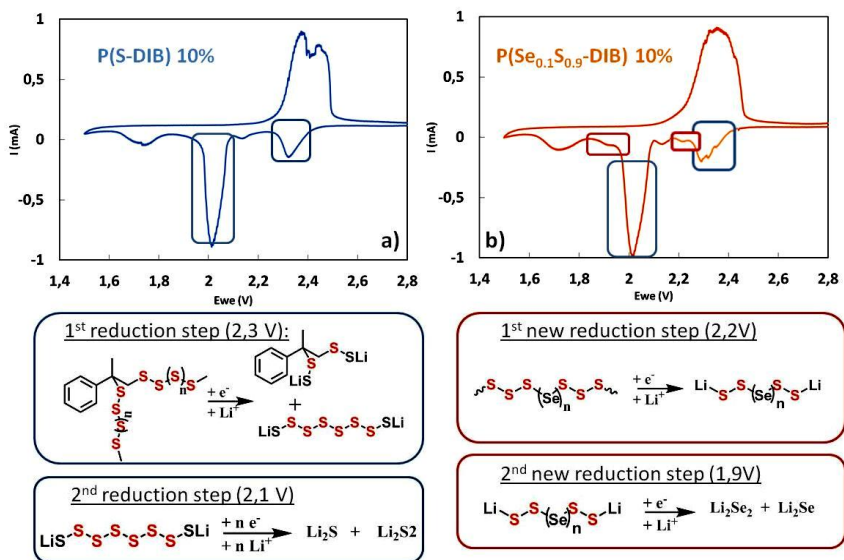
136

Figure 3.6: a) CV of P(S-DIB) polymer with 10 wt% of the organic comonomer DIB (top) and proposed reduction reaction at different voltages (bottom). b) CV of P(Se$_{0.1}$S$_{0.9}$-DIB) polymer with 10 wt% of the organic comonomer DIB (top) and proposed reduction reactions at new reduction processes observed in the CV (bottom).

First, cyclic voltammetry (CV) of the cells were carried out in order to observe the effect of the selenium content into the electrochemical properties of the polymer (Figure 3.6). The voltammograms of the neat poly(S-DIB) (Figure 3.5) shows a reduction peak at 2.30–2.35 V which is attributed to the conversion of sulfur to higher order linear polysulfides. The peak at 2.0 V is related to the further reduction of higher order polysulfides to lower order polysulfides, indicating multiple reaction feasibility of sulfur with lithium ions. The third small peak in the potential range of 1.70–1.75 V is attributed to the irreversible reduction of LiNO$_3$ additive in the electrolyte[33]. On the other hand, only one oxidation peak was observed at 2.35– 2.40 V in the subsequent charge process, corresponding to the transformation of lower ordered polysulfides to higher ordered polysulfides. The selenium activity was investigated in the CV of the poly(Se$_{0.1}$S$_{0.9}$-DIB) co-polymer (Figure 3.5), which was the material with the highest selenium amount. In this case, the broad oxidation peak suffers a shift to lower voltages; the maximum of the oxidation peak of the polymer containing
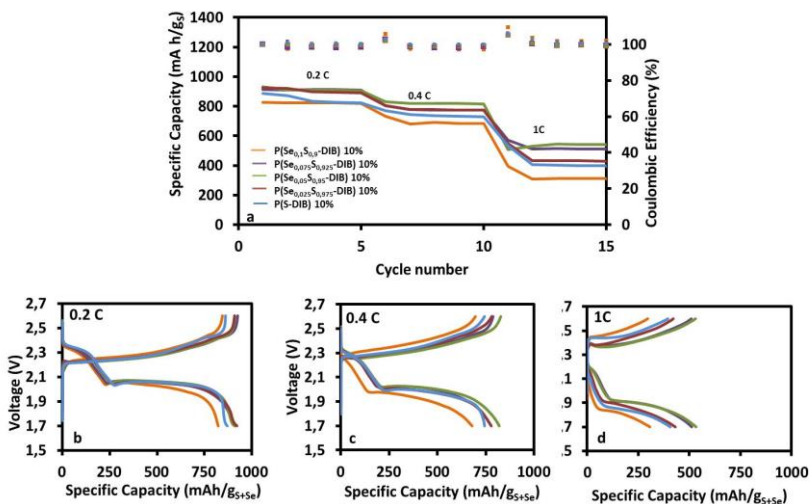
Figure 3.7: a) Effect of the C-rate on discharge capacity for the cathodes containing the series of P(Se$_x$S$_{1-x}$-DIB) with different Se-S ratios with 10 wt% of the organic comonomer DIB. Charge-discharge voltage profiles at b) 0.2C, c) 0.4C and d) 1C.

selenium appears at 2.30 V whereas the one of the polymer with bare sulfur is located at 2.35 V. This could be attributed to the higher contribution of selenium, which has a lower working voltage, to the overall oxidation step. Furthermore, two small peaks at 2.2 V and 1.9 V are observed. The peak at 2.2 V has been described as the formation of polysulfoselenide compounds, whereas the next peak at 1.9 V is the formation of lower order lithium selenides (Li$_2$Se). This reaction mechanism goes in agreement with the previous physicochemical characterization in which was proved that the Selenium was inserted in between sulfur segments.

Then, the charge discharge performance of the hybrid S-Se-Lithium cells at different C-rates was studied (Figure 3.7). It was found that the co-polymers containing 2.5, 5 and 7.5% in mol of selenium showed higher capacity than the standard P(S-DIB) polymer at every current density whereas the material with the highest content of selenium suffers a significant drop in the capacity. Interestingly, the materials with 5 and 7.5% in mol of selenium showed a

significant improvement in the capacity, especially at high C-rates showing 825 mAh g^{-1} at C/2,5 and 515 mAh g^{-1} at 1C in comparison with 730 mAh g^{-1} at C/2,5 and 402 mAh g^{-1} at 1C of the poly(S-DIB) polymers respectively Although we do not have an explanation for this result, a similar observation was reported in literature, in which selenium-sulfur alloys with selenium amounts in between 1 and 10% in mol showed the best electrochemical performance in terms of capacity at high C-rate and dropped at highest contents. Furthermore, Figure 3b), c) and d) shows the voltage profiles of the 2nd cycle at each current density. At 0.2 C two plateaus at around 2.3 and 2.05 V are clearly visible in the discharge curve for all of the materials, which is the characteristic behavior of the two step redox reaction of sulfur vs lithium in ether based electrolytes. As in previous reports, the addition of selenium does not change the shape of the voltage profile related with sulfur, however its own redox activity is unnoticed, even at high selenium content, due to the small contribution to the overall capacity.
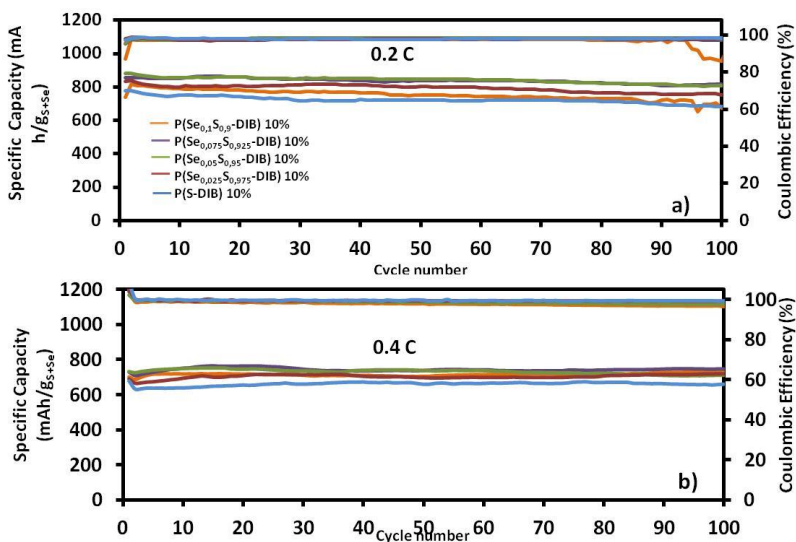

Figure 3.8: Long term cyclability test for the the cathodes containing the series of P(Se$_x$S$_{1-x}$-DIB) with different Se-S ratios with 10 wt% of the organic comonomer DIB at 0.2C (a) and 0.4C (b).

Lastly, long term cycling profiles of poly(S-DIB) and poly(Se$_x$S$_{1-x}$-DIB) at a moderate C-rate of 0.2 C and high C-rate of 0.4 C were carried out as shown in Figure 3.8 (Figure 3.9 magnified plots). As it can be observed the co-polymers containing selenium exhibited superior initial discharge capacities at moderate current densities (C/5), as well as higher capacity retention, especially the polymers with 5 and 7.5% in mol of selenium. The best co-polymers with 5.0 and 7.5% (in mol) showed initial values of 860 and 880 mAh g^{-1} respectively and for moderate C-rate of C/5. These polymers showed the lowest capacity loss per cycle, 0.14 and 0.4% in comparison with the 0.6% of capacity loss of the polymer with bare sulfur. The excellent performance of the hybrid sulfur-selenium co-polymers can be attributed to two main reasons as in the previous cases of S-Se lithium batteries. On one hand, the high electroactivity of the lowest order lithium selenides (Li$_2$Se) increase the reversibility of the battery, as there is a lower loss of active material by precipitation of redox-inactive materials (like Li$_2$S). On the other hand, it is though that the higher conductivity of selenium can enhance the performance of the battery by facilitating the
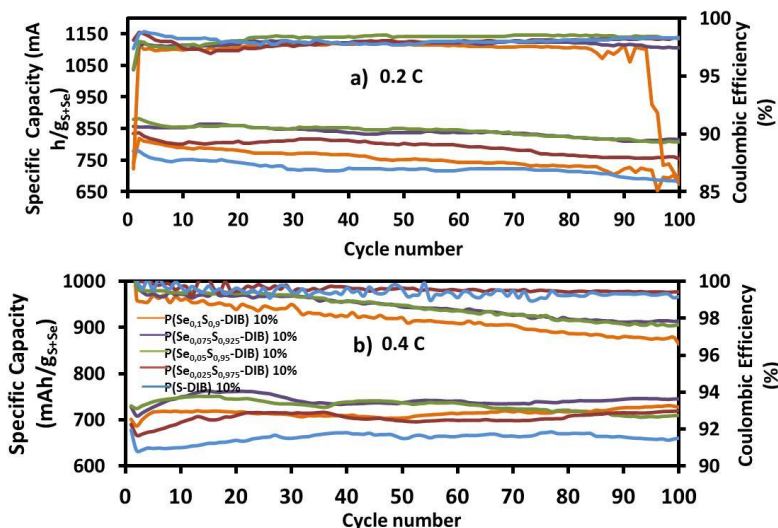

Figure 3.9: Magnified plots of the long term cyclability test for the the cathodes containing the series of P(Se$_x$S$_{1-x}$-DIB) with different Se-S ratios with 10 wt% of the organic comonomer DIB at 0.2C (a) and 0.4C (b).

electron transport through the active material.

4. Conclusions

In conclusion, the inverse vulcanization technique has been proved to be an easy and low energy method to obtain sulfur selenium materials which can be used as cathodes in lithium batteries in comparison with previously reported synthesis processes. Several characterization methods including NMR, Raman, DSC and TGA proved that a sulfur selenium hybrid copolymer was successfully synthesized. These co-polymers could be processed as powders using scalable and standard processing fabrication methods used for lithium-sulfur-selenium batteries. The principal feature of the Hybrid Sulfur-Selenium copolymers as Cathodic Materials for Lithium Batteries is the enhanced capacity retention at high C-rates and the low capacity decay during cycling. Interestingly for a lithium sulfur cell, the best performing material shows an excellent capacity value of 550 mAh g^{-1} at high C rate of 1C.

5. References

1.   Manthiram, A.; Chung, S.-H.; Zu, C., Lithium–Sulfur Batteries: Progress and Prospects. *Advanced Materials* 2015, **27** (12), 1980-2006.

2.   Urbonaite, S.; Poux, T.; Novák, P., Progress Towards Commercially Viable Li–S Battery Cells. *Advanced Energy Materials* 2015, **5** (16), n/a-n/a.

3.   Rosenman, A.; Markevich, E.; Salitra, G.; Aurbach, D.; Garsuch, A.; Chesneau, F. F., Review on Li-Sulfur Battery Systems: an Integral Perspective. *Advanced Energy Materials* 2015, **5** (16), n/a-n/a.

4.   Lu, Y.-C.; He, Q.; Gasteiger, H. A., Probing the Lithium–Sulfur Redox Reactions: A Rotating-Ring Disk Electrode Study. *The Journal of Physical Chemistry C* 2014, **118** (11), 5733-5741.

5.   Wujcik, K. H.; Velasco-Velez, J.; Wu, C. H.; Pascal, T.; Teran, A. A.; Marcus, M. A.; Cabana, J.; Guo, J.; Prendergast, D.; Salmeron, M.; Balsara, N. P., Fingerprinting Lithium-Sulfur Battery Reaction Products

by X-ray Absorption Spectroscopy. *Journal of The Electrochemical Society* 2014, **161** (6), A1100-A1106.

6.   Hofmann, A. F.; Fronczek, D. N.; Bessler, W. G., Mechanistic modeling of polysulfide shuttle and capacity loss in lithium–sulfur batteries. *Journal of Power Sources* 2014, **259**, 300-310.

7.   Cheng, X.-B.; Huang, J.-Q.; Peng, H.-J.; Nie, J.-Q.; Liu, X.-Y.; Zhang, Q.; Wei, F., Polysulfide shuttle control: Towards a lithium-sulfur battery with superior capacity performance up to 1000 cycles by matching the sulfur/electrolyte loading. *Journal of Power Sources* 2014, **253**, 263-268.

8.   Ji, X.; Lee, K. T.; Nazar, L. F., A highly ordered nanostructured carbon-sulphur cathode for lithium-sulphur batteries. *Nature Materials* 2009, **8** (6), 500-506.

9.   Liu, M.; Qin, X.; He, Y.-B.; Li, B.; Kang, F., Recent innovative configurations in high-energy lithium-sulfur batteries. *Journal of Materials Chemistry A* 2017, **5** (11), 5222-5234.

10.   Rehman, S.; Khan, K.; Zhao, Y.; Hou, Y., Nanostructured cathode materials for lithium-sulfur batteries: progress, challenges and perspectives. *Journal of Materials Chemistry A* 2017, **5** (7), 3014-3038.

11.   Xiang, Y.; Li, J.; Lei, J.; Liu, D.; Xie, Z.; Qu, D.; Li, K.; Deng, T.; Tang, H., Advanced Separators for Lithium-Ion and Lithium–Sulfur Batteries: A Review of Recent Progress. *ChemSusChem* 2016, **9** (21), 3023-3039.

12.   Cheng, L.; Curtiss, L. A.; Zavadil, K. R.; Gewirth, A. A.; Shao, Y.; Gallagher, K. G., Sparingly Solvating Electrolytes for High Energy Density Lithium–Sulfur Batteries. *ACS Energy Letters* 2016, **1** (3), 503-509.

13.   Xiao, J., Understanding the Lithium Sulfur Battery System at Relevant Scales. *Advanced Energy Materials* 2015, **5** (16), n/a-n/a.

14.   Eftekhari, A., The rise of lithium-selenium batteries. *Sustainable Energy & Fuels* 2017, **1** (1), 14-29.

15.   Lee, J. T.; Kim, H.; Oschatz, M.; Lee, D.-C.; Wu, F.; Lin, H.-T.; Zdyrko, B.; Cho, W. I.; Kaskel, S.; Yushin, G., Micro- and Mesoporous Carbide-Derived Carbon–Selenium Cathodes for High-Performance Lithium Selenium Batteries. *Advanced Energy Materials* 2015, **5** (1), 1400981-n/a.

16.   Abouimrane, A.; Dambournet, D.; Chapman, K. W.; Chupas, P. J.; Weng, W.; Amine, K., A New Class of Lithium and Sodium

Rechargeable Batteries Based on Selenium and Selenium–Sulfur as a Positive Electrode. *Journal of the American Chemical Society* 2012, **134** (10), 4505-4508.

17.   Cui, Y.; Abouimrane, A.; Lu, J.; Bolin, T.; Ren, Y.; Weng, W.; Sun, C.; Maroni, V. A.; Heald, S. M.; Amine, K., (De)Lithiation Mechanism of Li/SeS$_x$ (x = 0–7) Batteries Determined by in Situ Synchrotron X-ray Diffraction and X-ray Absorption Spectroscopy. *Journal of the American Chemical Society* 2013, **135** (21), 8047-8056.

18.   Xu, G.-L.; Ma, T.; Sun, C.-J.; Luo, C.; Cheng, L.; Ren, Y.; Heald, S. M.; Wang, C.; Curtiss, L.; Wen, J.; Miller, D. J.; Li, T.; Zuo, X.; Petkov, V.; Chen, Z.; Amine, K., Insight into the Capacity Fading Mechanism of Amorphous Se2S5 Confined in Micro/Mesoporous Carbon Matrix in Ether-Based Electrolytes. *Nano Letters* 2016, **16** (4), 2663-2673.

19.   Sun, F.; Cheng, H.; Chen, J.; Zheng, N.; Li, Y.; Shi, J., Heteroatomic Se$_n$S$_{8-n}$ Molecules Confined in Nitrogen-Doped Mesoporous Carbons as Reversible Cathode Materials for High-Performance Lithium Batteries. *ACS Nano* 2016, **10** (9), 8289-8298.

20.   Li, X.; Liang, J.; Zhang, K.; Hou, Z.; Zhang, W.; Zhu, Y.; Qian, Y., Amorphous S-rich S$_{1-x}$Se$_x$/C (x [≤] 0.1) composites promise better lithium-sulfur batteries in a carbonate-based electrolyte. *Energy & Environmental Science* 2015, **8** (11), 3181-3186.

21.   Chung, W. J.; Griebel, J. J.; Kim, E. T.; Yoon, H.; Simmonds, A. G.; Ji, H. J.; Dirlam, P. T.; Glass, R. S.; Wie, J. J.; Nguyen, N. A.; Guralnick, B. W.; Park, J.; SomogyiÁrpád; Theato, P.; Mackay, M. E.; Sung, Y.-E.; Char, K.; Pyun, J., The use of elemental sulfur as an alternative feedstock for polymeric materials. *Nature Chemistry* 2013, **5** (6), 518-524.

22.   Simmonds, A. G.; Griebel, J. J.; Park, J.; Kim, K. R.; Chung, W. J.; Oleshko, V. P.; Kim, J.; Kim, E. T.; Glass, R. S.; Soles, C. L.; Sung, Y.-E.; Char, K.; Pyun, J., Inverse Vulcanization of Elemental Sulfur to Prepare Polymeric Electrode Materials for Li–S Batteries. *ACS Macro Letters* 2014, **3** (3), 229-232.

23.   Dirlam, P. T.; Simmonds, A. G.; Kleine, T. S.; Nguyen, N. A.; Anderson, L. E.; Klever, A. O.; Florian, A.; Costanzo, P. J.; Theato, P.; Mackay, M. E.; Glass, R. S.; Char, K.; Pyun, J., Inverse vulcanization of elemental sulfur with 1,4-diphenylbutadiyne for cathode materials in Li-S batteries. *RSC Advances* 2015, **5** (31), 24718-24722.

24.   Gomez, I.; Mecerreyes, D.; Blazquez, J. A.; Leonet, O.; Ben Youcef, H.; Li, C.; Gómez-Cámer, J. L.; Bondarchuk, O.; Rodriguez-Martinez, L., Inverse vulcanization of sulfur with divinylbenzene: Stable and easy

143

processable cathode material for lithium-sulfur batteries. *Journal of Power Sources* 2016, **329**, 72-78.

25.   Gomez, I.; Leonet, O.; Blazquez, J. A.; Mecerreyes, D., Inverse Vulcanization of Sulfur using Natural Dienes as Sustainable Materials for Lithium–Sulfur Batteries. *ChemSusChem* 2016, **9** (24), 3419-3425.

26.   Worthington, M.; Kucera, R.; Albuquerque, I.; Gibson, C.; Sibley, A.; Slattery, A.; Campbell, J.; Alboaiji, S.; Muller, K.; Young, J.; Adamson, N.; Gascooke, J.; Jampaiah, D.; Sabri, Y.; Bhargava, S.; Ippolito, S.; Lewis, D.; Quinton, J.; Ellis, A.; Johs, A.; Bernardes, G.; Chalker, J. M., Laying Waste to Mercury: Inexpensive Sorbents Made from Sulfur and Recycled Cooking Oils. *Chemistry – A European Journal*, n/a-n/a.

27.   Worthington, M. J. H.; Kucera, R. L.; Chalker, J. M., Green chemistry and polymers made from sulfur. *Green Chemistry* 2017.

28.   Je, S. H.; Hwang, T. H.; Talapaneni, S. N.; Buyukcakir, O.; Kim, H. J.; Yu, J.-S.; Woo, S.-G.; Jang, M. C.; Son, B. K.; Coskun, A.; Choi, J. W., Rational Sulfur Cathode Design for Lithium–Sulfur Batteries: Sulfur-Embedded Benzoxazine Polymers. *ACS Energy Letters* 2016, **1** (3), 566-572.

29.   Boyd, D. A.; Baker, C. C.; Myers, J. D.; Nguyen, V. Q.; Drake, G. A.; McClain, C. C.; Kung, F. H.; Bowman, S. R.; Kim, W.; Sanghera, J. S., ORMOCHALCs: organically modified chalcogenide polymers for infrared optics. *Chemical Communications* 2017, **53** (1), 259-262.

30.   Anderson, L. E.; Kleine, T. S.; Zhang, Y.; Phan, D. D.; Namnabat, S.; LaVilla, E. A.; Konopka, K. M.; Ruiz Diaz, L.; Manchester, M. S.; Schwiegerling, J.; Glass, R. S.; Mackay, M. E.; Char, K.; Norwood, R. A.; Pyun, J., Chalcogenide Hybrid Inorganic/Organic Polymers: Ultrahigh Refractive Index Polymers for Infrared Imaging. *ACS Macro Letters* 2017, 500-504.

31.   Laitinen, R. S.; Pakkanen, T. A., Selenium-[77]NMR spectroscopic characterization of selenium sulfide ring molecules SenS8-n. *Inorganic Chemistry* 1987, **26** (16), 2598-2603.

32.   Laitinen, R.; Steudel, R., Vibrational spectroscopic investigations of

Chapter IV

Poly(anthraquinonyl sulfides): High Capacity Redox Polymers for Energy Storage
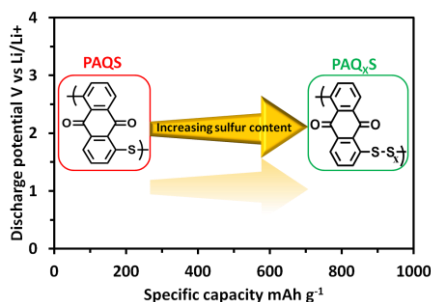
1. Introduction

In a sustainable planet, energy should be primarily provided by renewable sources such as solar or wind. Since most renewable energies are intermittent, electrochemical energy storage technologies such as batteries or supercapacitors are actively being developed[1]. Besides the improvement in terms of energy density and power capability, new concepts such as environmental impact, sustainability, and safety ought to be considered[2]. Today, most of the commercially available batteries do not fulfill those requirements since they contain toxic transition metals as part of their electrodes[2,3]. Therefore, developing alternative electrode materials is crucial nowadays. Among the most promising candidates, redox polymers are suitable, safe, and environmentally benign[4].

Redox polymers feature a lot of advantages such as film forming ability, flexibility, abundant resources, versatile chemical structures, tunable redox properties, and recyclability[5-9]. The most popular classes of redox polymers are conducting polymers, nitroxyl radical polymers, carbonyl polymers, and sulfur containing polymers[6]. Among redox polymers, carbonyl containing polymers such as polyimides, polyanthraquinones, or polyquinones are becoming the most promising ones due to its high cycling stability together with their abundance in nature showing high potential as electrode materials for next-gen battery systems[10].

Poly(anthraquinonyl sulfide) also known as PAQS is a very popular carbonyl polymer introduced as a high performance cathode for lithium batteries. PAQS combines the good reversibility of the anthraquinone moiety with the insoluble and stability of aromatic polymers. Furthermore, its relatively simple synthetic pathway allows its chemical combination with nanomaterials such as graphene or carbon nanotubes[11-14]. For this reason, PAQS was also successfully

implemented as cathode in several battery technologies such as sodium, magnesium and potassium batteries[15-17]. Although, PAQS batteries showed excellent cyclability its power storage is limited by its theoretical capacity value of which is 225 mAh g^{-1} [16]. In this work, we present a new family of PAQS type redox polymers with superior energy storage capacity. It is well-known that sulfur presents excellent electrochemical properties (1672 mAh g^{-1} and 2500 Whk g^{-1} vs Li/Li^{+}), low price, and availability[18,19]. In fact, the development of new sulfur polymers is leading the research of high capacity redox polymers for lithium−sulfur batteries[20-25]. For this reason, our strategy was to combine the high performance PAQS with the high capacity of sulfur into new hybrid polymers.

2. Experimental section

2.1 Materials and methods

1,5-Dichloroanthraquinone (DCAQ, Sigma Aldrich, 96%), Sodium sulfide anhydrous (Across Organics, 90+%), Sulfur (Sigma Aldrich, 99.5-100.5%), N-Methyl Pyrrolidone (NMP, Sigma Aldrich, 99%) were used as received.

In a 2-necked 100 ml round bottom flask equipped with a magnetic stir bar sodium sulfide and sulfur (amounts in 4.1) were added to 50 ml of NMP and placed in an oil bath preheated at 120 ºC. The mixture was stirred under nitrogen atmosphere until everything was dissolved when the solution showed dark colors. At this point DCAQ was added (amounts in table 4.1) and the reaction was left stirring overnight (16 hours). After this time a precipitated was observed in the dark solution. The reaction was filtrated and washed gently with hot water and acetone. The collected powders were dried in a vacuum oven during 24 hours prior to their characterization and application. The ATR-FTIR spectra were taken with a Nicolet 6700 FT-IR, Thermo Scientific Inc. The Raman analysis was performed in a DXR2 Raman Microscope from Thermo

Scientific with a 780 nm excitation laser. The solid state ^{13}C NMR spectra were recorded in a Bruker AVANCE 400 spectrometer. DSC thermograms were obtained in a Q2000 from TA instruments with two heating scans from -40 ^{0}C to 140 ^{0}C at 10 ^{0}C min^{-1} rate with a cooling scan of 50 ^{0}C min^{-1}. The TGAs of the materials were obtained in a in a Q500 from TA instruments in a heating rate of 10 ^{0}C min^{-1} under N$_2$ atmosphere.

	Na$_2$S		S$_8$		1,5-Dichloroanthraquinone		Yield
	Mol	Mass (g)	Mol	Mass (g)	Mol	Mass (g)	(% in wt)
PAQS	0.02	1.56	----	----	0.02	5.54	89%
PAQdS	0.02	1.56	0.02	0.64	0.02	5.54	78%
PAQpS	0.02	1.56	0.08	2.56	0.02	5.54	71%
PAQnS	0.02	1.56	0.16	5.12	0.02	5.54	57%

Table 4.1: Quantities in moles and grams needed for the synthesis of each poly(anthraquinonyl-polysulfide).

2.2 Electrochemical characterization

Positive electrodes were elaborated using 60% of active material. The selected polymers were dry ball milled prior to the cathode preparation, turning into a fine deep powder. Afterwards, a mixture of Ketjen Black 600JD (AkzoNobel) and the selected polymer was wet dry milled in ethanol during 3h. The mixture was dried and added to a solution of PVDF 5130 (SOLVAY) in NMP to form the cathodic slurry. The final solid content 30% slurries were prepared by mechanical mixer (RW 20 digital, IKA) at 600 rpm agitation rate. These slurries were blade cast onto a carbon coated aluminum foil (MTI Corp.) and dried at 60 ºC under dynamic vacuum during 12 hours before cell assembling. The cathodes were prepared with theoretical loadings of 2 mg cm^{-2}. One layer of commercial polyolefin separator Celgard 2500 separation soaked with 50 µL of 0.38 M solution of Bis(trifluoromethane)sulfonimide lithium salt (LiTFSI) (Sigma-Aldrich) and 0.32 M of lithium nitrate (LiNO$_3$) (Sigma-Aldrich) as additive, in 1/1

(v/v) mixture of dimethoxyethane (DME) (BASF) and dioxolane (DOL) (BASF), was placed between electrodes. Lithium metal (0.05 mm, Rockwood Lithium) was used as the anode in coin half cells (2025, Hohsen). Vacuum drying of electrodes and cell crimping has been performed in a dry room with dew point below -50 °C. Thereafter assembled cells were aged during 20 hours and then cycled by BaSyTec Cell Test System (Germany) at 25±1 °C by air conditioning.

3. Results and discussion

3.1 Synthesis

The synthetic route toward the sulfur-enriched PAQS polymers is depicted in figure 4.1. The reaction occurs via condensation of 1,5-dichloroanthraquinone with in situ formed sodium polysulfides[26]. First, sodium polysulfides of different lengths were synthesized by mixing sodium sulfide and elemental sulfur at different ratios in a polar high boiling solvent such as N-methyl pyrrolidone (NMP). This is known to result in a complex equilibrium of different polysulfide dianionic species[27]. Next, 1,5-chloroanthraquinone was added to this mixture and reacted under magnetic stirring overnight at 120 °C. As a result, a colored
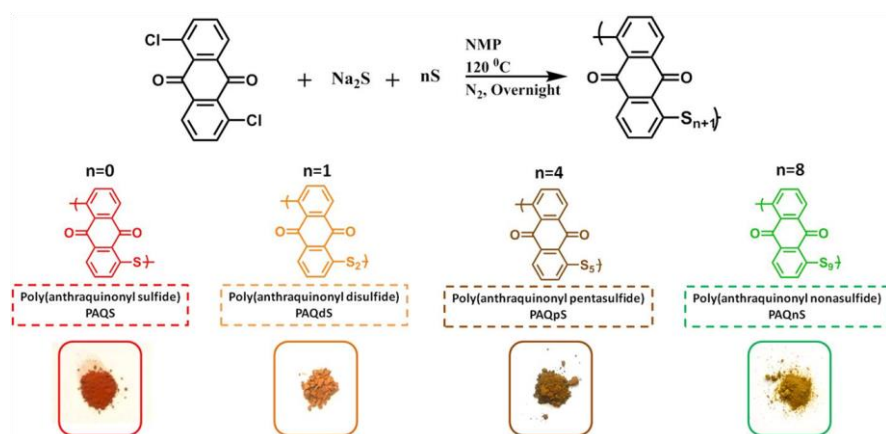

Figure 4.1: Top, synthesis reaction of Poly(anthraquinonyl sulfides). Bottom, proposed structures for the synthesized polymers with different sulfur equivalents with digital photographs showing the obtained powdery materials.

precipitate appeared in high yield, which was recovered by filtration, washed,

and dried under high vacuum. By changing the amount of sulfur into the initial reaction, we prepared four different polymers: poly(anthraquinonyl sulfide) PAQS reference with one sulfur atom, poly(anthraquinonyl disulfide) PAQdS with two sulfurs, poly(anthraquinonyl pentasulfide) PAQpS with five sulfurs, and poly(anthraquinonyl nonasulfide) PAQnS with nine sulfurs. The polymers were analyzed by elemental analysis in order to elucidate its elemental compositions (Table 4.1). As it can be observed, the values obtained of all the polymers are very close from the theoretical values which confirms the different ratios between organic and sulfur into the poly(anthraquinonyl sulfides). It is worth to note that the initial polysulfides are in a complex equilibrium which should lead to polymer segments with different lengths of sulfur atoms. Therefore, the

	Carbon (%)		Hydrogen (%)		Sulfur (%)	
	Theor.	Exp.	Theor.	Exp.	Theor.	Exp.
PAQS	70.3	67.1	2.9	2.5	13.4	12.7
PAQdS	61.7	58.6	2.9	2.1	23.5	19.5
PAQpS	45.7	50.7	1.9	1.9	43.6	32.2
PAQnS	33.9	33.3	1.4	1.2	58.2	53.0

number of sulfur atoms x in each formula should be taken as an average.

Table 4.2: Elemental analysis results of the obtained Poly(anthraquinonyl-polysulfide) polymers

3.2 Physicochemical characterization

As mentioned before, the poly(anthraquinonyl-polysulfide) PAQxS were obtained as powders. The reference PAQS was recovered as a light red powder, whereas PAQdS as a light brown powder, PAQpS as a dark brown powder, and PAQnS as a light green powder as showed in the pictures of figure 4.1. These powders were insoluble in common organic solvents such as chloroform, dimethylformamide or N-methyl pyrrolidone. For this reason, the

polymer characterization was carried out by solid state ^{13}C NMR, FTIR, and Raman Spectroscopy. The solid state ^{13}C NMR spectra of the 1,5-chloroanthraquinone monomer, the reference PAQS polymer and two new polymer PAQdS and PAQnS are shown in Figure 4.2 b). The bottom spectra of the monomer shows four different signals at 133, 139, 143, and 146 ppm corresponding to the aromatic carbons and one additional signal at 186 ppm related to the carbonyl carbon of the anthraquinone. In the case of PAQS, the set of signals related to the aromatic carbons is disturbed and turned into a very broad set of signals. As expected, the PAQxS show similar signals in the ^{13}C NMR spectra. It is also worth mentioning that, along with the sulfur addition, the signals become sharper and more defined. This effect may be due to the larger physical separation between the anthraquinone moieties from each other that causes lower NMR disturbance as sulfur is not active in NMR. Comparing with the spectra of the monomer with the PAQnS, can be observed that the set of signals at 143 ppm shift to lower ppms (140 ppm). It is also worth mentioning that the signal at 147 ppm is related with the carbon (b) in the 1,5-dichloroanthraquinone spectra, but to the carbon (f) in the case of PAQnS
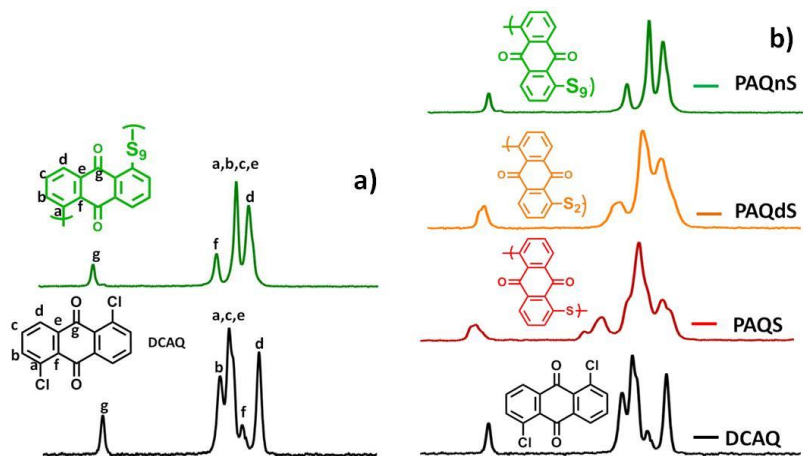

Figure 4.2: Solid State ^{13}C NMR spectra of the initial monomer DCAQ and resulting polymers PAQS, PAQdS and PAQnS. a) Assignation of the different signals for the initial monomer (bottom) and the obtained PAQnS (top). b) Comparison between the initial monomer (DCAQ) and the obtained polymers PAQS, PAQdS and PAQnS.

(Figure 4.2 a)).

The FTIR spectra of Figure 4.3 compare the initial DCAQ monomer and the resulting poly(anthraquinonyl sulfides) polymers. It is clearly seen that the spectra of the polymers are very similar to the one of the starting material DCAQ. This is explained by the chemical similarities of the organic part. However, there is a clear difference in the region in between 1350 and 1500 cm^{-1}. Here the band at 1430 cm^{-1} related to the C−Cl bond from DCAQ, disappears completely after the polymerizations and a new band appears at 1410 cm^{-1}. This complete disappearance and the new band corresponding to the new C−S bond formed points out the total consumption of DCAQ monomer to form PAQxS polymers[28]. As expected, the same signals were observed in all polymers, as shown in Figure 4.3 b).

Raman spectroscopy is a known technique for investigating the vibrations related with the polysulfide segments[29]. Figure 4.4 shows the Raman spectra of poly(anthraquinonyl sulfides) polymers with the reference spectra of PAQS and
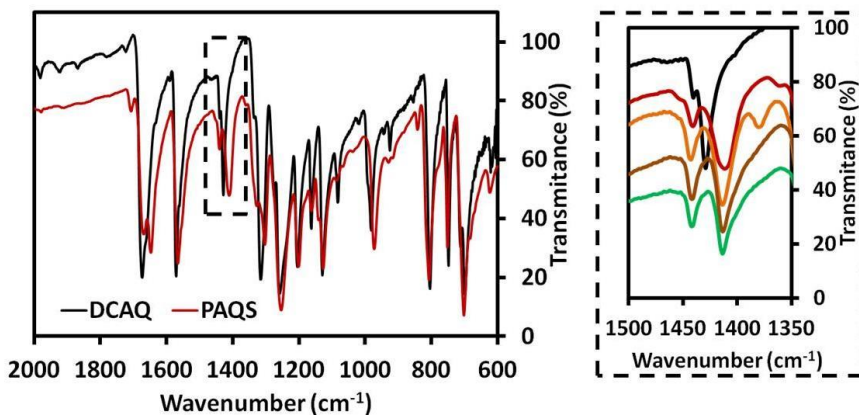

Figure 4.3: a) FTIR-ATR spectra of the obtained polymer P(AQS) (red) compared with the monomer, DCAQ (black). b) Zoomed, the region between 1350-1500 cm^{-1} of the used monomer DCAQ (black), and the obtained polymers PAQS (red), PAQdS (light brown), PAQpS (dark brown) and PAQnS (green).
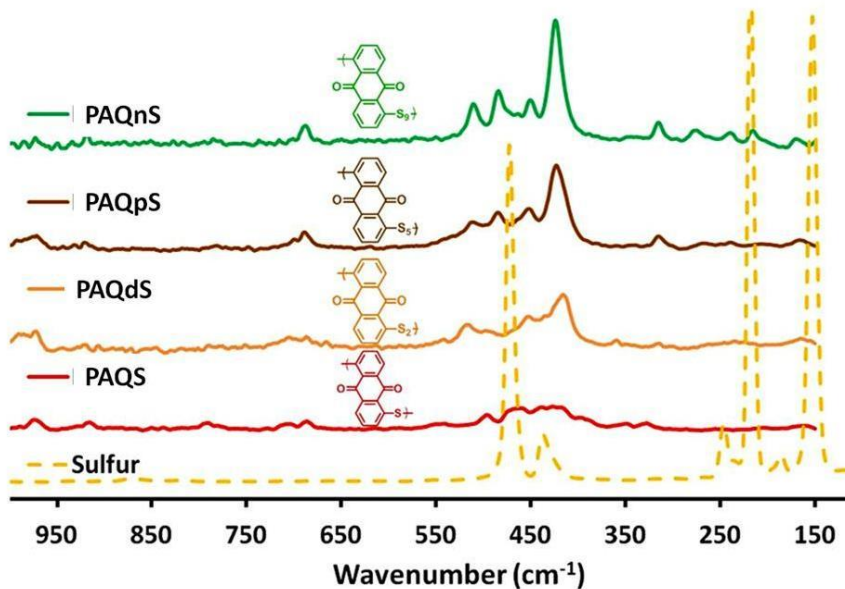
Figure 4.4: Raman spectra of the obtained polymers PAQS (red), PAQdS (light brown), PAQpS (dark brown) and PAQnS (green) compared with the spectrum of Sulfur (yellow dotted line).

elemental sulfur. As a first observation, the poly(anthraquinonyl sulfides) polymers do not show any band related to the reference elemental sulfur and are significantly different than the PAQS spectrum. The Raman spectrum of PAQS does not show clear bands associated with polysulfides since in theory PAQS doesńt have any S−S bond in its structure. Interestingly in the case of PAQxS, signals between 400 and 550 cm^{-1} appear which are related with the stretching of S−S bonds. With the increasing of sulfur amount going from PAQdS, PAQpS and PAQnS these signals grow and get more defined. Additionally, at the highest sulfur content PAQnS, some small signals at lower wavenumbers appear (150−250 cm^{-1}). These signals are related with the torsion and deformation vibrations of the polysulfide chains. This could further suggest that as the polysulfide chain gets longer, increasing the flexibility of the chains what promotes other kind of vibrations apart from stretching.

154

Next, the thermal properties poly(anthraquinonyl sulfides) with respect to the reference PAQS and elemental sulfur were studied by Differential Scanning Calorimetry (DSC) and Thermogravimetric Analysis (TGA). In Figure 4.5 a) the DSC thermograms are displayed. As it can be observed, the PAQxS polymers do not show a clear glass transition temperature, which is a normal behavior or these aromatic base rigid materials. It is also worth to mention that there is no melting peak of unreacted elemental sulfur in the thermograms, indicating that there is not remaining elemental sulfur in the final polymers. The thermal stability of the polymers was studied by TGA, as shown in Figure 4.5 b). PAQS reference polymer shows very high thermal stability, almost up to 500 °C. This behavior is typical in aromatic sulfide polymers, known for their high chemical, mechanical, and thermal stability. Interestingly, with the increase of the sulfur part, the thermal stability decreases. The weak S−S bonds start to break, promoting the degradation of the material at lower temperatures. Furthermore, high sulfur content polymers show a degradation step at 260 °C for PAQpS with a weight loss of 12% and 200 °C for PAQnS loosing 35% of weight, which seems to be due to the degradation of polysulfide segments. These weight losses are not consistent with the amount of sulfur in the polymers, which was
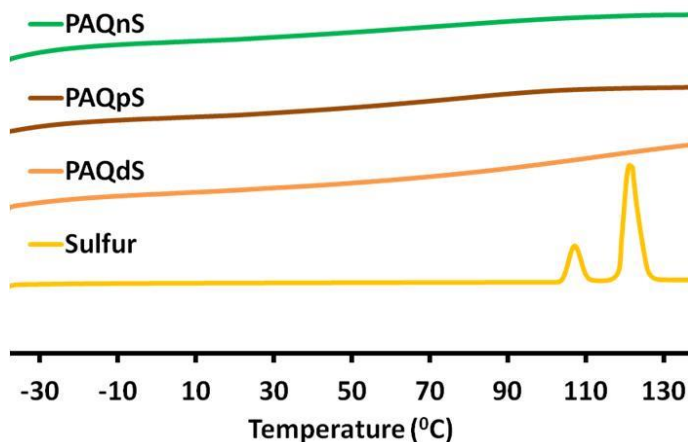

Figure 4.5: 1st Cycle of the DSC thermograms of the obtained polymers PAQdS (light brown), PAQpS (dark brown) and PAQnS (green) compared with the spectrum of Sulfur (yellow).
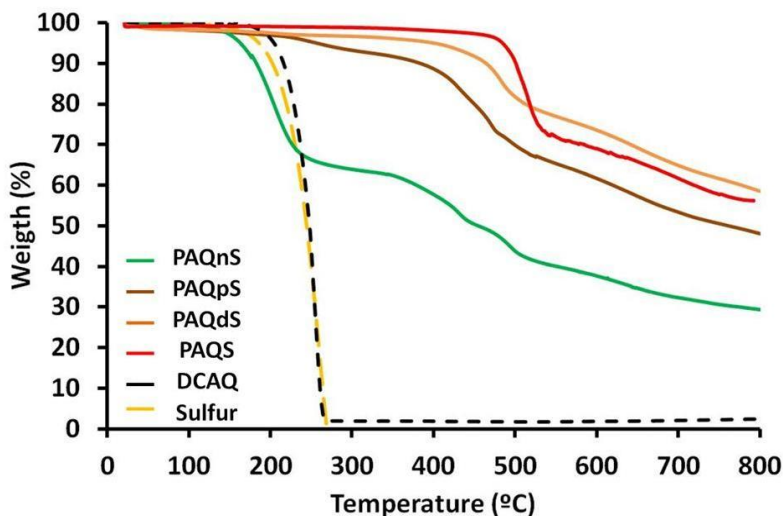
Figure 4.6: TGA thermograms of obtained polymers PAQS (red), PAQdS
(light brown), PAQpS (dark brown) and PAQnS (green). For comparison the
thermograms of the monomer (DCAQ, dotted black) and sulfur (dotted yellow)
are shown.

previously studied by elemental analysis. This might due to the distribution of
sulfur in the backbone. At low sulfur content (PAQS, or PAQdS), sulfur is
directly bonded to high molecular weight moieties that have high thermal
stability, therefore, the degradation of polysulfides does not occur. When the
sulfur amount in the polymer is increased (PAQpS, PAQnS), the sulfur in
between the anthraquinone moieties tend to form small sulfur molecules that
can degrade at low temperatures and sublimate. However, the sulfur directly
bonded to the organic part does not sublimate, indicating lower sulfur content
than the real one.

3.3 Electrochemical characterization

As mentioned at the beginning of this article, PAQS presents excellent
electrochemical performance as cathodic material in lithium batteries. However,
its limited capacity hinders its extended application in batteries. The addition of
sulfur should in theory enhance the electrochemical properties of PAQS.

Considering the proposed structures (Figure 4.6) and the redox reaction mechanism (Figure 4.7), the theoretical capacity was calculated to be 225 mAh/g for the reference PAQS, 397 mAh/g for PAQdS, 732 mAh/g for PAQpS, and 976 mAh/g for PAQnS (Figure 4.6). Interestingly, the value of theoretical capacity the poly(anthraquinonyl sulfides) PAQxS show between 2 and 4 times increase in capacity with respect to the known PAQS.

Therefore, cathodes containing the poly(anthraquinonyl sulfides) were assembled into coin cells using metallic lithium as anode. Figure 4.8 shows the cyclic voltagrams of PAQS reference and PAQnS as a representative example of the PAQxS polymers. As reported in previous articles, PAQS shows a broad signal between 2 and 2.5 V that includes the two redox processes associated
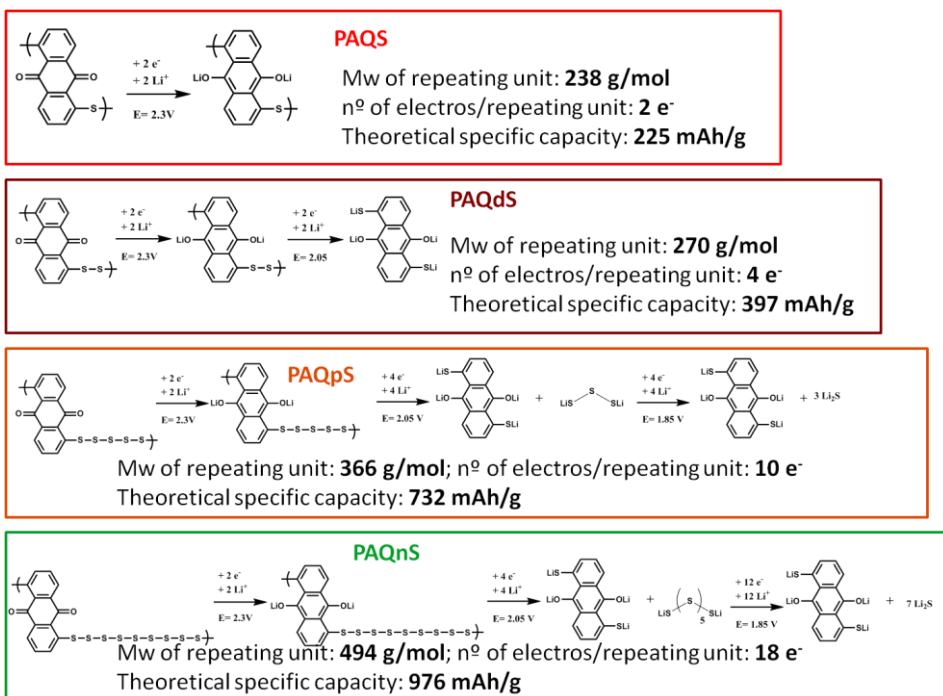

Figure 4.7: Reduction reaction mechanism proposal of the obtained polymers PAQS (red), PAQdS (light brown), PAQpS (dark brown) and PAQnS (green), and their specific capacity based in the reduction mechanism.
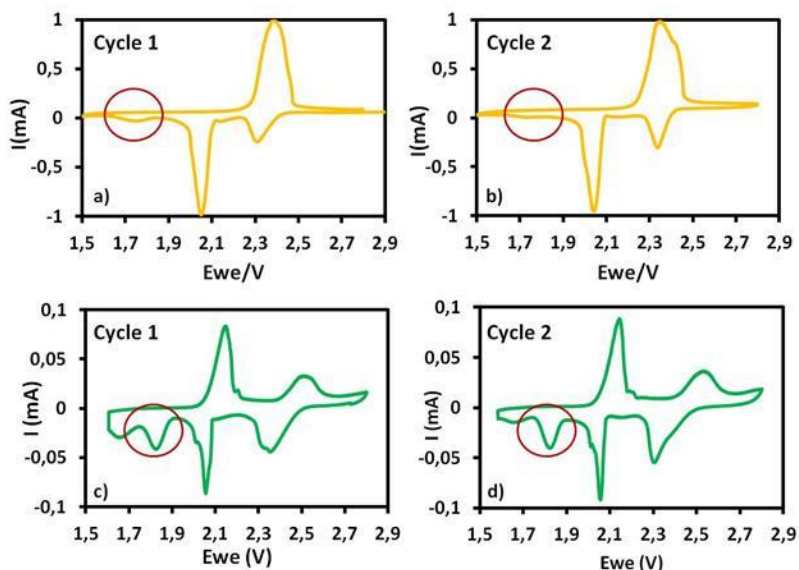
Figure 4.9: Cyclic voltammetry of different cycles of a) elemental sulfur (Cycle 1), b) elemental sulfur (Cycle 2) and c) PAQnS (Cycle 1), d) PAQnS (Cycle 2)..

with the anthraquinone moiety[15-17]. Interestingly, the cyclic voltagram of the sulfur enriched PAQnS is significantly different. PAQnS shows two oxidation peaks at 2.1 and 2.6 V and three reduction peaks at 1.75, 2.0, and 2.3 V. The peaks at high voltages are related to the oxidation reduction process of the anthraquinone moieties[15-17]. This process is narrower and shifted to higher potentials as compared to the PAQS reference. The peaks at low voltage correspond to the oxidation/reduction processes of the polysulfides moieties. Elemental sulfur shows two reduction peaks at 2.3 and 2.0 V (Figure 4.9 a,b). These peaks are related with the reduction of elemental cyclic sulfur allotropes, S8 and others, into high order linear lithium polysulfides and further reduction of these polysulfides into shorter Li_2S_x species. The second reduction peak has been described as the reduction of high order lithium polysulfides into Li_2S and Li_2S_2 passing through intermediate length Li_2S_x. Interestingly, the PAQnS, show the reduction peak at 2.0 V, which matches with the second reduction step of elemental sulfur, and a new one at 1.85 V, that it does not show the conventional sulfur cathodes. It is worth to point out that, unlike the elemental

sulfur, this peak does not disappear in the second cycle, what can indicate that is related to a reversible redox process (Figure 4.9 c,d). Interestingly, this third peak matches with the one observed for small linear sulfur molecules S_2 and S_3 16 which show the reduction of the small sulfides at 1.85 V[31]. The cyclic voltagrams of the other poly(anthraquinonyl sulfides) not shown here are similar to the one of PAQnS polymer. The only difference is the relative intensity between the signals of the anthraquinone and polysulfides moiety which varies depending on the polymer composition.

In order to investigate the impact of the addition of sulfur in the polymers, lithium battery coin cells were further investigated. To further confirm the combination of the redox processes in the PAQnS, in Figure 4.10 the voltage profile of the second cycle of the long-term cycling experiment is shown. First,
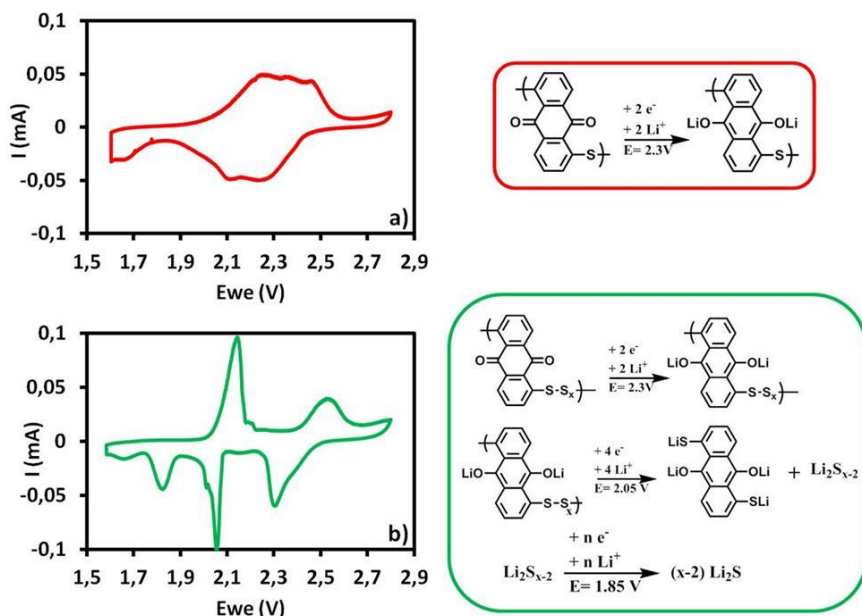

Figure 4.8: Second cycle of the Cyclic voltammetry of cathodes containing a) PAQS and b) PAQnS. In the right of each voltagram, the proposed redox processes of each material at each reduction voltage.

PAQS shows the reduction plateau at an average voltage of 2.2 V and the oxidation plateau at 2.3 V, result that agrees with the previously showed cyclic voltametry (Figure 4.8). As expected from the cyclic voltametry experiments, the PAQnS shows a multistep profile both in the reduction either in the oxidation. During the discharge a first plateau at around 2.3 V can be observed, with a discharge capacity of around 100 mAh g^{-1}. This first redox process might be related with the anthraquinone moiety present in the polymer. Comparing with the redox profile of the PAQS, the reduction potential has shifted to higher voltages, what matches with the shif previously observed. During the reduction, two new plateaus are visible, a long one at around 2.0 V, related with the second reduction process described in the cyclic voltametry of the PAQnS (Figure 4.8 b). This process may be related to the breaking of the polysulfide segments of the polymer and gives a capacity of around 300 mAh g^{-1} and the last one at 1.85 V, the final reduction of short lithium sulfides to Li2S, achieving a capacity of 150 mAh g^{-1}. All in all the experimental capacity value observed in the case of PAQnS exceeds more than twice the one of PAQS. The other poly(anthraquinonyl sulfides) show intermediate behaviors between those two. Additionally, in the first cycle of the cyclic voltagrams of elemental sulfur, PAQS and PAQnS, an irreversible reduction peak can be observed at 1.65−1.75 V that disappears in the second cycle (Figures 4.8 and 4.9). This peak is associated with the irreversible reduction of the lithium nitrate (LiNO$_3$) and the formation of the stable SEI layer in the surface of the lithium anode[30].

Next, we cycled the PAQxS/lithium coin cells at different rates. As it can be observed in the Figure 4.10 a), PAQS shows the excellent electrochemical behavior previously reported with negligible capacity fading with the increase of the current density and maintained almost a constant capacity of around 145 mAh g^{-1}. The sulfur-enriched PAQnS shows higher capacity of PAQS, showing an average capacity of 356 mAh g^{-1} at 0.1 mA, 255 mAh g^{-1} at 0.25 mA, 220 mAh g^{-1} at 0.5 mA, 205 mAh g^{-1} at 1 mA, and 180 mAh g^{-1} at 2 mA. The PAQnS shows a different trend in which a high capacity fading can be observed in the
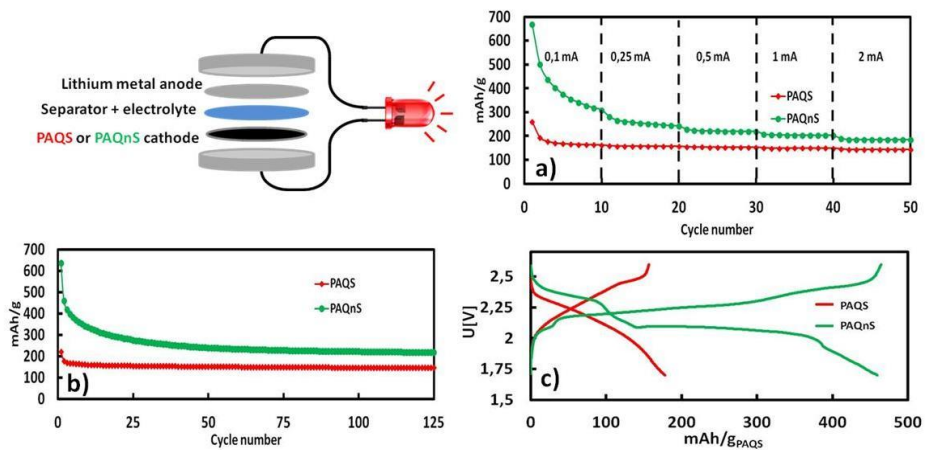
Figure 4.10: a) Effect of current intensity for different PAQS (red) and PAQnS (green) electrodes on discharge capacity. b) Galvanostatic long term cycling performance at 0.25 mA PAQS (red) and PAQnS (green) electrodes on discharge capacity. c) Voltage profiles of the 2nd cycle of the long term cycling performance for PAQS (red) and PAQnS (green). At the top left of the image, a schematic representation of the coin cell configuration.

first 10 cycles, but it tends to stabilize during cycling. Afterward, long cyclability tests were performed on identical cells, as can be observed in Figure 4.10 b). On the one hand, the PAQS shows the same cyclability behavior as previously reported, with almost constant 150 mAh g^{-1} and no capacity fading during cycling and very stable Coulombic efficiency above 99%. On the other hand, PAQnS shows a different cycling profile. Even though the first discharge above from 600 mAh g^{-1} (64% of the theoretical capacity), there is a drastic capacity fading in the first 10 cycles of almost 50% loss. In the next 15 cycles still there is a smaller capacity fading of 10% of capacity loss. Finally, at cycle 30, the capacity stabilizes at 230 mAh g^{-1} and is maintained almost constant up to 125 cycles. The Coulombic efficiency is always above 95%.

This behavior is typical of lithium sulfur battery system, where the capacity usually suffers a severe loss during the first charge/discharge cycles due to the dissolution of the lithium polysulfide intermediates in the electrolyte and the mechanism of sulfur electrochemistry[32]. It is worth mentioning that in typical LiS

batteries this capacity fading continues in during the whole long cycling process. In the case of PAQnS cathodes, we observed an initial capacity lost; however, in this case the capacity is maintained almost constant for more than 100 cycles with negligible capacity fading. This is very similar to the longterm charge/discharge profile of the organic polymer PAQS. This data points out the combination of the PAQxS cathodes show features of sulfur batteries like very high initial capacity, capacity loss in the first cycles but also the advantages of PAQS polymers such as high stability of the capacity toward long cycling and high C-rates.

4. Conclusion

To conclude, this work presents the synthesis and characterization of new poly(anthraquinonyl sulfides) PAQxS redox polymers. The polymers were synthesized by coupling of in situ formed sodium polysulfides with dichloroanthraquinone. Interestingly, the anthraquinone/polysulfide ratio could be varied leading to different PAQxS. These polymers were characterized by ATR-FTIR and solid state ^{13}C NMR for the organic part and Raman spectroscopy for the sulfur part. These sulfur enriched PAQxS powders combine the excellent redox behavior anthraquinone and polysulfide moieties. The cyclic voltammetry showed a dual reversible redox activity associated with both redox couples anthraquinone and polysulfides. Interestingly, the poly(anthraquinione nonasulfide) PAQnS showed very high experimental initial capacity values in lithium coin cells above 600 mAh g^{-1} at high C-rate and good cyclability. Whereas the typical capacity drop of sulfur cathods is observed, PAQxS electrodes showed stable capacity values of >225 mAh g^{-1} after 100 cycles improving PAQS. The further use of these poly(anthraquinonyl sulfides) as high capacity redox polymers for energy storage in different batteries is under development in our laboratories.

5. References

1. Yang, Z.; Zhang, J.; Kintner-Meyer, M. C. W.; Lu, X.; Choi, D.; Lemmon, J. P.; Liu, J., Electrochemical Energy Storage for Green Grid. *Chemical Reviews* **2011,** *111* (5), 3577-3613.

2. Larcher, D.; Tarascon, J. M., Towards greener and more sustainable batteries for electrical energy storage. **2014,** *7*, 19.

3. Liang, Y.; Tao, Z.; Chen, J., Organic Electrode Materials for Rechargeable Lithium Batteries. *Advanced Energy Materials* **2012,** *2* (7), 742-769.

4. Choi, J. W.; Aurbach, D., Promise and reality of post-lithium-ion batteries with high energy densities. *Nature Reviews Materials* **2016,** *1*, 16013.

5. Muench, S.; Wild, A.; Friebe, C.; Häupler, B.; Janoschka, T.; Schubert, U. S., Polymer-Based Organic Batteries. *Chemical Reviews* **2016,** *116* (16), 9438-9484.

6. Casado, N.; Hernández, G.; Sardon, H.; Mecerreyes, D., Current trends in redox polymers for energy and medicine. *Progress in Polymer Science* **2016,** *52* (Supplement C), 107-135.

7. Suga, T.; Aoki, K.; Nishide, H,; Ionic Liquid-Triggered Redox Molecule Placement in Block Copolymer Nanotemplates toward an Organic Resistive Memory, *ACS Macro Letters.* **2015**, 4 (9), 892-896.

8. Casado, N.; Hernández, G.; Veloso, A.; Devaraj, S.; Mecerreyes, D.; Armand, M., PEDOT Radical Polymer with Synergetic Redox and Electrical Properties. *ACS Macro Letters* **2016** *5* (1), 59-64

9. Suga, T.; Sakata, M.; Aoki, K.: Nishide, H.; Synthesis of pendant radical- and Ion-Containing Block Copolymers via Ring-Opening Methatesis Polymerization for Organic Resistive Memory *ACS Macro Letters.* **2014**, 3 (8), 703-707

10. Häupler, B.; Wild, A.; Schubert, U. S., Carbonyls: Powerful Organic Materials for Secondary Batteries. *Advanced Energy Materials* **2015,** *5* (11), 1402034.

11. Jian, Z.; Liang, Y.; Rodríguez-Pérez, I. A.; Yao, Y.; Ji, X., Poly(anthraquinonyl sulfide) cathode for potassium-ion batteries. *Electrochemistry Communications* **2016,** *71* (Supplement C), 5-8.

12. Song, Z.; Zhan, H.; Zhou, Y., Anthraquinone based polymer as high performance cathode material for rechargeable lithium batteries. *Chemical Communications* **2009,** (4), 448-450.

13. Pan, B.; Huang, J.; Feng, Z.; Zeng, L.; He, M.; Zhang, L.; Vaughey, J. T.; Bedzyk, M. J.; Fenter, P.; Zhang, Z.; Burrell, A. K.; Liao, C., Polyanthraquinone-Based Organic Cathode for High-Performance Rechargeable Magnesium-Ion Batteries. *Advanced Energy Materials* **2016.**

14. Bitenc, J.; Pirnat, K.; Bančič, T.; Gaberšček, M.; Genorio, B.; Randon-Vitanova, A.; Dominko, R., Anthraquinone-Based Polymer as Cathode in Rechargeable Magnesium Batteries. *ChemSusChem* **2015,** *8* (24), 4128-4132.

15. Lee, W.; Suzuki, S.; Miyayama, M., Electrochemical Properties of Poly(Anthraquinonyl Sulfide)/Graphene Sheets Composites as Electrode Materials for Electrochemical Capacitors. *Nanomaterials* **2014,** *4* (3), 599.

16. Song, Z.; Xu, T.; Gordin, M. L.; Jiang, Y.-B.; Bae, I.-T.; Xiao, Q.; Zhan, H.; Liu, J.; Wang, D., Polymer–Graphene Nanocomposites as Ultrafast-Charge and -Discharge Cathodes for Rechargeable Lithium Batteries. *Nano Letters* **2012,** 12 (5), 2205–2211.

17. Vizintin, A.; Bitenc, J.; Kopač Lautar, A.; Pirnat, K.; Grdadolnik, J.; Stare, J.; Randon-Vitanova, A.; Dominko, R., Probing electrochemical reactions in organic cathode materials via in operando infrared spectroscopy. *Nature Communications,* **2018**, 9 (1), 661.

18. Chung, W. J.; Griebel, J. J.; Kim, E. T.; Yoon, H.; Simmonds, A. G.; Ji, H. J.; Dirlam, P. T.; Glass, R. S.; Wie, J. J.; Nguyen, N. A.; Guralnick, B. W.; Park, J.; SomogyiÁrpád; Theato, P.; Mackay, M. E.; Sung, Y.-E.; Char, K.; Pyun, J., The use of elemental sulfur as an alternative feedstock for polymeric materials. *Nature Chemistry,* **2013,** *5* (6), 518-524.

19. Simmonds A. G., Griebel J. J., Park J., Kim K. R., Chung W. J., Oleshko V. P., Kim J., Kim E. T., Glass R. S., Soles C. L., Sung Y.-E., Char K., Pyun J., Inverse vulcanization of elemental sulfur to prepare polymeric electrode materials for Li-S batteries. *ACS Macro Letters* **2014**, (3), 229-232.

20. Dirlam, P. T.; Glass, R. S.; Char, K.; Pyun, J., The use of polymers in Li-S batteries: A review. *Journal of Polymer Science, Part A: Polymer Chemistry*, **2017**, 55(10), 1635-1668.

21. Gomez, I.; Mecerreyes, D.; Blazquez, J. A.; Leonet, O.; Ben Youcef, H.; Li, C.; Gómez-Cámer, J. L.; Bondarchuk, O.; Rodriguez-Martinez, L., Inverse vulcanization of sulfur with divinylbenzene - stable and easy processable cathode material for LiS batteries. *Journal of Power Sources* **2016,** 329, 72–78.

22. Gomez, I.; Leonet, O., Blazquez, J. A.; Mecerreyes, D., Inverse Vulcanization of Sulfur with Natural Dienes as Sustainable Materials for LiS batteries. *ChemSusChem* **2016**, 9 (24), 3419–3425.

23. Je, S. H.; Hwang, T. H.; Talapaneni, S. N.; Buyukcakir, O.; Kim, H. J.; Yu, J.-S.; Woo, S.-G.; Jang, M. C.; Son, B. K.; Coskun, A.; Choi, J. W., Rational Sulfur Cathode Design for Lithium–Sulfur Batteries: Sulfur-Embedded Benzoxazine Polymers. *ACS Energy Letters,* **2016**, 1 (3), 566–572.

24. Zhang, Y.; Griebel, J. J.; Dirlam, P. T.; Nguyen, N. A.;Glass, R. S.; Mackay, M. E.; Char, K.; Pyun, J., Inverse vulcanization of elemental sulfur and styrene for polymeric cathodes in Li-S batteries. *Journal of Polymer Science Part A: Polymer Chemistry*, **2016**, 55 (1), 107-116.

25. Gomez, I.; Leonet, O., Blazquez, J. A.; Mecerreyes, D., Hybrid SulfurSelenium Co-polymers as Cathodic Materials for Lithium Batteries, *ChemElectroChem,* **2017.**

26. Fahey, D. R.; Hensley, H. D.; Ash, C. E.; Senn, D. R., Poly(p-phenylene sulfide) Synthesis: A Step-Growth Polymerization with Unequal Step Reactivity. *Macromolecules* **1997,** *30* (3), 387-393.

27. Seel, F.; Güttler, H.-J.; Simon, G.; Więckowski, A., *Colored sulfur species in EPD-solvents.* **1977**, 49, 45-54.

28. Krishnakumar, V.; Xavier, R. J., Vibrational analysis of 1,4-diaminoanthraquinone and 1,5-dichloroanthraquinone: A joint FTIR, FT–Raman and scaled quantum mechanical study. *Spectrochimica Acta Part A: Molecular and Biomolecular Spectroscopy* **2005,** *61* (8), 1799-1809.

29. Eckbert B., S. R., Molecular spectra of sulfur molecules and solid sulfur allotropes. In *Elemental sulfur and sulfur-rich compounds II*, T., S., Ed. Springer: Topic in current chemistry, 2003; Vol. 231.

30. S. S. Zhang, *Electrochimica Acta* **2012**, 70, 344–348.

31. Xin, S.; Gu, L.; Zhao, N.-H.; Yin, Y.-X.; Zhou, L.-J.; Guo, Y.-G.; Wan, L.-J., Smaller Sulfur Molecules Promise Better Lithium–Sulfur Batteries. *Journal of the American Chemical Society* **2012,** *134* (45), 18510-18513.

32. Kolosnitsyn, V.S.; Kusmina, E.V.; Karaseva, E.V. On the reasons for low sulphur utilization in the lithium-sulphur batteries *Journal of the Power Sources* **2015,** *274* (15), 203-210.

166

Chapter V

Sulfur Polymers meet Poly(ionic liquid)s: Bringing new properties to both polymer families
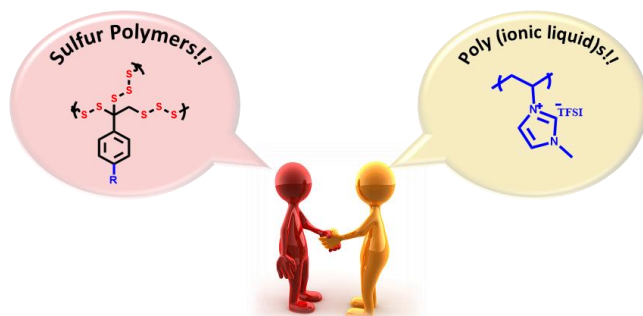
1. Introduction

New polymers with specific properties are searched to fulfil the demands in emerging application areas such as energy, optics, electronics or biomedicine[1–3]. Among them, sulfur containing polymers and poly(ionic liquid)s are two of the emerging synthetic macromolecules which are finding a variety of applications. On the one hand, sulfur containing polymers have unique properties given by the presence of sulfur with specific chemistry such as redox or dynamic polysulfide bonds and low solubility[4]. Sulfur containing polymers are finding applications in areas such as lithium sulfur batteries, high refractive index materials, self-healing plastics and mercury capture materials[5–8]. On the other hand, poly(ionic liquid)s have emerged as a new class of polyelectrolytes combining the properties of ionic liquids such as ionicity, ionic conductivity, thermal and electrochemical stability and tunable solubility[9–11]. Poly(ionic liquid)s are finding many different applications as polymer electrolytes in batteries or solar cells, electronics devices, gas membranes for CO_2 separation, vitrimers, catalysis, lubricants, water purification or biomedicine[12–16].

Having this in mind, we hypothesized that the combination of both chemistries, sulfur containing polymers and poly(ionic liquid)s could lead to new polymers with unique properties and applications. For instance, two of the limitations of sulfur are its limited solubility and low conductivity. Here, the introduction of ionic groups could be used to tune the solubility of sulfur containing polymers in water or organic solvents or to bring about some ionic conductivity. To the best of our knowledge, these two polymer chemistries have not been combined before. In order to do so, we followed a reaction recently reported by Pyun et al. between sulfur and styrene which opens new possibilities to copolymerize sulfur with polar monomers such as triazines, acrylates and polar styrenics[17]. Using this strategy, in this paper we present the synthesis and characterization of new sulfur containing poly(ionic liquid)s. For this purpose, first we investigated the copolymerization between sulfur and the styrenic functional monomer 4-

vinylbenzyl chloride. Taking advantage of the high solubility of the poly(sulfur-vinylbenzyl chloride) system, we carried out an easy post-functionalization based on quaternization and anion exchange leading to new sulfur containing poly(ionic liquid)s. These original new polymers showed features of both sulfur containing polymers and poly(ionic liquid)s into the same material.

2. Experimental Section

2.1 Materials and methods

Sulfur (Sigma-Aldrich, 99.5-100.5%), 4-vinylbenzyl chloride (Sigma-Aldrich, 90%), N-methyl imidazole (Sigma-Aldrich, 99%), n-Hexanes (Scharlab, Synthesis grade), Tetrahydrofuran (Scharlab, Synthesis grade) were used as received.

2.2.1 Synthesis of poly(sulfur-co-4-vinylbenzyl chloride) (P(S-VBC))

In a 100 ml round bottom flask equipped with a magnetic stir bar elemental sulfur was added and placed into an oil bath preheated at 130 ºC. After the melting of sulfur, 4-vinylbenzyl chloride was added via syringe (see masses in table 5.1). During the first hour the mixture showed a yellow turbid solution, that afterwards become totally transparent. The monomer consumption was monitored via NMR until the 4-vinylbenzyl chloride was totally consumed. At this point the reaction media was a brownish viscous fluid that solidified after cooling. This bulk was dissolved in THF and purified via flash column chromatography in order to remove the unreacted elemental sulfur using n-hexanes as eluent for elemental sulfur and THF for P(S-VBC) polymers. The final polymer was isolated by rotary evaporation of THF yielding to opaque yellow viscous liquids. Yields: P(S-VBC) 1: 43%; P(S-VBC) 2: 65%; P(S-VBC) 3: >90%.

Sample	Sulfur		4-Vinylbenzyl chloride	
	Mass (g)	Mol	Mass (g)	Mol
P(S-VBC) 1	7.0	0.218	3.0	0.020
P(S-VBC) 2	5.0	0.156	5.0	0.033
P(S-VBC) 3	3.0	0.093	7.0	0.046

Table 5.1: *Masses and mol amounts for the inverse vulcanization reaction of sulfur with 4-vinylbenzyl chloride.*

2.2.2 Synthesis of poly(Sulfur-co-4-vinylbenzyl methylimidazolium) TFSI (P(S-VBMIm) TFSI)

Quaternization procedure: In a 100 ml round bottom flask equipped with a magnetic stir bar 1 g of the purified P(S-VBC) polymer was dissolved in 40 ml of $CHCl_3$ and placed in an oil bath preheated at 65 ºC. Subsequently N-Methylimidazole was added and the reaction was stirred overnight. Afterwards, a clear red oil precipitate could be observed in the bottom of the flask. The $CHCl_3$ was decanted and the precipitate was washed 3 times with 10 ml of $CHCl_3$. Afterwards, the product was dissolved in MeOH and the solvent was removed by rotary evaporation. The product was dissolved in distilled water and purified by dialysis for one night in order to remove the excess of N-methylimidazole. Afterwards the polymer was dried in the rotavaporator and in a vacuum oven at 40 ºC overnight yielding a brittle transparent red film. Yields: P(S-VBMImC) 1: 67%; P(S-VBMImC) 2: 60%; P(S-VBMImC) 3: 57%.

Anion exchange procedure: In a 100 ml Erlenmeyer flask, 1g of P(S-VBMImC) was dissolved in 50 ml of deionized water. Lithium bis(trifluorosulfonyl) imide (LiTFSI) was added in excess in a 0.2 g ml^{-1} solution in water. Immediately a light orange precipitate could be observed. The resulting mixture was further

stirred 1 h. Afterwards the product was filtrated and washed several times with deionized water. The filtrate was dried under vacuum for 1 day. The yields in all cases were stoichiometric.

2.2.3 Polymer characterization

NMR analyses were performed in a Bruker AVANCE 300 spectrometer with CDCl$_3$ and d^6-DMSO (Deutero GmbH) as solvents. The molecular weight was investigated in a Waters chromatograph (waters chromatography, Milford, MA, USA) equipped with four 5 mm Waters columns (300 mm × 7.7 mm) connected in series with increasing pore sizes (100, 1000, 105, 106 Å) with THF as a mobile phase, with Poly(Styrene) standards and Toluene as a marker. The thermal properties were studied in a Q2000 for DSC measurements and in a Q500 for thermogravimetric analyses, both from TA instruments. DSC thermograms were obtained with two heating scans from 40 ºC to 140 ºC at 10 ºC min^{-1} rate with a cooling scan of 50 ºC min^{-1}. The thermograms of the TGA were done in a in a heating rate of 10 ºC min^{-1} under N$_2$ atmosphere.

The ionic conductivity was studied by EIS (electrochemical impedance spectroscopy) with an Autolab 302N Potentiostat Galvanostat with temperature controlled by a Microcell HC station. The sample was prepared by drop casting a circular membrane (Ø = 11 mm) with a thickness of 140 µm. The membranes were placed between two stainless steel electrodes and sealed in a Microcell under inert atmosphere in a globe box to avoid the contact of the sample with moisture. The measurements were carried out between 20 °C and 60 °C with a step of 10 °C. The frequency range was set from 0.1 MHz to 0.1 Hz and the amplitude was 10 mV.

Cyclic Voltametry: A mixture of Ketjen Black 600JD (AkzoNobel) and the selected co-polymer was wet dry milled in ethanol during 3 h. The mixture was dried and added to a solution of PVDF 5130 (SOLVAY) in NMP to form the

cathodic slurry. These slurries were blade cast onto a carbon coated aluminum foil (MTI Corp.) and dried at 60 ºC under dynamic vacuum during 12 hours before cell assembling. One layer of commercial polyolefin separator Celgard 2500 separation soaked with 50 mL of 0.38 mol L^{-1} solution of Bis(trifluoromethane)sulfonimide lithium salt (LiTFSI) (Sigma-Aldrich) and 0.32 mol L^{-1} of lithium nitrate ($LiNO_3$) (Sigma-Aldrich) as additive, in 1/1 (v/v) mixture of dimethoxyethane (DME) (Gotion) and dioxolane (DOL) (Gotion), was placed between electrodes. Lithium metal (0.05 mm, Rockwood Lithium) was used as the anode in coin half cells (2025, Hohsen). The cells were tested from 1.5 to 2.8 V at 10 mV s^{-1}.

3. Results and Discussion

3.1. Copolymerization of sufur and 4-vinylbenzyl chloride

In a first step the inverse vulcanization between sulfur and 4-vinylbenzyl choride (VBC) was investigated. This reaction was carried in bulk at 130 ºC by melting of sulfur and dropwise addition of VBC (Figure 5.1). This temperature was chosen since appeared to be the optimal one for the copolymerization between sulfur and styrene. As it can be seen in the pictures, the reaction mixture changed from a transparent yellow liquid aspect to a brownish viscous liquid. Upon cooling the final product was obtained as a glassy brown solid. Using this method, three different copolymers were synthesized by varying the initial sulfur:4-vinyl benzyl chloride weight ratio 70 S:30 VBC (P(S-VBC)1), 50 S: 70 VBC (P(S-VBC)2) and 30 S:70 VBC (P(S-VBC)3). The monomer conversion was followed during the reaction time by ^{1}H NMR spectroscopy. As it can be seen in Figure 5.1b, the reaction is faster at high sulfur contents and the reaction times range from 3 hours in the case where VBC is 30 wt%, to 4.5 h in the case of 50 wt% VBC and 9 hours in the case of 70 wt% VBC. It is worth to mention that in all the cases, an induction period of about 1 h is observed which
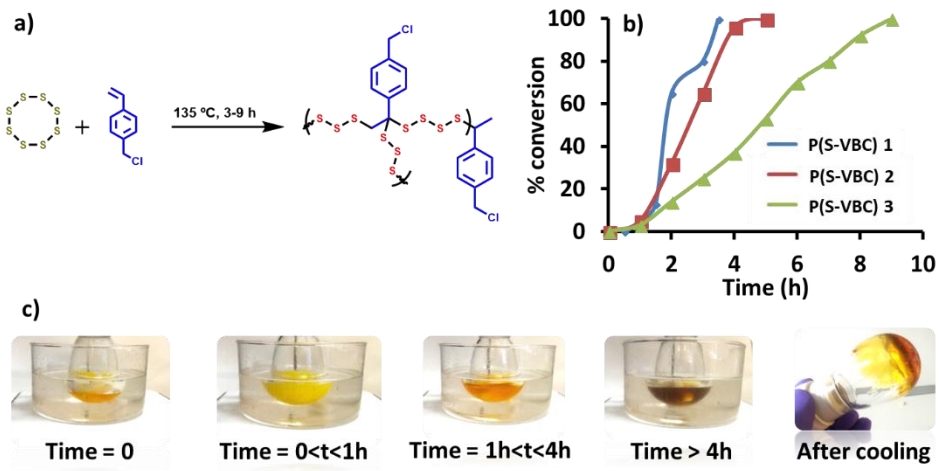
Figure 5.1: a) Synthetic scheme of the copolymerization between sulfur and 4-vinylbenzyl chloride; b) Conversion of 4-vinuylbenzyl chloride during the reaction as followed by 1H NMR; c) Digital images of the reaction mixture at different reaction times.

goes together with a visual observation of an initial turbid reaction mixture which becomes clear and homogeneous.

After copolymerization the P(S-VBC) polymers were purified by flash chromatography in order to eliminate the un-reacted sulfur. The purified copolymers resulted soluble in organic solvents such as tetrahydrofuran, chloroform and dimethylsulfoxide and therefore they could be characterized by solution NMR and gel permeation chromatography. Figure 5.2 a) compares the ^{1}H NMR spectrum of 4-vinylbenzyl chloride and the obtained poly(sulfur-co-4-vinylbenzyl chloride) from an initial 70 wt% sulfur ratio (P(S-VBC) 1). As it can be observed, the signals due to the vinylic protons between 5 and 7 ppm completely disappear indicating the total reaction of the double bonds. On the other hand, the methylene signal close to the chlorine atom at 4.6 ppm and the aromatic signals between 7 and 8 ppm are maintained showing a broader aspect typical of polymeric compounds. In the region between 1.5 and 4 ppm a

variety of small peaks are observed which are associated to the methylene protons of the polymer chain directly linked to other methylene units or sulfur atoms. These peaks are similar to the observed ones previously in the copolymerization of sulfur with styrene.

The ^{1}H NMR spectra of the three copolymers with varying composition present similar features. However, depending on the initial feed ratio the poly(sulfur-co-4-vinylbenzyl chloride) copolymers were different, from a viscous liquid in the case of the one synthesized of P(S-VBC)3 to soft solids in the other two cases P(S-VBC)1-2. In order to quantify the final composition of the copolymers we quantified the recovered sulfur after flash chromatography and we carried out elemental analysis into the three copolymers. As shown in Table 1 and table S3, the obtained poly(sulfur-co-4-vinylbenzyl chloride) copolymers showed a wt% composition of 45.5 wt% P(S-VBC)1, 44.8 wt% P(S-VBC)2, and 35.1wt% P(S-VBC)3 in sulfur, respectively. Furthermore, the molecular weight of these copolymers was analyzed by Size Exclusion Chromatograpy (Figure 5.2 b). As
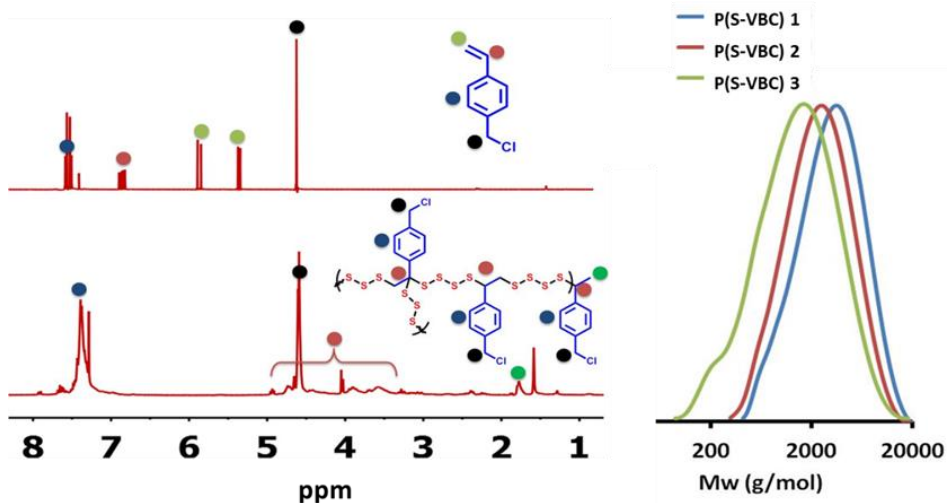

Figure 5.2: a) 1H NMR spectra of 4-vinylbenzyl chloride (top) and P(S-VBC) 1. b) GPC traces of the obtained P(S-VBC) copolymers with different feed ratios.

Sample	Sulfur recovered	Final yield
P(S-VBC) 1	54.5%	45%
P(S-VBC) 2	22.5%	60%
P(S-VBC) 3	---	>90%

Table 5.2: Sulfur recovered from the purification processes and the yield obtained from the final polymer.

it can be observed, the copolymers showed low molecular weights following the observed trends in previously reported poly(sulfur-co-styrene) copolymers. It is also worth to indicate that the higher the initial sulfur ratio, the higher the molecular weight of the copolymers which shows values of 3800, 3000 and 2000 g mol^{-1} and dispersity values of 1.6, 1.4 and 2.4 for P(S-VBC)1-3, respectively.

In order to study the stability of the functional group of the monomer to the inverse vulcanization reaction conditions, the model reaction of elemental sulfur with benzyl chloride was performed, and the resulting product was studied by NMR. In figure 5.3 a) ^{1}HNMR spectrum of benzyl chloride is compared with the obtained product. As can be observed, the NMR shifts and integration are exactly the same in both cases, what initially suggest that the isolated product is essentially benzyl chloride, which has not reacted in any way with elemental sulfur. In order to further confirm this affirmation, the structure of the obtained

Sample	C %		H %		S %	
	Theor.*	Obt.	Theor.*	Obt.	Theor. *	Obt.
P(S-VBC) 1	21.2 %	39%	1.5%	3.1%	70%	45.5%
P(S-VBC) 2	35.4%	40.8%	2.5%	3.0%	50%	44.8%
P(S-VBC) 3	49.5%	45.5%	3.5%	3.5%	30%	35.1%

*Calculated from the initial feed ratios

Table 5.3: Elemental analysis of the different polymers obtained from the inverse vulcanization of sulfur with 4-Vinylbenzyl chloride.
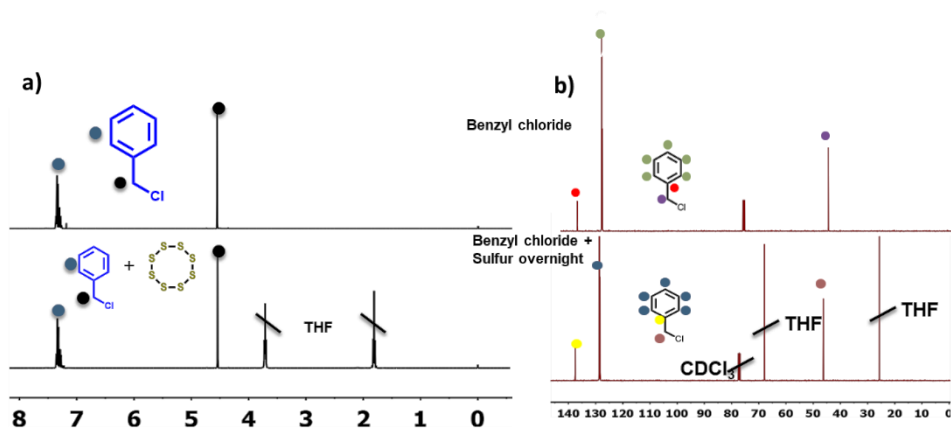
Figure 5.3: a) ^{1}HNMR of benzyl chloride (top) and benzyl chloride treated with sulfur overnight. b) ^{13}CNMR of benzyl chloride (top) and benzyl chloride treated with sulfur overnight

product was studied by ^{13}CNMR. As can be observed in figure 5.3 b), the spectra of the benzyl chloride shows carbons related with the aromatic region can be identified at 130 and 140 ppm and the carbons of the methylene groups bonded to the chlorine moiety at 45 ppms. The comparison between the spectra of the benzyl chloride before and after the treatment with sulfur show neither differences in the chemical shift of the signals nor new peaks.

3.2 Synthesis of poly(sulfur-co-vinyl benzyl imidazolium) poly(ionic liquid)s

The sulfur containing poly(ionic liquid)s were synthesized by post-functionalization of the previously described P(S-VBC) copolymers (Figure 5.4 a). In a first step, these copolymers were quaternized using N-methyl imidazole. After 14 hours of reaction, the new copolymer was obtained as a red oil which phase separated from the chloroform solvent. After drying, the poly(sulfur-co-vinylbenzyl imidazolium) chloride (P(S-VBMImC)) was obtained as a red glassy solid. Interestingly, after reaction the quaternized copolymer became solube in polar solvents such as methanol and even water. In the final step, the anion exchange of the chloride anion by a typical anion of the ionic liquid world such

177

as bis(trifluoromethanesulfonyl)imide (TFSI) was carried out. The anion exchange reaction was quite straightforward by simple dissolution of the quaternized copolymer in water and addition of LiTFSI salt. Almost instantaneously, the newly formed poly(sulfur-co-vinylbenzyl imidazolium) TFSI (P(S-VBMImTFSI)) precipitated in water and it was recovered and dried. This copolymer was not soluble in very polar solvents such as water and methanol, but readily soluble in polar aprotic solvents such as acetone and dimethylformamide. The P(S-VBMImTFSI) copolymers formed red soft self-
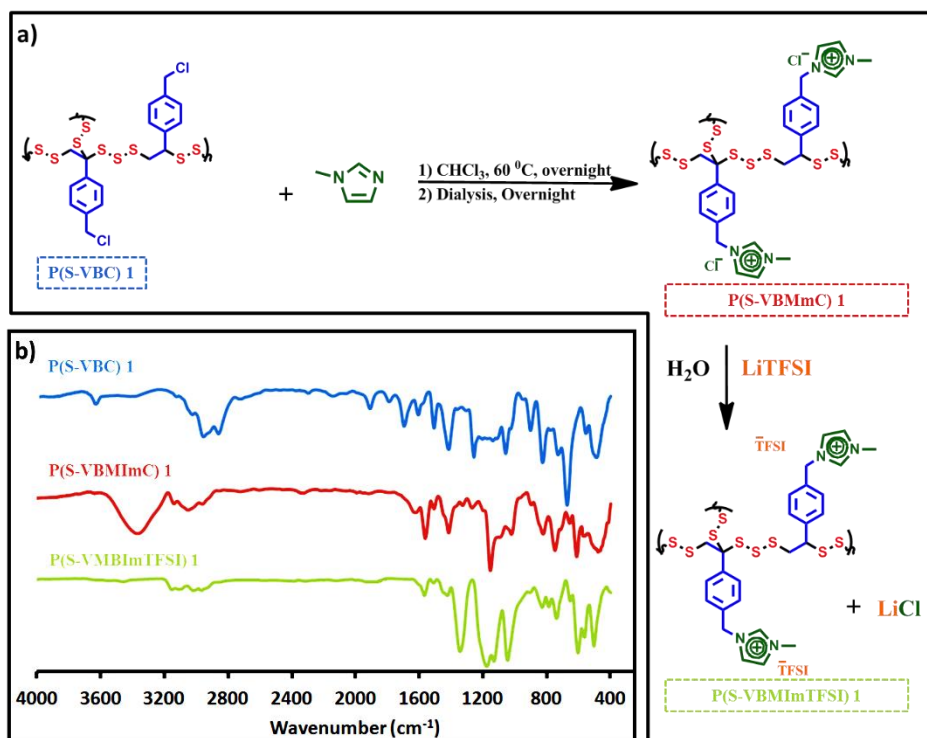

Figure 5.4: a) Synthetic scheme of the post-polymerization modification reactions towards sulfur containing poly(ionic liquid)s. b) ATR-FTIR spectra of the initial poly(sulfur-co-4-vinylbenzyl chloride) (P(S-VBC)1, top), quaternized poly(sulfur-co-4-vinylbenzyl imidazolium)chloride (P(S-VBMImC)1, medium) and final poly(sulfur-co-4-vinylbenzyl imidazolium)TFSI (P(S-VBMImTFSI)1, bottom).

standing films whereas the initial P(S-VBMImC) formed very brittle films.

The quaternization and anion exchange reactions were confirmed by chemical characterization of the copolymers by NMR and FTIR spectroscopy. Figure 5.4 b) compares the FTIR spectrum of the initial P(S-VBC) 1, quaternized P(S-VBMImC) 1 and final P(S-VBMImTFSI). The spectrum of the initial product shows the characteristic bands of the aromatic and the aliphatic C-H vibrations at >3000, 1605, 1508 ,1409 and 832 cm⁻¹. Besides the band associated to the methylene-chlorine groups are clearly visible at 1256 cm⁻¹ (CH$_2$-Cl wagging) and in the region between 700 and 600 cm⁻¹ (C-Cl stretching). Interestingly, these bands disappear completely in the spectra of the quaternized copolymers and new bands related with the imidazolium moieties are present in the spectra of the following products. Namely, the band at 3100 cm⁻¹ related to the halogen bonds, C=C band at 1564 cm⁻¹ and C-C-N stretching at 1159 and 754 cm⁻¹. The
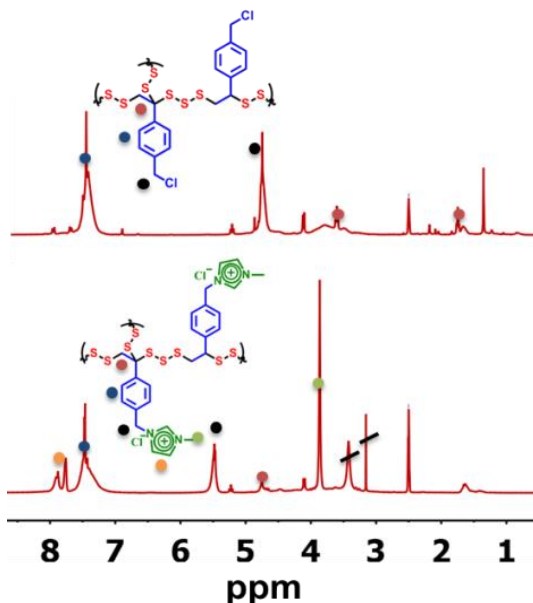

Figure 5.5: ¹HNMR of P(S-VBC) 1 (top) and P(S-VBMImC) 1 (bottom).

complete modification of the alkyl chloride was also confirmed in the ^{1}H NMR spectra showed in figure 5.5. The spectrum of the quaternized poly(sulfur-co-4-vinylbenzyl imidazolium) chloride does not show any of the initial signal of the methylene group bonded at the chlorine atom at 4.5 ppm. Furthermore, new signals at 7.7 ppm associated to the imidazolium ring and 3.9 ppm of the methylene close to it can be found.

Furthermore, the anion exchange reaction and the chemical nature of the P(S-VBMImTFSI) could be confirmed by FTIR. The chloride to TFSI anion exchanged resulted in disappearance of the band at >3100 cm^{-1} related to the halogen atom and the appearance of strong and characteristic bands of the TFSI anion at 1374, 1180, 1134 and 1042 cm^{-1}. Besides this change, the rest of the bands are very similar on the three spectra (Figure 5.4b).

3.3 Thermal and electrochemical characterization of poly(sulfur-co-vinyl benzyl imidazolium) poly(ionic liquid)s

The thermal properties of the poly(sulfur-co-vinyl benzyl imidazolium) poly(ionic liquid)s were investigated by Differential Scanning Calorimetry (DSC) and
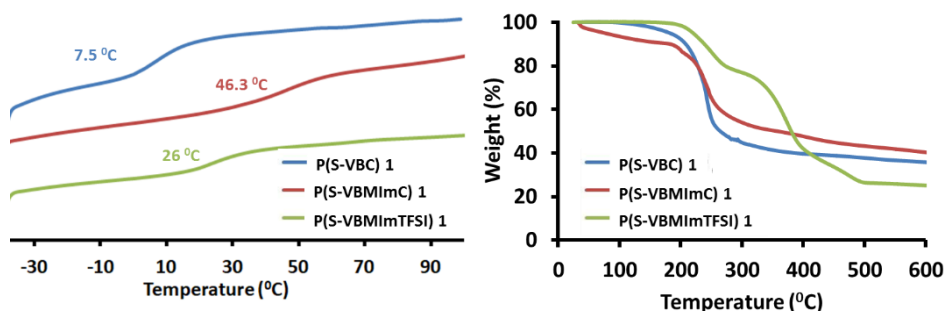

Figure 5.6: a) DSC thermograms and TGA thermograms of poly(sulfur-co-4-vinylbenzyl chloride) (P(S-VBC) 1), quaternized poly(sulfur-co-4-vinylbenzyl imidazolium)chloride (P(S-VBMImC) 1) and final poly(sulfur-co-4-vinylbenzyl imidazolium)TFSI (P(S-VBMImTFSI) 1).
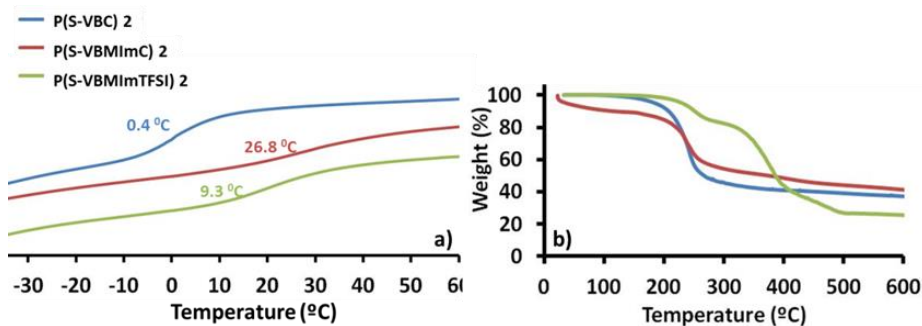
Figure 5.7: a) DSC thermograms of P(S-VBC) 2 (blue), P(S-VBMImC) 2 (red) P(S-VBMIm TFSI) 2 (green) polymers. b) TGA thermograms of of P(S-VBC) 2 (blue), P(S-VBMImC) 2 (red) and P(S-VBMIm TFSI) 2 (green) polymers.

thermogravimetric analysis (TGA) (Figure 5.6). As it can be observed in the DSC data shown in Figure 5.6a), all the copolymers were amorphous and showed clear glass transition temperatures. The initial P(S-VBC) 1 presented a low Tg value of 7.5 ºC quite similar to the previously reported poly(sulfur-co-styrene) systems. On the other hand, the quaternized P(S-VBMImC) showed a high Tg value of 46.2 ºC which is expected from the rigid imidazolium-chloride units. However, the final P(S-VBMImTFSI) shows a lower Tg value of 26 ºC. This drop in glass transition is expected and observed before for poly(ionic
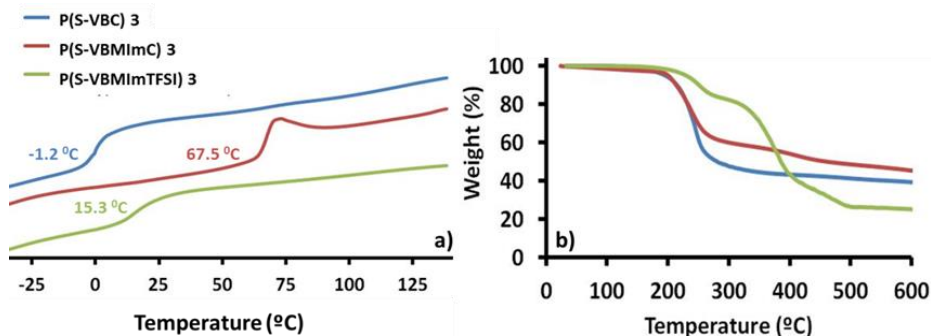

Figure 5.8: a) DSC thermograms of P(S-VBC) 3 (blue), P(S-VBMImC) 3 (red) and P(S-VBMIm TFSI) 3 polymers. b) TGA thermograms of of P(S-VBC) 3 (blue), P(S-VBMImC) 3 (red) and P(S-VBMIm TFSI) 3 (green) polymers.

181

liquid)s where the chloride anion is substituted by TFSI.

The three different copolymers showed also a different behavior in the TGA thermograms showed in Figure 5.6b). As it can be observed, the P(S-VBC) showed a degradation step at 200 ⁰C with a weight loss of 43 wt% which can be associated to the sulfur content. The P(S-VBMImC) presented a similar TGA behavior but in this case the initial weight loss is 34% which is understood due to the decreased presence of sulfur in this copolymer. As observed with other poly(ionic liquid)s, the P(S-VBMImTFSI) showed the higher thermal stability with only a 23 wt% loss at 200 ⁰C. AS it can be observed in figure 5.6 and 5.7, this degradation behavior can be extended to the rest of copolymers with different initial sulfur feed ratios.

As discussed in the introduction, we expect that the new sulfur containing poly(ionic liquid)s present both properties of sulfur containing polymers and poly(ionic liquid)s. One known feature of poly(ionic liquid)s is their *high ionic* conductivity which is known also as a limitation in the case of sulfur containing copolymers. In particular, poly(ionic liquid)s having TFSI counter-anions show high ionic conductivity values. To corroborate this, we measured the ionic conductivity of our copolymers by electrochemical impedance spectroscopy. As
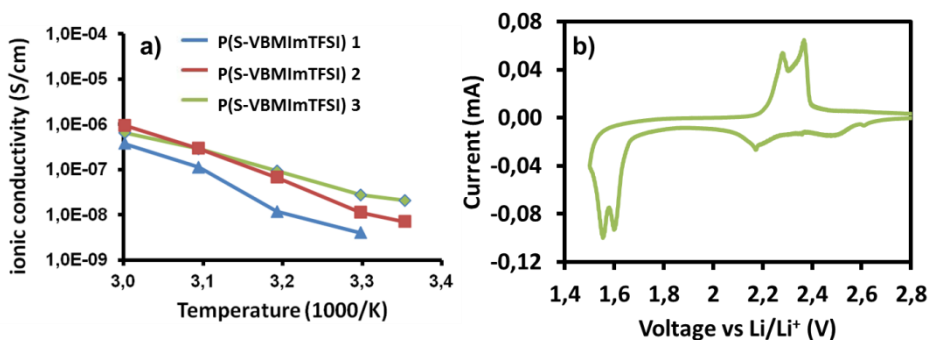

Figure 5.8: a) Ionic conductivity vs temperature of P(S-VBMImTFSI)1-3 and b) Cyclic voltagram of the P(S-VBMImTFSI) 1.

it can be observed in figure 5.8 a), the three poly(sulfur-co-4-vinylbenzyl imidazolium)TFSI copolymers show ionic conductivity values between 10^{-9} and 10^{-6} S/cm which are very high for sulfur containing polymers. The subtle differences between the three different polymers are related to the changes observed in their glass transition temperatures. Although this values are relatively low when compared to the best polymer ion conductors (10^{-3} S/cm), they compared favorably to sulfur materials which show a very low conductivity value of 10^{-14} S/cm.

On the other hand, one typical feature of sulfur containing polymers which is not observed in poly(ionic liquid) is their redox properties. It is well known the reversibility of the S-S bonds are redox active which allows sulfur containing polymers to be used as cathodic materials in lithium-sulfur batteries. In order to study this, we investigated the cyclic voltammetry vs Li/Li$^+$ of the P(S-VBMImTFSI) 1 copolymer. The cyclic voltammetry shown in Figure 5.8 b) shows two quasi-reversible reduction peaks at 2.45 and 2.17 V and two overlapped oxidation peaks at 1.6 V. Although in particular the oxidation peaks are displaced as compared to pure sulfur, it is clearly seen that the sulfur containing poly(ionic liquid)s present some interesting redox properties.

3.4 Application of poly(sulfur-co-vinyl benzyl imidazolium) poly(ionic liquid)s

The synthesis and characterization of these new sulfur based poly(ionic liquid)s have proved that both chemistries, namely the high sulfur content polymers and the chemistry of poly(ionic liquid)s, have been successfully combined obtaining a material with synergetic properties of tunable solubility, ionic conductivity and redox activity. Therefore, in order to take advantage of these features, the high sulfur content poly(ionic liquid)s have been applied in two different scenario. On one hand, the water soluble P(S-VBMImC) have been used as a stabilizer for waterborne nanometric sulfur. And on the other hand the ionically conductive

P(S-VBMImTFSI) have been applied in lithium sulfur battery either as additive in the cathode or in the electrolyte*.*

3.4.1 Waterborne sulfur nanoparticles suspension stabilized by P(S-VBMImC) poly(ionic liquid).

Poly(ionic liquid)s have the ability be used as stabilizers for a wide window of nano-objets, from polymer particles to metal nanoparticles[18,19]. In this case a dispersion of sulfur nanoparticles in water with sulfur based Poly(ionic liquid)s as surfactants was synthesized. An aqueous solution of $Na_2S_2O_3$ was treated with oxalic acid and by disproponation reaction elemental sulfur was synthesized in form of nanoparticles that tend to agglomerate and precipitate as micrometric sulfur (figure 5.10 a))[20]. It was studied by Paria et al that these
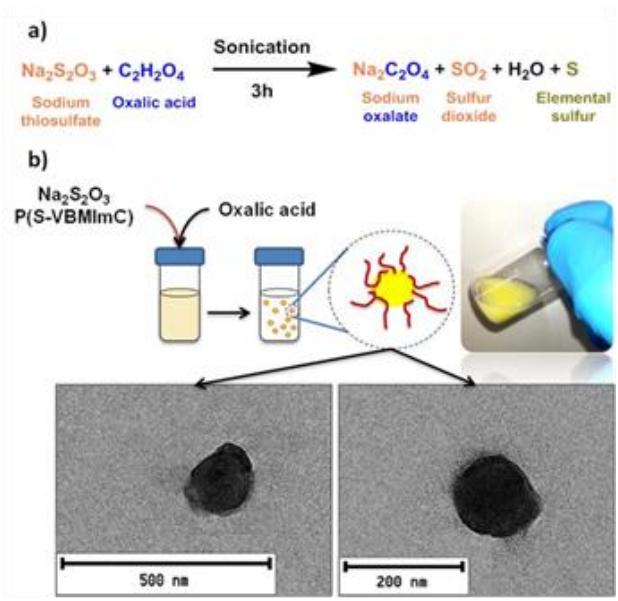

Figure 5.10: a) Disproponation reaction of sodium thiosulfate with oxalic acid to form waterborne elemental sulfur. b) Schematic representation of the preparation of sulfur nanoparticles dispersion from sodium thiosulfate and stabilized by the poly(ionic liquid) P(S-VBMImC). In the bottom, SEM images of the obtained sulfur nanoparticles

sulfur nanoparticles could be stabilized using different commonly used surfactants. In this case the previously synthesized Poly(Sulfur-VBMImC) 2 was used as stabilizer, it is our belief, that the sulfur backbone of the high sulfur content polymer presents a high affinity for the sulfur particle, and the ionic moiety has the ability to stabilize the particle in aqueous phase. The synthesis was done under sonication mixing, as was proved by Paria et al that were the condition under the sulfur nanoparticles presented the lowest particle size[21]. After the completion of the disproponation reaction the particle size was studied by TEM. As can be observed in figure 5.10 b), particles around 200 nm were obtained. The particle showed a spherical like shape, and the presence of the Poly(Sulfur-VBMImC) 2 polymer can be observed in the surface of the particle.

3.4.2 P(S-VBMImTFSI) as additive in lithium sulfur cells.

Another field of application where the poly(ionic liquid)s are showing excellent results is in energy storage systems[9,22]. More specifically in lithium sulfur system, cationic polymers have attracted attention as advanced binders as they can lead to both, higher ionic conductivity in the cathode structure, what enhances the Lithium ion transport towards the sulfur particles, and the ability to trap polysulfide by electrostatic interactions[23]. Therefore, as the presented
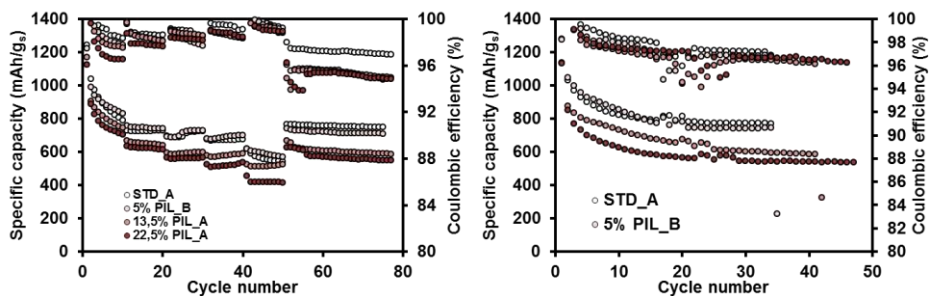

Figure 5.11: a) Effect of C-rate on capacity for cathodes containing 5, 13,5 and 22,5 wt% of P(S-VBMImTFSI) as additive, with a standard sulfur cathode as comparison. b) Cyclability studies of cathodes containing 5, 13,5 and 22,5 wt% of P(S-VBMImTFSI) as additive, with a standard sulfur cathode as comparison

polymers possess good ionic conductivity, the P(S-VBMImTFSI) has been applied as an additive in the cathode formulation. Furthermore, these materials have shown some redox activity, what can be translated into an increase in the capacity of the battery. There have been tried 3 different amount of sulfur based poly(ionic liquid) by replacing 5%, 13.5% or 22.5% of carbon weight. In Figure 5.11 the C-rate capability and cycling stability of the bare cathodes, cathodes with 5 wt%, 13.5 wt% and 22.5 wt% of P(S-VBMImTFSI) in the cathode are shown. As can be observed, in C-rate capability the bare cathode shows the best performance, by delivering around 900 mAh g^{-1} at C/10, 760 mAh g^{-1} at C/5, 720 mAh g^{-1} at C/2.5, 700 mAh g^{-1} at 1C and 600 mAh g^{-1} at 2C, recovering to almost 800 mAh g^{-1} at C/5 for long cycling stability study. The addition of 5 wt% of P(S-VBMImTFSI) into the cathode appears to have no significant effect in the capacity, however the coulombic efficiency remains below the CE of the bare cathode, specially in the subsequent cycling stability study at C/5 where the capacity is similar, but the coulombic efficiency decreases below 96%. The other two concentrations have more dramatic effect either in the capacity, where the cathode with 13.5 wt% of the sulfur bases poly(ionic liquid) shows 800 mAh g^{-1} at C/10, 660 mAh g^{-1} at C/5, 590 mAh g^{-1} at C/2.5, 570 mAh g^{-1} at 1C and 550 mAh g^{-1} at 2C, recovering to around 600 mAh g^{-1} at C/5 for long cycling stability study; and the cathodes with 22.5 wt% of P(S-VBMImTFSI) performs 700 mAh g^{-1} at C/10, 630 mAh g^{-1} at C/5, 560 mAh g^{-1} at C/2.5, 530 mAh g^{-1} at 1C and 420 mAh g^{-1} at 2C, recovering to almost 550 mAh g^{-1} at C/5 for long cycling stability study.

Similar trend can be found in cycling stability study at C/10 where the bare cathode shows an initial capacity of 1300 mAh g^{-1} and is stabilized at 800 mAh g^{-1} with a coulombic efficiency above 96% in cycle 30; whereas the cathodes with the sulfur based poly(ionic liquid) shows poorer performance such as 780 mAh g^{-1} with 5%, 600 mAh g^{-1} with 13.5% and 565 mAh g^{-1} with 22.5 wt% of P(S-VBMImTFSI). This detrimental effect can be related with the high solubility of the P(S-VBMImTFSI) in the electrolyte solvents. This could lead to a diffusion

of the polymer out from the cathode, compromising the cathode structure and leading to cathodic areas that are no connected to the conductive network in contact with the current collector, what heads to lower capacity.

After this unsuccessful trial, and taking advantage of the high solubility of these materials in organic solvents, the P(S-VBMImTFSI) poly(ionic liquid)s were used as additives in the electrolyte. Wang et al, who reported the use high sulfur content polymers made from inverse vulcanization reaction as additive in the electrolyte[24] . They claim that the high sulfur content polymer promotes formation of more stable and flexible SEI layers due to the synergetic effect of the presence of organic units that serve as a plasticizer of the SEI layer and the Li-containing inorganic units that provide Li conductive pathways. Motivated by this report, the novel sulfur based poly(ionic liquid)s were used as additives in the electrolyte with the aim of having a hybrid SEI layer in which the organic part would not only have this plastisizer effect, but also it would enhance the ionic conductivity of the SEI thank to the ionic nature of the organic part. In this way, electrolytes containing 1, 10 and 50 wt% dissolved P(S-VBMImTFSI) were used as electrolytes in a lithium sulfur cell. In figure 5.12 the electrochemical results are depicted. As it can be observed, for the long cycling stability study
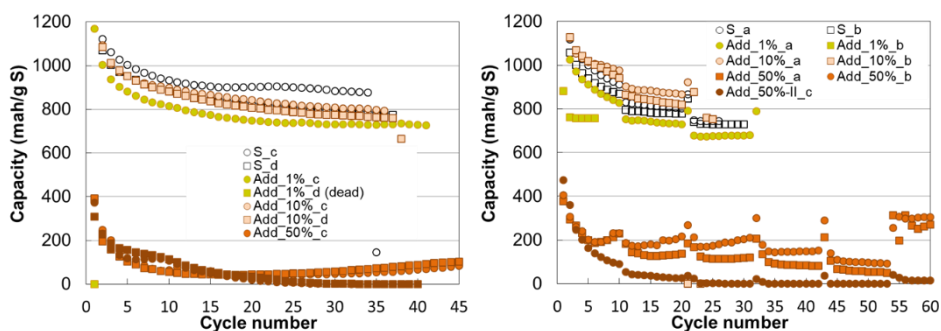

Figure 5.12: a) Effect of C-rate on capacity for coin cells containing 1, 10 and 50 wt% of P(S-VBMImTFSI) as additive in the electrolyte, with a standard electrolyte as comparison. b) Cyclability studies of coin cells containing 1, 10 and 50 wt% of P(S-VBMImTFSI) as additive in the electrolyte, with a standard electrolyte as comparison

the cell with standard electrolyte shows excellent capacity of 880 mAh g_s^{-1} at cycle 50 with a coulombic efficiency above 99%. However, the cells with the P(S-VBMImTFSI) show lower values either of capacity at cycle 50; 713 mAh g_s^{-1} for 1%, 742 mAh g_s^{-1} for 10% and 50 mAh g_s^{-1} for 50 wt% of P(S-VBMImTFSI) in the electrolyte and coulombic efficiency. Although further studies have not done, a possible hypothesis could pass through two scenarios. On one hand, the sulfur based poly(ionic liquid)s posses a limited sulfur rank in the backbone, what can promote the formation of low order lithium sulfides that are known to have detrimental effects in the battery by passivating the anode with an insulator SEI layer[25]. On the other hand, the imidazolium based poly(ionic liquid)s have limited electrochemical stability, what can lead to unforeseen side reactions with undesired side products[26]. For this reason, we believe that the sulfur based poly(ionic liquid) can have a promising future by a proper design of the material by optimizing the chemistry of the synthesis of high sulfur polymer as well as the post-polymerization modification.

4. Conclusions

In this chapter, the chemistries of sulfur containing polymers and poly(ionic liquid)s have been combined for the first time. This was carried out by the inverse vulcanization and copolymerization of sulfur and 4-vinylbenzyl chloride followed by post-modification quaternization and anion exchange reactions. All the chemical as well as thermal characterizations confirmed the successful synthesis of sulfur containing poly(ionic liquid)s. The sulfur poly(ionic liquid)s combine some properties related to its poly(ionic liquid) nature such as anion-dependent solubility (water vs organic solvents) and high ionic conductivity as well as properties related to its sulfur content such redox activity. All in all, this combination brings about polymers with new properties such as sulfur-containing polymers soluble in water, sulfur-containing polymers with high ionic conductivity or redox active poly(ionic liquid)s. This unique combination of properties shows promise for different applications of these new polymers in

wide range of different areas. In this chapter, the water soluble P(S-VBMImC) have been successfully used as stabilizer for waterborne sulfur nanoparticles, whereas the ionically conductive P(S-VBMImTFSI) was applied as additive in lithium sulfur cells. Although the last experiment resulted infructuous, we believe that by a proper design of the sulfur based poly(ionic liquid) can have a beneficial effect in the electrochemical performance of a lithium sulfur battery.

5. References

1. Higashihara, T. & Ueda, M. Recent progress in high refractive index polymers. *Macromolecules* **48,** 1915–1929 (2015).

2. Mantione, D., del Agua, I., Sanchez-Sanchez, A. & Mecerreyes, D. Poly(3,4-ethylenedioxythiophene) (PEDOT) derivatives: Innovative conductive polymers for bioelectronics. *Polymers* **9,** (2017).

3. Casado, N., Hernández, G., Sardon, H. & Mecerreyes, D. Current trends in redox polymers for energy and medicine. *Progress in Polymer Science* **52,** 107–135 (2016).

4. Griebel, J. J., Glass, R. S., Char, K. & Pyun, J. Polymerizations with elemental sulfur: A novel route to high sulfur content polymers for sustainability, energy and defense. *Progress in Polymer Science* **58,** 90–125 (2016).

5. Gomez, I., Leonet, O., Blazquez, J. A. & Mecerreyes, D. Inverse Vulcanization of Sulfur using Natural Dienes as Sustainable Materials for Lithium–Sulfur Batteries. *ChemSusChem* **9,** 3419–3425 (2016).

6. Crockett, M. P. *et al.* Sulfur-Limonene Polysulfide: A Material Synthesized Entirely from Industrial By-Products and Its Use in Removing Toxic Metals from Water and Soil. *Angewandte Chemie - International Edition* **55,** 1714–1718 (2016).

7. Griebel, J. J. *et al.* Dynamic Covalent Polymers via Inverse Vulcanization of Elemental Sulfur for Healable Infrared Optical Materials. *ACS Macro Letters* **4,** 862–866 (2015).

8. Hasell, T., Parker, D. J., Jones, H. A., McAllister, T. & Howdle, S. M. Porous inverse vulcanised polymers for mercury capture. *Chem. Commun.* **52,** 5383–5386 (2016).

9. Yuan, J., Mecerreyes, D. & Antonietti, M. Poly(ionic liquid)s: An update. *Progress in Polymer Science* **38,** 1009–1036 (2013).

10. Shaplov, A. S., Ponkratov, D. O. & Vygodskii, Y. S. Poly(ionic liquid)s: Synthesis, properties, and application. *Polymer Science Series B* **58,** 73–142 (2016).

11. Qian, W., Texter, J. & Yan, F. Frontiers in poly(ionic liquid)s: syntheses and applications. *Chem. Soc. Rev.* **46,** 1124–1159 (2017).

12. Isik, M. *et al.* Cholinium-based ion gels as solid electrolytes for long-term cutaneous electrophysiology. *J. Mater. Chem. C* **3,** 8942–8948 (2015).

13. Bara, J. E. in *Absorption-Based Post-combustion Capture of Carbon Dioxide* 259–282 (2016). doi:10.1016/B978-0-08-100514-9.00011-1

14. Isik, M. *et al.* Sustainable Poly(Ionic Liquids) for CO2 Capture Based on Deep Eutectic Monomers. *Acs Sustainable Chemistry & Engineering* **4,** 7200–7208 (2016).

15. Porcarelli, L. *et al.* Single-Ion Block Copoly(ionic liquid)s as Electrolytes for All-Solid State Lithium Batteries. *ACS Applied Materials and Interfaces* **8,** 10350–10359 (2016).

16. Hendriks, B., Waelkens, J., Winne, J. M. & Du Prez, F. E. Poly(thioether) Vitrimers via Transalkylation of Trialkylsulfonium Salts. *ACS Macro Letters* **6,** 930–934 (2017).

17. Zhang, Y. *et al.* Inverse vulcanization of elemental sulfur and styrene for polymeric cathodes in Li-S batteries. *Journal of Polymer Science, Part A: Polymer Chemistry* **55,** 107–116 (2017).

18. Fernandes, A. M. *et al.* From Polymer Latexes to Multifunctional Liquid Marbles. *ACS Applied Materials & Interfaces* **7,** 4433–4441 (2015).

19. Marcilla, R. *et al.* Nano-objects on a round trip from water to organics in a polymeric ionic liquid vehicle. *Small* **2,** 507–512 (2006).

20. Chaudhuri, R. G. & Paria, S. Synthesis of sulfur nanoparticles in aqueous surfactant solutions. *Journal of Colloid and Interface Science* **343,** 439–446 (2010).

21. Chaudhuri, R. G. & Paria, S. Growth kinetics of sulfur nanoparticles in aqueous surfactant solutions. *Journal of Colloid and Interface Science* **354,** 563–569 (2011).

22. Qian, W., Texter, J. & Yan, F. Frontiers in poly(ionic liquid)s: syntheses and applications. *Chem. Soc. Rev.* **46,** 1124–1159 (2017).

23. Vizintin, A., Guterman, R., Schmidt, J., Antonietti, M. & Dominko, R. Linear and Crosslinked Ionic Liquid Polymers as Binders in Lithium-Sulfur Battery. *Chemistry of Materials* (2018). doi:10.1021/acs.chemmater.8b02357

24. Li, G. *et al.* Organosulfide-plasticized solid-electrolyte interphase layer enables stable lithium metal anodes for long-cycle lithium-sulfur batteries. *Nature Communications* **8,** (2017).

25. Simmonds, A. G. *et al.* Inverse vulcanization of elemental sulfur to prepare polymeric electrode materials for Li-S batteries. *ACS Macro Letters* (2014). doi:10.1021/mz400649w

26. Sun, X.-G. *et al.* Bicyclic imidazolium ionic liquids as potential electrolytes for rechargeable lithium ion batteries. *Journal of Power Sources* (2013). doi:10.1016/j.jpowsour.2013.02.061

Conclusions

194

The aim of this thesis has been the development of novel high sulfur content polymeric materials for energy storage application in lithium sulfur batteries. In the frame of this work, a variety of different polymers have been presented addressing different synthetic strategies by exploring different sulfur chemistries and either changing the monomers, changing the chalcogenide part, the synthetic method or by post polymerization functionalization method. The most important conclusions will be highlighted in the following points:

1. In the first chapter Divinyl benzene proved to be a good comonomer for the inverse vulcanization of sulfur. The reaction resulted to be faster than with 1,3-Diisopropenyl benzene, yielding to amorphous and yellow materials. These polymers resulted to be more rigid what eases the processability of the active material what enhances the electrochemical performance, showing excellent capacity of above 700 mAh g^{-1} with a cycle life of 500 cycles.

2. In the second chapter, it was proven that the inverse vulcanization reaction is not restricted to aromatic monomers. Furthermore, it was demonstrated that green and sustainable monomers can be used by simple adjustments in the synthesis. The physicochemical characterization proved the successful polymerization showing different structures of the polymeric materials. These polymers were electrochemically tested, presenting stable capacities of around 700 mAh g^{-1} at 200 cycles at C/5. By this result it was proved the classical behavior of stable capacity retention of the inverse vulcanized material with the copolymerization of sulfur with novel sustainable based monomers.

3. In the third chapter, combining of the sulfur-selenium binary system at high temperature and the inverse vulcanization process hybrid sulfur-

selenium copolymers were obtained. These materials were physicochemically characterized showing both features, the successful polymerization as well as the hybridization of sulfur with selenium. Furthermore, the battery results proved a synergetic performance of good cycle life of an inverse vulcanized polymer with a stable capacity of 800 mAh g^{-1} at cycle 100 at C/5 and a higher C-rate capability of sulfur-selenium materials, such as an improvement of 100 mAh g^{-1} at 1C versus a standard sulfur polymer.

4. In the fourth chapter, the combination of the ability of sulfur to form long polysulfide dianionic species in EPD solvents along with the step growth polymerization reaction of alkyl or benzyl dihalides with sodium sulfide was explored. Furthermore, a commonly used organic redox molecule, anthraquinone, was used as organic comonomer. The synthesis yield to insoluble powders that were characterize by different solid-state methods. The electrochemical characterization showed the redox combination of polysulfide segments with the anthraquinone moieties and the test at coin cell level showed high initial capacity of 600 mAh g^{-1}, and high cycle life of 125 cycles at 0.25 mA.

5. And finally, a sulfur based Poly(ionic liquid) was obtained for the first time taking advantage of the sulfur-styrene system A functional styrenic monomer was used, 4-vinylbenzyl chloride, with a subsequent post-polymerization modification by a simple nucleophilic substitution. In this way, a material with synergetic properties of both polymer families such as redox properties ionic conductivity and tunable chemistry solubility could be obtained broadening application window of high sulfur content polymeric materials.

Curriculum Vitae

Mr Iñaki Gomez
Date of Birth: 4th of October 1989 in Donostia – San Sebastian
Nationality: Spanish
Address: Asteasuain 3, 2ºB, 20160 Lasarte-Oria, Spain

Fundación Cidetec, Energy Storage Materials for Energy Unit
Parque Científico y Tecnológico de Gipuzkoa Pº Miramón, 188, 20014 Donostia - San Sebastián
Phone: +34685703583, e-mail: igomez@cidetec.es

WORKING EXPERIENCES

April 2018 - present; **Fundación Cidetec, Energy Storage:** Junior researcher at Materials for Energy Division focused in the development of Lithium Sulfur Batteries.

September 2014 – April 2018: **BERC Polymat, Donostia – San Sebastian;** Predoctoral researcher. Development of high sulfur content polymers as active redox materials for energy storage applications. Supervised by Prof. David Mecerreyes (Polymat) and Dr. Alberto Blazquez (Cidetec). Framed within IPeS ERC project.

January 2017 – July 2017: **University of Arizona, Tucson, United States**, Visiting researcher in the Prof. Jeffrey Pyun laboratory. Synthesis and development of novel functional high sulfur content polymers.

EDUCATION

2014–2018; **University of the basque country, faculty of chemistry science, Donostia – San Sebastian:** PhD in applied chemistry and polymeric materials. PhD project under the supervision of Prof. David Mecerreyes and Dr. Alberto Blazquez. Development of high sulfur content polymers as active redox materials for energy storage applications.

197

2013–2014; **University of the basque country, faculty of chemistry science, Donostia – San Sebastian:** Master degree in applied chemistry and polymeric materials. Master project under the supervision of Prof. David Mecerreyes, development of novel Poly(ionic liquid)s based on chlorocuprate anions.

2007-2013; **University of the basque country, faculty of chemistry science, Donostia – San Sebastian**: Bachelor´s degree in Chemistry, speciality in macromolecular chemistry.

TECHNICAL SKILLS

Characterization techniques: NMR (^{1}H, ^{13}C, ^{77}Se liquid and ^{13}C solid state), **Infrared spectroscopy** (FTIR), **Raman spectroscopy, Gel Permeation Chromatography** (SEC-GPC), **Differential Scanning Calorymetry** (DSC)**, Thermogravimetric analysis** (TGA), **Dynamic Mechanical Thermal Analysis** (DMTA).

Electrochemical testing: Cathode processing (Slurry, blade cast and battery assembly of Li-sulfur cells with different configuration and components), **BaSyTec** (software and hardware).

Software: Office (Word, Excel, Power Point, Access), **TA analysis** (Interpretation of DSC, TGA and reology data), **MestreNova** (Interpretation of NMR data), **ChemBioDraw** (Chemical drawing and database), **SciFinder, Mendeley.**

KNOWLEDGE & EXPERIENCES

Languages: Spanish – mother language, English – fluent writing and speaking, Basque – Fluent writing and speaking

Lab experiences: Planing of the synthesis and explanation of the results, independent or teamwork. Organic synthesis; poly(ionic liquid) synthesis, isolation and purification; bulk copolymerization and sulfur chemistry; emulsion polymerization. Characterization with NMR, FTIR, elemental analysis, Raman, DSC, SEM, etc. Assembly of Li batteries (coin cell), electrochemical measurements with BaSyTech and interpretation of the measurements.

BIBLIOGRAPHY

Published articles:

1 - I. Gomez, D. Mecerreyes, J. A. Blazquez, O. Leonet, H. Ben Youcef, C. Li, J. L. Gómez-Cámer, O. Bondarchuk, L. Rodriguez-Martinez, *J. Power Sources* **2016**, *329*, 72–78.

2 - I. Gomez, O. Leonet, J. A. Blazquez, D. Mecerreyes, *ChemSusChem* **2016**, *9*, 3419–3425.

3 - I. Gomez, D. Mantione, O. Leonet, J. A. Blazquez, D. Mecerreyes, *ChemElectroChem* **2018**, *5*, 260–265.

4 - I. Gomez, O. Leonet, J. Alberto Blazquez, H. J. Grande, D. Mecerreyes, *ACS Macro Lett.* **2018**, *7*, 419–424.

5 - I. Gomez, A. F. Anastro, O. Leonet, J. A. Blazquez, H.-J. Grande, J. Pyun, D. Mecerreyes, *Macromol. Rapid Commun.* **2018**, *0*, 1800529.

Conference Contributions:

1- Suspol Summer School, Donostia - San Sebastian, Spain, June 2014, Organizing cometee

2- JIP-JEPO, Donostia - San Sebastian, Spain, September 2015: Organizing cometee

3- ABAA8, Bilbao, Spain, October 2015: Poster "Innovative sulphur rich copolymers as high performance cathodes for lithium sulphur batteries"

4- 5th Workshop "Lithium Sulfur Batteries", Dresde, Germany, November 2016: "Inverse vulcanization of sulfur with natural dienes as sustainable materias for lithium sulfur batteries"

5- ACS Meeting, San Francisco, CA, United States, April 2017: Poster "Inverse vulcanization of sulfur with natural dienes as sustainable materias for lithium sulfur batteries"